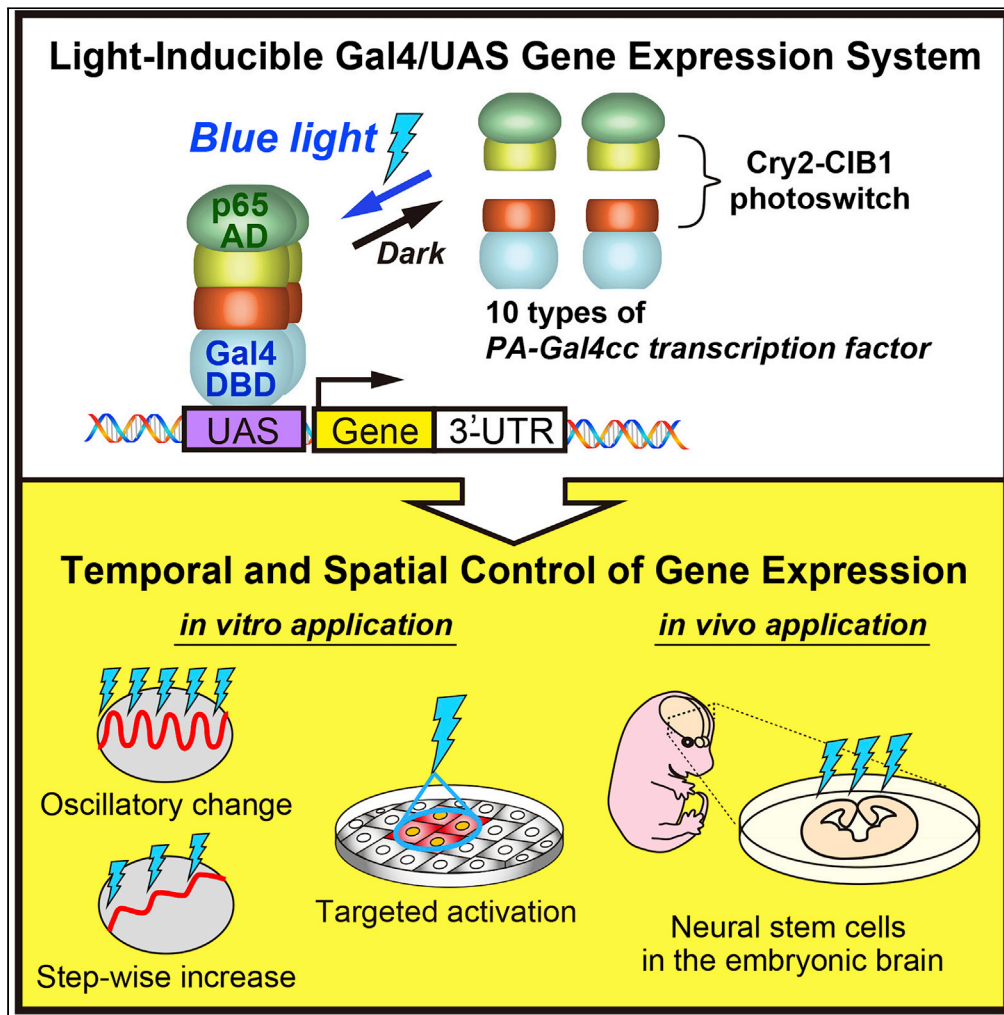## Article

Optimization of Light-Inducible Gal4/UAS Gene Expression System in Mammalian Cells

Mayumi Yamada,
Shinji C. Nagasaki,
Yusuke Suzuki,
Yukinori Hirano,
Itaru Imayoshi

imayoshi.itaru.2n@kyoto-u.ac.jp

HIGHLIGHTS

Photoactivatable (PA)-Gal4cc transcription factors are developed in mammalian cells

The PA-Gal4cc activities are controlled by blue light

The PA-Gal4cc allows precise temporal and spatial control of gene expression

The PA-Gal4cc can be applied to various types of cells *in vitro* and *in vivo*

Article

Optimization of Light-Inducible Gal4/UAS Gene Expression System in Mammalian Cells

Mayumi Yamada,[1,2,3,4] Shinji C. Nagasaki,[1] Yusuke Suzuki,[1,2,4] Yukinori Hirano,[4,5] and Itaru Imayoshi[1,2,3,5,6,7,8,*]

SUMMARY

Light-inducible gene expression systems represent powerful methods for studying the functional roles of dynamic gene expression. Here, we developed an optimized light-inducible Gal4/UAS gene expression system for mammalian cells. We designed photoactivatable (PA)-Gal4 transcriptional activators based on the concept of split transcription factors, in which light-dependent interactions between Cry2-CIB1 PA-protein interaction modules can reconstitute a split Gal4 DNA-binding domain and p65 transcription activation domain. We developed a set of PA-Gal4 transcriptional activators (PA-Gal4cc), which differ in terms of induced gene expression levels following pulsed or prolonged light exposure, and which have different activation/deactivation kinetics. These systems offer optogenetic tools for the precise manipulation of gene expression at fine spatiotemporal resolution in mammalian cells.

INTRODUCTION

Over the course of development, homeostatic maintenance, and environmental responses of multicellular organisms, gene expression patterns in cells are dynamically altered. To precisely analyze the functional roles of dynamic gene expression changes, tools that allow spatiotemporal control at fine resolution are needed. Light-control systems are powerful methods to artificially regulate cellular functions at fine spatiotemporal resolution, including gene expression control (Crefcoeur et al., 2013; Hallett et al., 2016; Horner et al., 2017; Imayoshi et al., 2013; Konermann et al., 2013; Motta-Mena et al., 2014; Pathak et al., 2017; Polstein and Gersbach, 2012; Shimizu-Sato et al., 2002; Wang et al., 2012; Yazawa et al., 2009; Quejada et al., 2017; Yamada et al., 2018; Liu et al., 2012; Muller et al., 2013). By applying diverse types of photoactivatable (PA) molecules originally cloned from plants, fungi, and bacteria, such as light-switchable enzymes or protein interaction modules, the application of these optogenetic tools has expanded to studies of the regulation of many different cellular functions and biological activities.

The Gal4/UAS system is a binary gene expression system primarily used in *Drosophila*, although it has also been applied to zebrafish and mammalian model organisms (Fischer et al., 1988; Brand and Perrimon, 1993). Gal4, a transcription factor originally cloned from yeast, contains a DNA-binding domain (DBD) and a transcription activation domain (AD), and binds to a specific sequence, UAS (upstream activation sequence). It activates transcription from a basal promoter placed downstream of UAS. The Gal4/UAS system has two major advantages. First, the UAS results in the expression of downstream genes at much higher levels than endogenous tissue-specific promoters. Therefore, this amplification process allows for high levels of gene expression. Second, expression vectors or transgenic animals with Gal4 and UAS constructs are widely used in many different research models. By combining these substantial resources, it is possible to induce expression of the gene of interest in a desired cell type/tissue at a high level at the desired time.

For the precise manipulation of gene expression at fine spatiotemporal resolution in mammalian cells, we designed a blue light-inducible Gal4/UAS gene expression system based on the concept of split transcription factors. In this system, light-dependent interactions between Cry2-CIB1 PA-protein interaction modules can reconstitute a split Gal4 DBD and p65 transcription AD. We adapted the *Arabidopsis thaliana*-derived blue light-responsive heterodimer formation module consisting of the cryptochrome 2 (Cry2) photoreceptor and its specific binding protein cryptochrome-interacting basic-helix-loop-helix 1 (CIB1)

[1]Research Center for Dynamic Living Systems, Graduate School of Biostudies, Kyoto University, Kyoto 606-8501, Japan

[2]Institute for Frontier Life and Medical Sciences, Kyoto University, Kyoto 606-8507, Japan

[3]World Premier International Research Initiative–Institute for Integrated Cell-Material Sciences, Kyoto University, Kyoto 606-8501, Japan

[4]Medical Innovation Center/SK Project, Graduate School of Medicine, Kyoto University, Kyoto 606-8507, Japan

[5]The Hakubi Center, Kyoto University, Kyoto 606-8302, Japan

[6]Japan Science and Technology Agency, Precursory Research for Embryonic Science and Technology, Saitama 332-0012, Japan

[7]Present address: Research Center for Dynamic Living Systems, Graduate School of Biostudies, Kyoto University, Shogoin-Kawahara 53, Sakyo-ku, Kyoto 606-8507, Japan

[8]Lead Contact

*Correspondence: imayoshi.itaru.2n@kyoto-u.ac.jp

https://doi.org/10.1016/j.isci.2020.101506

(Wu and Yang, 2010; Kennedy et al., 2010; Taslimi et al., 2016). This was because the Cry2-CIB1 PA-protein interaction system is efficient and reversible and had therefore already been exploited in previously developed PA gene expression systems (Hallett et al., 2016; Taslimi et al., 2016; Quejada et al., 2017; Yamada et al., 2018).

Here, we optimized light-inducible Gal4/UAS gene expression systems via comprehensive functional screening of candidate constructs of the PA-Gal4 transcriptional activator (PA-Gal4cc) in mammalian cells. Each PA-Gal4cc has a different light-induced transcription efficacy and activation/deactivation kinetics. The conventional Gal4/UAS system is widely used in different research models, such as expression vectors or transgenic animals with UAS regulatory sequences; therefore our light-controlled PA-Gal4cc transcriptional activators will allow the optogenetic manipulation of genes of interest in broad fields of biology.

RESULTS

Functional Screening of Optimized PA-Gal4cc Transcription Factors

Previously, several light-inducible Gal4/UAS systems were developed using yeast cells. However, some such systems optimized in yeast cells (Hallett et al., 2016) do not function efficiently in mammalian cells (Figure S1 and our unpublished data). Therefore, we carried out functional screening of candidate PA-Gal4 transcriptional activator constructs in the immortalized human embryonic kidney cell line HEK293T (Figures 1 and S2–S13 and Table S1). To avoid a possibility that saturated expression of the stable reporter product might mask the differences of light-induced gene expression levels, we applied the destabilized luciferase reporter Ub-NLS-luc2 (Figures 1B and S14) and placed the *Ascl1* 3′ UTR sequence just downstream of Ub-luc. This is known to result in a shorter mRNA half-life and prevent accumulation of the reporter activity in the measured cells (Imayoshi et al., 2013; Luker et al., 2003; Voon et al., 2005; Masamizu et al., 2006). We used two types of the Gal4 DBD, because existence of internal dimerization domain reportedly inhibits nuclear localization of the transcription factor in combination with the light-induced dimerization system (Pathak et al., 2017). In the short version, for constructs of the Gal4 DBD, we used the sequences containing Gal4 residues 1–65. The long version constructs of Gal4 DBD contain its original dimerization domain in addition to the DBD (residues 1–147). For functional screening of these candidate PA-Gal4 transcriptional activator constructs, we used the short or long Gal4 constructs as the split DBD, together with the transcription AD of p65 (p65 AD). We confirmed the strong activity of p65 AD with a comparison to VP16 and VP64 AD (Figure S15) (Wang et al., 2012). In addition to the Cry2-CIB1 system, we also screened constructs of PA-Gal4 activators using other optical dimer formation systems, such as Magnet (Kawano et al., 2015) (Figure S10), tunable light-controlled interacting protein tags (TULIPs) (Strickland et al., 2012) (Figure S11), and original light-inducible dimer/improved light-inducible dimer (oLID/iLID) (Guntas et al., 2015; Hallett et al., 2016) (Figures S12 and S13). However, most constructs did not yield efficient light-inducible transcriptional activity in our functional screening studies. Therefore, we focused on PA-Gal4 constructs using the Cry2-CIB1 system (Figures 1 and S2–S9 and Tables S1–S4).

Arabidopsis thaliana-derived Cry2 and CIB1 were originally regulatory components of development and growth in plants, acting via circadian clock control. Cry2 has two domains, the N-terminal photolyase homology region (PHR) and the cryptochrome C-terminal extension. PHR is a domain that noncovalently binds to the chromophore flavin adenine dinucleotide (FAD). Cry2 binds the basic-helix-loop-helix (bHLH) transcription factor CIB1 in a blue light-specific manner. Truncated versions of the Cry2 and CIB1 essential domains act as a blue light-dependent heterodimer formation module, and several point mutations of Cry2 result in faster or slower photocycles (Kennedy et al., 2010; Liu et al., 2012; Taslimi et al., 2016; Yamada et al., 2018; Hughes et al., 2012). Because these Cry2/CIB1 variants and their respective pairs have different binding affinities, kinetics, and background activity in the dark, we undertook detailed investigations of combinations of the different Gal4 DBD, p65 AD, and Cry2/CIB1 variants (Figures 1 and S2–S9).

Of the 180 tested constructs using the Cry2-CIB1 system, 64 showed light-dependent increases (>5-fold) of the luciferase transcription reporter (Figures 1 and S2–S9). This was more common for the construct sets incorporating the short version of Gal4 DBD. Of the 64 light-inducible Gal4 activator constructs, 16 yielding a >5-fold increase and 33 with a >10-fold increase contained the short version of Gal4 DBD. This might due in part to the nuclear clearing phenotype of Cry2-fused proteins (Pathak et al., 2017), which was reported to be dependent on the presence of a dimerization domain contained within Cry2-fused proteins. In contrast, the long version of the Gal4 DBD construct has an inherent dimerization domain.
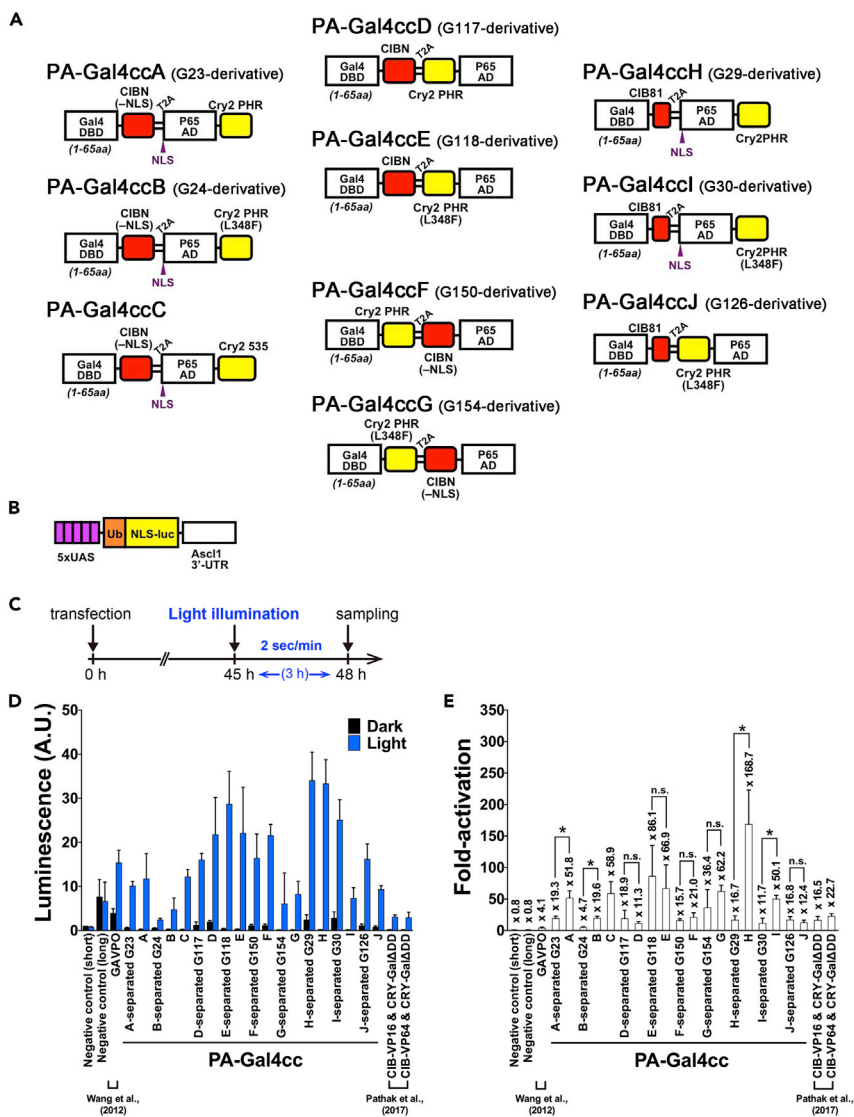
Figure 1. Generation of the Photoactivatable (PA)-Gal4cc Transcriptional Activators

(A) Schematic illustration of the PA-Gal4cc constructs. Yellow boxes indicate Cry2 variants, and red boxes indicate CIB1 variants adapted in this study. Codon optimization for efficient expression in mammalian cells was performed for all Cry2 and CIB1 derivatives.

(B) The reporter construct used in this experiment consisted of 5x UAS, Ub-NLS-luc2, and *Ascl1* 3′ UTR sequences.

(C) Experimental time course.

(D) Validation of light-dependent regulation of the PA-Gal4cc constructs in transiently transfected HEK293T cells. Ten selected candidate construct pairs that showed low basal background and significant induction (e.g., "PA-Gal4cc-A ~ J-separated" constructs) were modified as single expression plasmids, in which the PA-module-tethered Gal4 DBD and p65 AD were co-expressed together with a T2A self-cleaving peptide (i.e., PA-Gal4cc-A ~ J). The pEF-Gal4 DBD short and pEF-p65 AD and pEF-Gal4 DBD long and pEF-p65 AD without any PA dimer formation molecules were co-transfected as the negative control (short) and the negative control (long), respectively.

(E) Fold-increase of luciferase activity (light/dark). The previously developed PA-Gal4 transcription activators (Wang et al., 2012; Pathak et al., 2017) were included for comparison. PHR, photolyase homology region; NLS, nuclear localization signal. The data represent mean values ±standard deviation (SD) (n = 9) from three independent experiments; Each experiment consisted of three replicates. Luciferase assay data of the negative control (short) in the dark were used for the correction of data of each construct. The values in bar graphs and summary of the statistical comparisons were also displayed in Table S1. *p < 0.05; two-tailed Student's t test between the results of each separated and T2A construct pair.

We selected 10 construct pairs for subsequent validation (PA-Gal4cc-separated A ~ J in Figure 1 and Table S1) because of their low levels of background activity in the dark and their consistent light-induced gene expression. Importantly, the selected pairs exhibited lower background activity than GAVPO (Wang et al., 2012; Imayoshi et al., 2013) in the dark (Tables S1–S3). In the construct screening experiments, PA-module-tethered Gal4 DBD and p65 AD were expressed separately from the two independent expression plasmids. When the PA-Gal4 construct was expressed from a single expression plasmid in which the PA-module-tethered Gal4 DBD and p65 AD were co-expressed together with a T2A self-cleaving peptide (Kim et al., 2011), light-induced transcriptional activity was preserved or increased (Figures 1D and 1E and Table S1). This could be due to the improved simultaneous expression efficiency of the PA-module-tethered Gal4 DBD and p65 AD in each transfected cell using T2A-based bicistronic expression vectors. We finally selected these 10 constructs on the T2A vectors and designated them "PA-Gal4ccA ~ PA-Gal4ccJ" (Figure 1A).

In the candidate construct screening studies for PA-Gal4cc, the cells were exposed to pulsed blue light (e.g., 2-s pulse every minute) for only 3 h before cell sampling (Figures 2A–2C). When cells were exposed to similar blue light pulses (2-s pulse every minute) for longer time periods (e.g., 24 h), the induced transcription reporter activity for PA-Gal4cc was increased (Figures 2D–2F). Most of the constructs had essentially similar or superior activities to the light-insensitive constitutively active Gal4 transcriptional activator Gal4-VN8x6 (Salghetti et al., 2000) (Figures 2E and Tables S2 and S3). The rank order of the degree of induced gene expression between the PA-Gal4cc constructs was mostly same for 3- and 24-h illumination (Figure S16).

## Light Dose-Dependent Transcriptional Activity of PA-Gal4cc

One important advantage of a light-inducible gene expression system is the ease of tuning gene expression levels by modifying illumination protocols. We investigated the effects of (1) the duration of the blue light on-phase in the on-off cycle (Figure 3A) and (2) the number of blue light pulses applied (Figure 3D).

We observed an expected blue light duration-dependent increase of luciferase reporter activity in PA-Gal4cc-transduced HEK293T cells (Figures 3B and 3C), indicating that fine control of downstream gene expression was achieved by changing the duration of blue light illumination in the on-phase of the cycle. The duration-dependent significant changes were observed in PA-Gal4ccB, G, H, and I (Figure 3C). We also observed increased luciferase reporter activity dependent on the number of light pulses (Figures 3E and 3F). The light pulse number-dependent significant changes were observed in PA-Gal4ccC, G, H, and I (Figure 3F). However, sensitivity to limited duration or numbers of blue light pulses and linear responses to multiple exposures varied between the PA-Gal4cc constructs. For instance, PA-Gal4ccA, D, E, F, and J were sensitive to short pulses or a single pulse of blue light but did not show further significant increases on multiple pulses. In contrast, PA-Gal4ccB, C, G, H, and I exhibited increased reporter gene expression depending on the duration or number of pulses of blue light. In both cases, fine control of gene expression levels with GAVPO was difficult to achieve in the transient transfection experiments using HEK293T cells (Figure 3). This is because the leaky activity of GAVPO in the dark was high and significant luciferase activity was already induced before exposure to blue light.

Temporal Characteristics of PA-Gal4cc

Because of the rapid activation and deactivation kinetics of the previously developed PA-Tet-OFF/ON system (Yamada et al., 2018), in which the same Cry2-CIB1 switch was applied, it might be expected that PA-Gal4cc could be used for dynamic control of downstream gene expression. The original Cry2 is rapidly activated by exposure to light, and then spontaneously dissociates from CIB1 with a half-life of ~5.5 min (Kennedy et al., 2010; Taslimi et al., 2016). We validated the temporal characteristics of each PA-Gal4cc construct by exposure to short pulses of light (2 min) and monitored luciferase reporter expression levels in real time (Figure 4A).

Analyzing HEK293T cells transiently transfected with PA-Gal4cc and UAS-Ub-NLS-luc2 reporter we found that the temporal patterns of blue light pulse-induced luciferase activity was different for the different constructs (Figures 4 and S17). When we compared the on-kinetics of PA-Gal4cc constructs with GAVPO, most of the tested constructs, with the exception of PA-Gal4ccF and I, had significantly lower values than GAVPO (Figure 4B). Light-induced gene expression did not cease rapidly in cells transiently transfected with GAVPO and PA-Gal4cc. However, the off-kinetics of PA-Gal4ccD, E, G, I, and J were significantly shorter
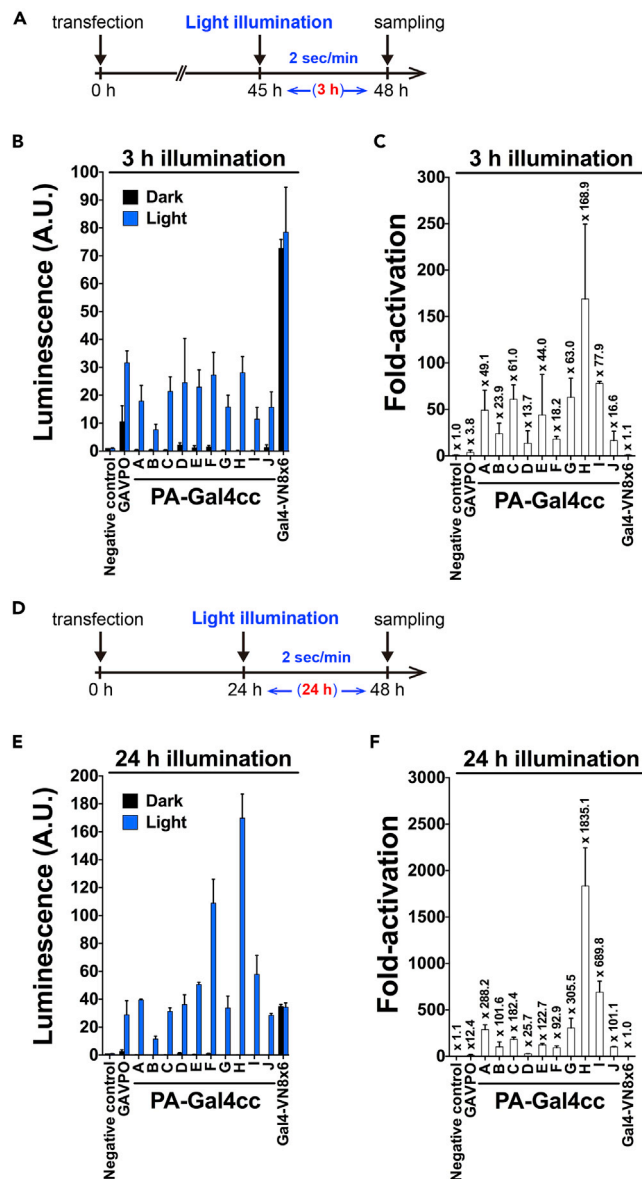
Figure 2. Comparison of Two Different Light Exposure Protocols to Activate PA-Gal4cc-Mediated Transcription

(A) Illumination protocol used for the luciferase assay is indicated.

(B and C) Validation of light-induced luciferase reporter activities by PA-Gal4cc constructs in transiently transfected HEK293T cells. Measured luciferase activities (B) and fold-increase of luciferase activity (Light/Dark) (C). The pEF-Gal4-VN8x6 plasmid was used for expressing the light-insensitive constitutively active Gal4 transcriptional activator. The pEF-Gal4 DBD short and pEF-p65 AD without any PA dimer formation molecules were co-transfected as the negative control. The rank order of the degree of fold activation was as follows: PA-Gal4cc-H, I, G, C, A, E, B, F, J, D. The data represent mean values ± SD (n = 9) from three independent experiments; each experiment consisted of three replicates.

(D) Illumination protocol with prolonged exposure used for the luciferase assay is indicated. The light wavelength and radiant energy were the same as (A).

(E and F) Validation of light-induced luciferase reporter activities by PA-Gal4cc constructs in transiently transfected HEK293T cells. Measured luciferase activities (E) and fold-increase of luciferase activity (Light/Dark) (F). The rank order of the degree of fold activation was as follows: PA-Gal4cc-H, I, G, A, C, E, B, J, F, D. The data represent mean values ± SD (n = 6) from three independent experiments; each experiment consisted of duplicates. The values in bar graphs and summary of the statistical comparisons were also displayed in Tables S2 and S3. The rank orders of PA-Gal4cc in the two experiments were summarized in Figure S16.
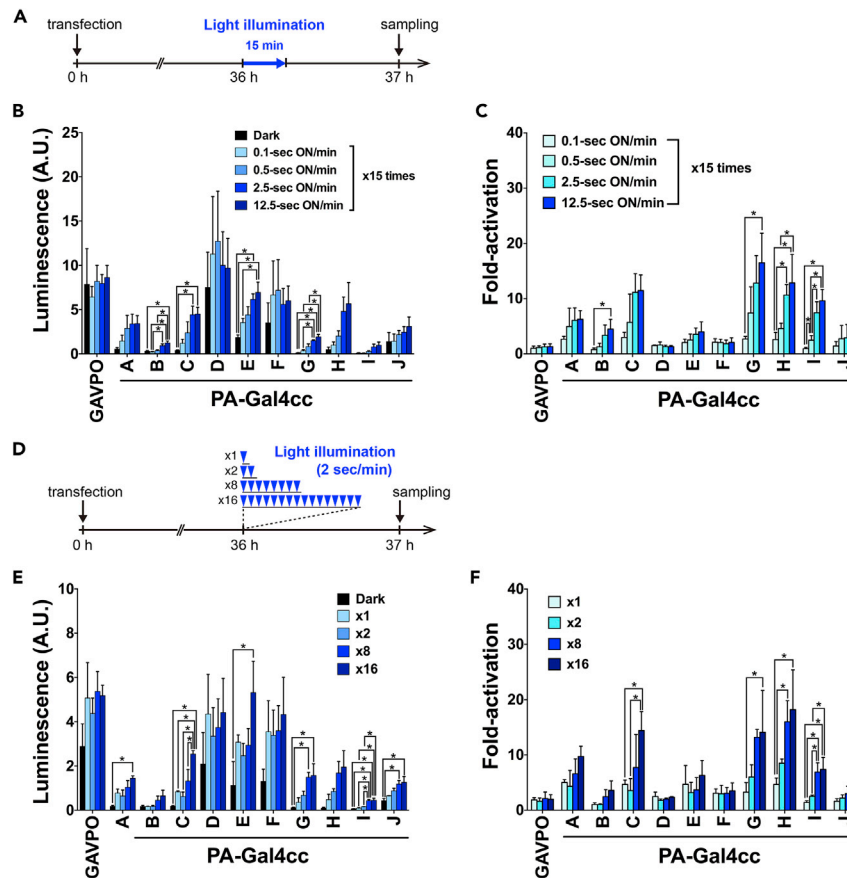
Figure 3. Light-Dose-Dependent Control of PA-Gal4cc Transcriptional Activity

(A) Schematic representation of experimental conditions for testing the effects of the duration of blue light on-phase in the on-off cycle.

(B and C) Blue light duration-dependent increase in measured luciferase activities (B) and fold-increase of luciferase activity (Light/Dark) (C) in PA-Gal4cc transiently transfected HEK293T cells. The data represent mean values $\pm$ SD (n = 8) from three independent experiments.

(D) Schematic representation of experimental conditions for analyzing the effects of the number of applied blue light pulses.

(E and F) Light pulse number-dependent increase in measured luciferase activities (E) and fold-increase of luciferase activity (Light/Dark) (F) in PA-Gal4cc transiently transfected HEK293T cells. The data represent mean values $\pm$ SD (n = 7) from three independent experiments. The data represent mean $\pm$ SD. *$p < 0.05$; one-way ANOVA followed by Tukey's posthoc test.

than GAVPO, indicating that the former are excellent candidates for rapid and dynamic gene expression control (Figure 4C).

We conducted similar experiments using normal, stable luciferase reporters (luc2 in Figure S17A). The activation and deactivation kinetics of light-induced gene expression were extended when the reporter is constructed with normal, stable luciferase (Yamada et al., 2018). Indeed, we observed extended activation and deactivation kinetics of light-induced gene expression with PA-Gal4cc (Figures S17B and S17C). The rank order of the on/off-kinetics of the different PA-Gal4cc constructs was also mostly preserved among these reported constructs with different half-lives (Figure S18).

In the earlier construct validation studies (Figures 1, 2, and 3) we had analyzed the mass effects of multiple blue light pulses. When we periodically applied short-term blue light pulses with different periods at 3, 6, and 12 h and monitored the luciferase reporter expression level in real time, different types of dynamic gene expression patters were induced among the PA-Gal4cc and destabilized/normal luciferase reporter
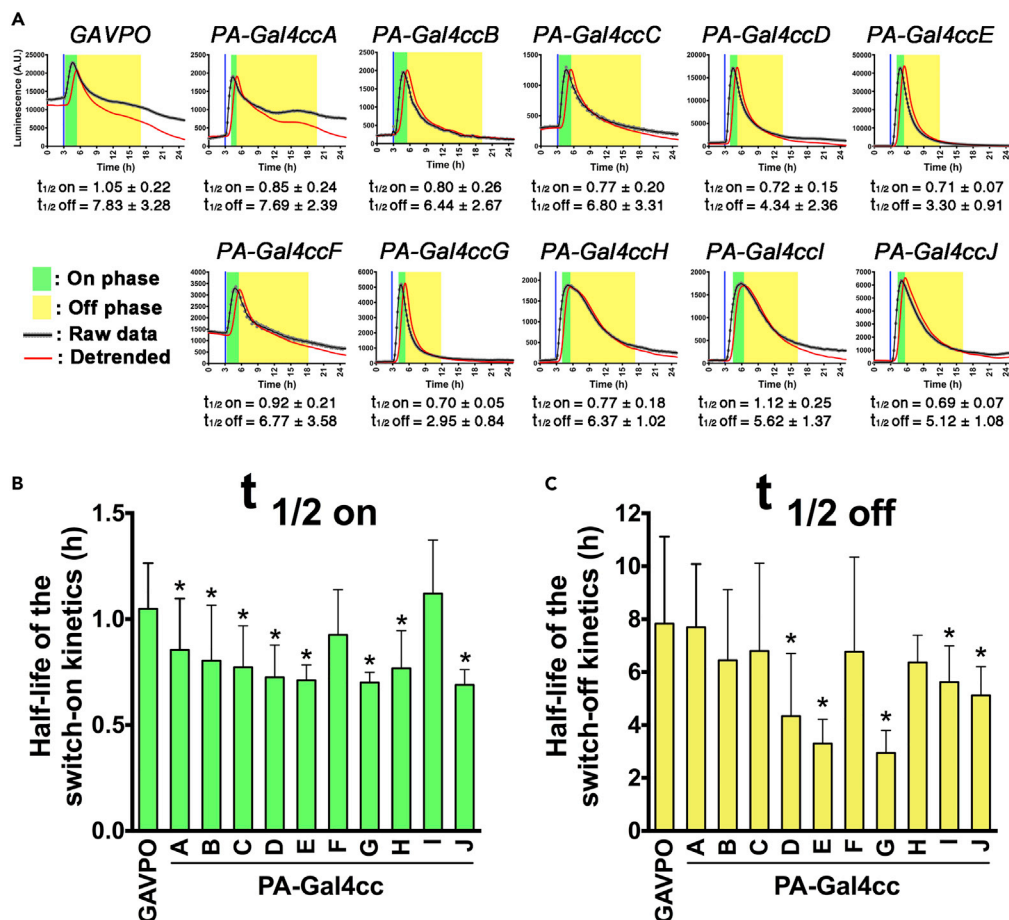
Figure 4. Temporal Features of the PA-Gal4cc Transcriptional Activators

(A) HEK293T cell transfected with the PA-Gal4cc constructs and 5x UAS-Ub-NLS-luc2-Ascl1 3′ UTR reporter were exposed to a single blue light pulse. The timing of blue light exposure is indicated by vertical blue lines. The blue light was applied to cells 30 h after the transfection. The transcription on- and off-phases are highlighted in green and yellow, respectively. (B and C) Using the single light pulse data set, kymograph analysis was used to determine the half-lives of the switch-on (B) and switch-off (C) kinetics of the PA-Gal4cc transcriptional activators. The data represent mean ± SD. *p < 0.05; one-way ANOVA followed by Dunnett's posthoc test (GAVPO versus each PA-Gal4cc). The rank order of the half-life of the switch-on/off kinetics between the PA-Gal4cc constructs was summarized in Figure S18.

constructs (Figures 5 and S19). For example, in the case of destabilized UAS-Ub-NLS-luc2, experiments with 12-h periodic illumination, most of the PA-Gal4cc induced oscillatory gene expression with minimum accumulation of the reporter (Figure 5A). Under blue light irradiation with a 6-h period, a stepwise increase in luciferase reporter activity was observed in PA-Gal4ccH- or I-transfected cells (Figure 5B). In addition to PA-Gal4ccH and I, PA-Gal4cc J also induced stepwise increase of the reporter under blue light irradiation with a 3-h period (Figure 5C). In contrast, PA-Gal4ccE and G still induced oscillatory expression with 3-h periodic illumination (Figure 5C). These differences in the induced gene expression patterns might be attributable to the different activation/deactivation kinetics of each PA-Gal4cc. For instance, PA-Gal4ccE and G had a significantly shorter half-life of off-kinetics and would more easily induce oscillatory expression of downstream genes (Figures 4 and 5).

Reporter expression dynamics were also changed when we used a more stable reporter construct (i.e., UAS-normal luc2-reporter) (Figure S19A). Most of the PA-Gal4cc constructs showed a stepwise increase type of reporter expression under blue light illumination with a 3-h period (Figure S19D). Thus, by changing the reporter protein half-lives as well as the light exposure pattern, different gene expression patterns (e.g., oscillatory change or stepwise increase) can be induced with the same PA-Gal4cc. For example, under blue
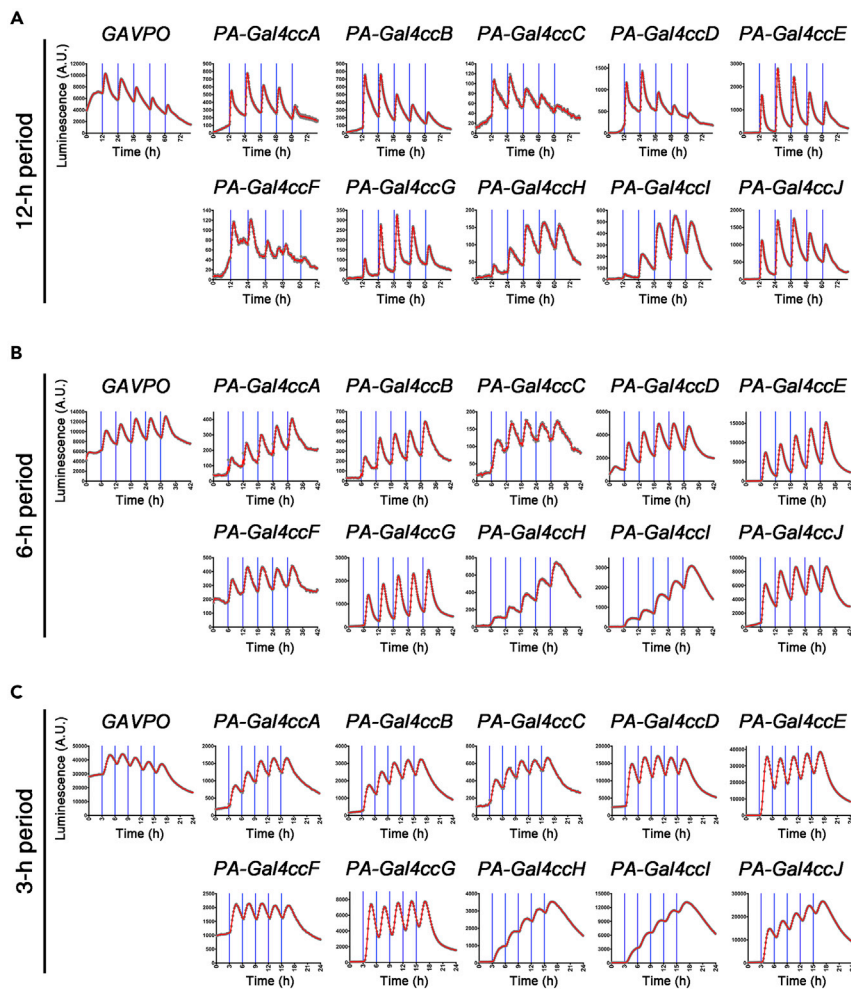
Figure 5. Periodic Activation of the PA-Gal4cc Transcriptional Activators

(A–C) Transiently transfected HEK293T cells, in which PA-Gal4cc and 5x UAS-Ub-NLS-luc2-Ascl1 3′ UTR reporter had been introduced via lipofection, were repeatedly exposed to blue light pulses at 12- (A), 6- (B), or 3-h (C) intervals. The timing of blue light exposure is indicated by vertical blue lines. The first blue light illumination was initiated 24 h after the transfection. Experiments were repeated at least three times with similar results.

light irradiation with a 3-h period, PA-Gal4ccE induced an oscillatory pattern with the unstable UAS-Ub-NLS-luc2-reporter, but a stepwise increase pattern with the stable UAS-luc2-reporter.

Application of PA-Gal4cc together with Lentivirus Vectors

To reduce experimental variability due to different cellular transfection efficiencies, we used lentivirus vectors to stably express PA-Gal4ccE, one of the fastest cycling PA-Gal4ccs, in HEK293T cells and to integrate the reporter construct (Figures 6 and S20). Consistent with the co-transient transfection data of PA-Gal4ccE and destabilized luciferase reporter, the reporter activity was greatly enhanced in the stable PA-Gal4ccE cells exposed to blue light relative to cells left in the dark. When we applied blue light pulses with different periods, robust oscillatory expression was induced at 3, 6, and 12 h (Figures 6A–6C, S20E, S20G, and S20I). However, to develop stable cells manifesting reliable blue light responsiveness, multiple rounds of selections with drug/fluorescence-activated cell sorting were required to purify transduced cells that have higher copy numbers of lentivirus vectors and expression levels of PA-Gal4ccE (Figure S21). In contrast, when we generated GAVPO-expressing stable cells, one single round of drug selection was sufficient (Figure S21). Furthermore, these stable cells in which GAVPO and the UAS-Ub-NLS-luc2-reporter were integrated with lentivirus vectors exhibited efficient and reliable blue light-inducible gene expression and
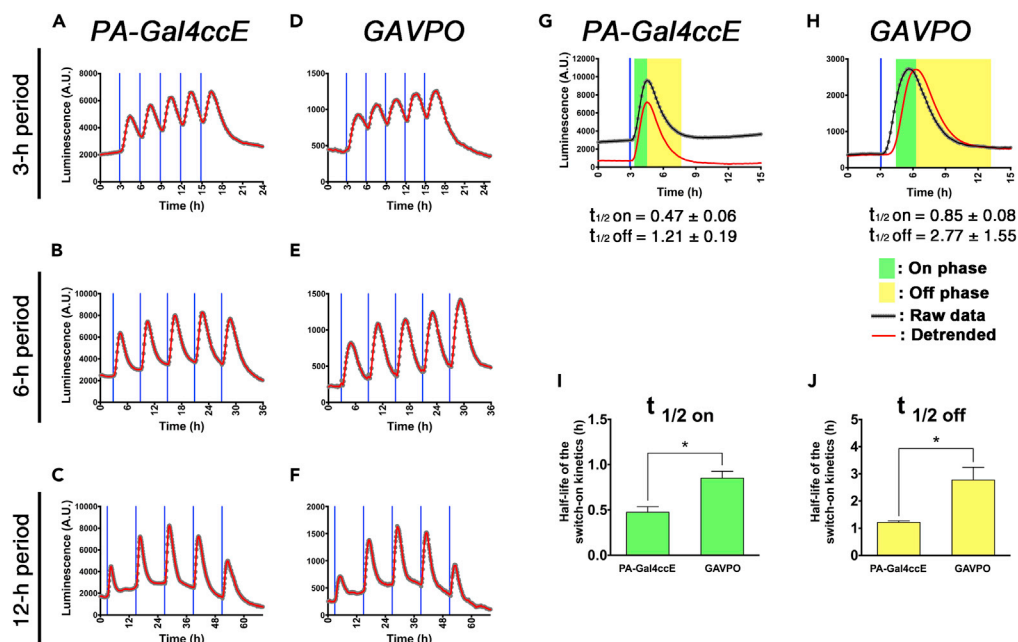
Figure 6. Light-Induced Gene Expression Control with PA-Gal4cc-Expressing Lentiviral Vectors

(A–F) The PA-Gal4ccE or GAVPO lentiviral vector-transduced HEK293T cells were repeatedly exposed to blue light pulses at 3- (A and D), 6- (B and E), or 12-h (C and F) intervals. The reporter construct consisted of 5x UAS, Ub-NLS-luc2, and *Hes1* 3′ UTR sequences. The timing of blue light exposure is indicated by vertical blue lines. Experiments were repeated at least three times with similar results.

(G and H) PA-Gal4ccE (G)- and GAVPO (H)-introduced HEK293T cells were exposed to a single blue light pulse.

(I and J) Using the single light pulse data set, kymograph analysis was used to determine the half-lives of the switch-on (I) and switch-off (J) kinetics of light-induced gene expression. The data represent mean ± SD. *$p < 0.05$; two-tailed Student's t test.

also showed rapid activation/deactivation kinetics (Figures 6D–6F, S20B, S20D, S20F, S20H, and S20J). Although stably transfected GAVPO is significantly slower than PA-Gal4ccE (Figures 6G–6J), the reliability and temporal kinetics were dramatically improved compared with the results of transient transfection experiments (Figure S20). These findings indicate that GAVPO is more suitable for experiments in which stable cells expressing this factor at not-too-high levels can be prospectively screened and identified. In contrast, due to the lower background activity of PA-Gal4cc, this is more suitable for transient transfection experiments where the rigorous control of PA transcription factor expression levels is more difficult and transfection efficiencies are more variable between cells.

Targeted Activation of PA-Gal4cc in Spatially Restricted Cells

Next, we examined whether we could spatially control gene expression in targeted cells. To test this, we equipped a bioluminescence imaging microscope with a digital mirror device (DMD) to stimulate the targeted cells. We tested PA-Gal4ccE and H in such spatial control gene expression experiments. After exposure to a blue light pulse, bioluminescence imaging revealed that luciferase expression in PA-Gal4cc-transfected HEK293T cells with the UAS-Ub-NLS-luc2 reporter occurred in the areas determined by the DMD device (Figure 7). These results indicated that spatial control of gene expression is feasible using the PA-Gal4cc/UAS-system.

Validation of PA-Gal4cc in Brain Slice Cultures

Finally, we tested the ability of the PA-Gal4cc/UAS system to induce light-triggered gene expression in tissues other than cultured cell lines. To this end, we examined PA-Gal4cc activity in neural stem/progenitor cells of the developing mouse forebrain (Figure 8). We transfected the PA-Gal4ccE expression plasmid together with the UAS-Ub-NLS-luc2 reporter into neural stem/progenitor cells using *ex utero* electroporation methods. When tissue slices derived from the electroporated brain were periodically illuminated by blue light at 3- (Figures 8B and 8C) and 6-h (Figures 8D and 8E) periods, oscillatory reporter expression
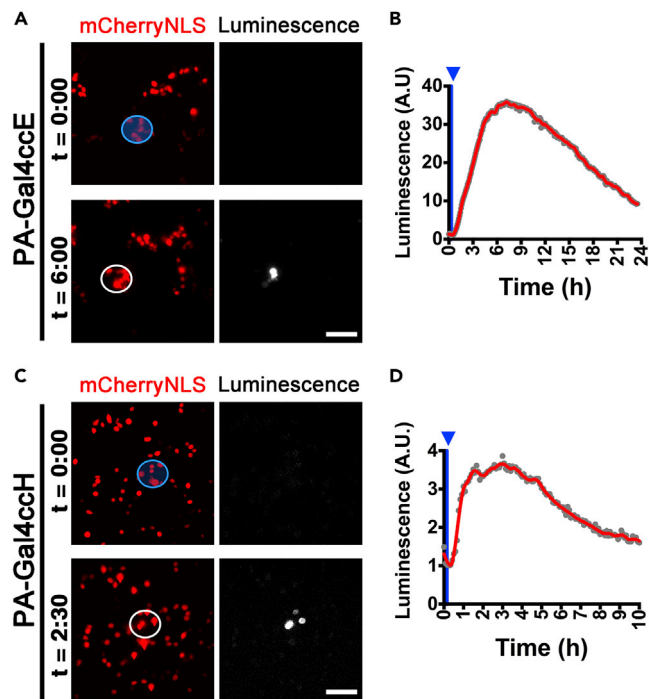
Figure 7. Spatially Controlled Regulation of PA-Gal4cc Transcriptional Activators by Patterned Light Illumination
(A–D) Targeted cell populations were illuminated by patterned light generated by a digital mirror device (DMD). The patterned light, indicated by blue circles, was applied to HEK293T cells in which the PA-Gal4ccE (A and B) and PA-Gal4ccH (C and D) were transiently introduced by lipofection. (B and D) Light-induced reporter expression was quantified after patterned light illumination in the white circled regions. The timing of blue light exposure is indicated by blue arrowheads. Experiments were repeated at least three times with similar results. 86.0% $\pm$ 19.0% and 83.3% $\pm$ 28.9% showed light-induced reporter expressions in the PA-Gal4ccE- and PA-Gal4ccH-transfected cells, respectively. Scale bars, 100 μm.

was observed in the ventricular/subventricular zone where the neural stem/progenitor cells are preferentially located (Imayoshi and Kageyama, 2014a, 2014b). These findings suggest that PA-Gal4cc can be introduced into cells by various different methods, including electroporation, as well as lipofection and with lentiviral vectors. We also documented efficient blue light-induced gene expression in primary cultured cells, such as neural stem/progenitor cells of acutely prepared embryonic brain slices.

DISCUSSION

Here we describe a set of improved PA-Gal4cc transcriptional activators for the spatiotemporal control of gene expression in mammalian cells. To develop PA-Gal4cc transcriptional activators, we carried out functional screening by investigating the following parameters of the candidate constructs: (1) Gal4 DBD elements, (2) Cry2/CIB1 truncation and point mutations, (3) Cry2/CIB1 configuration (i.e., N-terminal or C-terminal fusion), and (4) expression vector structures necessary for efficient expression in target cells. We finally selected 10 PA-Gal4cc transcriptional activators (PA-Gal4cc A ~ J) with different light-induced transcription efficacy and activation/deactivation kinetics. Importantly, all selected PA-Gal4cc had low background activity in the dark, achieving reliable dynamic gene expression control with minimal leaky transcription before light exposure. In our PA-Gal4cc, PA-module-fused Gal4 DBD and p65 AD are co-expressed together with a T2A self-cleaving peptide. The IRES sequence, another tool for co-expression of two polypeptides, is sometimes used for the reconstitution of synthetic transcription factors by light (Quejada et al., 2017). The size of the IRES sequence is much greater than the DNA sequence encoding the T2A peptide, and its integration in expression vectors reduces the level of gene expression. This may limit the application of PA transcription factors to viral vectors in which the size of the inserted sequence is limited and a shorter sequence is preferred for preparing high-titer virus purified products. One concern when using the T2A peptide is that the residue peptides of cleaved T2A may change the properties of
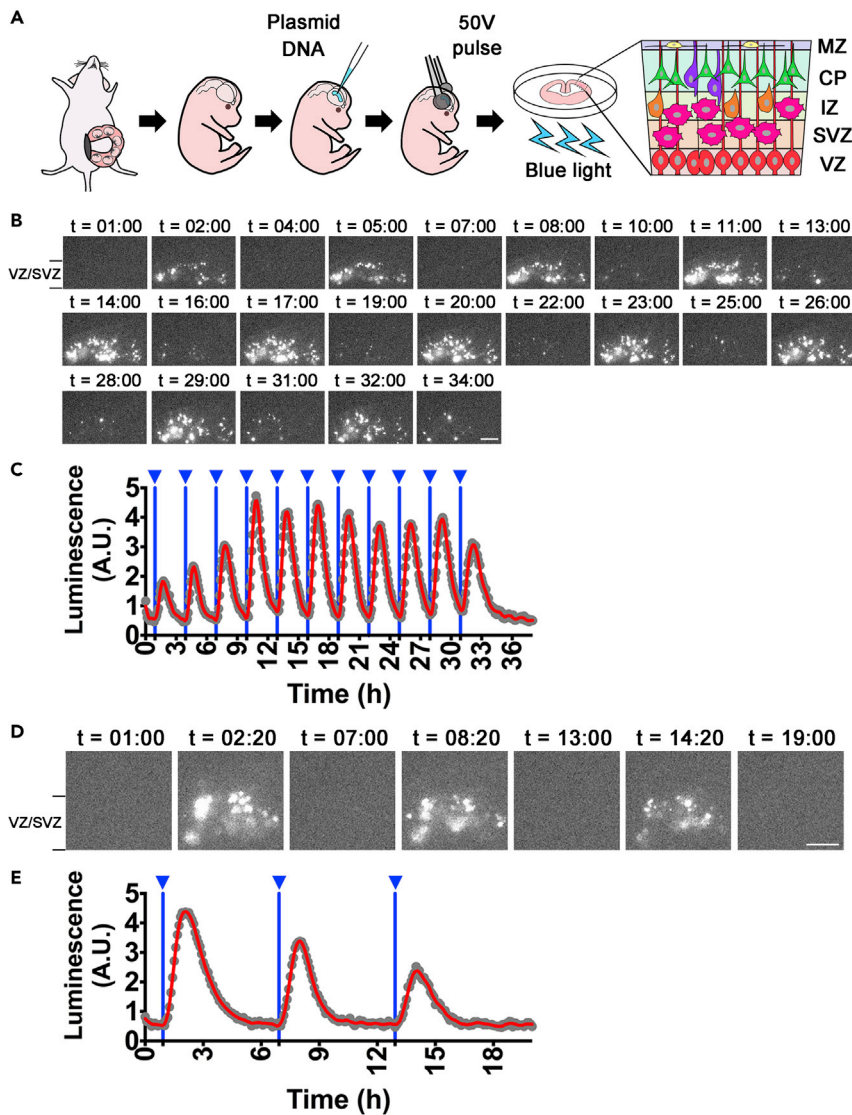
Figure 8. Optogenetic Manipulation of Gene Expression in Brain Slices

(A) PA-Gal4ccE with 5x UAS-Ub-NLS-luc2-Ascl1 3' UTR reporter was introduced into neural stem/progenitor cells of the developing brain by *ex utero* electroporation. The electroporated brain was immediately extracted from the embryo and sliced on tissue culture membrane.

(B–E) Blue light was periodically applied to the slice over a 3- (B and C) and a 6-h period (D and E) and reporter activity was monitored. Blue light-induced luciferase expression was observed in the neural stem/progenitor cells of the ventricular and subventricular zones (VZ/SVZ). Scale bars, 200 μm. MZ, marginal zone; CP, cortical plate; IZ, intermediate zone.

the expressed functional molecules, in this case, the efficiency of the reconstitution of Cry2/CIB1-fused Gal4 DBD and p65AD. However, this concern was not relevant for our PA-Gal4cc because the light-induced transcriptional activity was preserved in the separately expressed vectors and T2A-based bicistronic expression vectors (Figure 1 and Tables S1–S3).

In our construct screening, we used p65 AD as a transcription AD. In previous reports that developed the light-activatable Gal4/UAS system in mammalian cells, VP16 AD or VP64 AD were applied (Pathak et al., 2017; Quejada et al., 2017). Although they identified constructs that showed strong light-induced gene expressions, the structures of the identified optimal constructs were different from the constructs developed in our study, in terms of the applied Cry2/CIB1 truncation and point mutations and Cry2/CIB1 configurations. These results indicate

that, when the different kinds of molecular elements are applied in development of synthetic light-reconstitutable transcription factors, rigorous functional screenings must be required to identify the optimal constructs.

For reliable and fine cellular gene expression control by light, high sensitivity to light, large dynamic range of induced gene expression, and low background transcription activity in the dark are required. To reduce the effects of photo-toxicity resulting from exposure to intense light, high sensitivity is essential for achieving gene expression control using lower-power and/or short-duration light pulses. A requirement for prolonged light exposure also reduces the temporal resolution of gene expression control. To artificially control the magnitude of gene expression as well as the timing (e.g., initiation and termination), light-inducible gene expression systems having large dynamic ranges are needed. Here, we validated more than 200 candidate PA-Gal4 transcriptional activator constructs. The sensitivity to light and dynamic range of induced gene expression levels varied depending on the PA modules used, and their different temporal features, such as activation/deactivation kinetics. Indeed, the selected 10 PA-Gal4cc-A ~ J constructs had different light-induced transcription efficacies and temporal features (Figures 2, 3, 4, 5, S17, and S19 and Tables S1–S4). For example, PA-Gal4ccE or G had significantly faster on/off-kinetics than the other PA-Gal4ccs and is therefore more suitable for generating oscillatory gene expression patterns (Figures 5, S18, and S19 and Table S4). In contrast, PA-Gal4ccH and I and are more suitable for inducing accumulated-type gene expression, such as stepwise increases, and this might be partially attributed to relatively slower on/off-kinetics of PA-Gal4ccH and I than that of PA-Gal4ccE and G (Figures 5, S18, and S19 and Table S4). Regarding the maximum light-induced gene expression level, PA-Gal4ccH showed higher values than other the other PA-Gal4ccs (Figures 2 and S16 and Table S4). In terms of light sensitivity, PA-Gal4ccD and E are very sensitive and can be fully activated by very dim light or a small number of light pulses (Figure 3 and Table S4). All things considered, PA-Gal4ccE could be the first choice when the experiment type needs rapid activation/deactivation of gene expressions and/or the blue light illumination power or exposure time is limited. In contrast, when the experiment type prefers higher induced gene expression levels and prolonged repeated light exposures are permitted, PA-Gal4ccH is more suitable.

In the selected PA-Gal4cc constructs, different sets of Cry2 and CIB1variants were used. However, the light-induced transcription activation/deactivation kinetics of the PA-Gal4cc constructs did not closely correlate with the reported photocycle differences of the Cry2/CIB1 variant pairs. For example, PA-Gal4ccE, the fastest cycling PA-Gal4cc, has a Cry2 PHR module with the L348F slow photocycle mutation (~24-min half-life). The off-kinetics of PA-Gal4ccE was significantly shorter than that of PA-Gal4ccD, in which a wild-type Cry2 PHR module (~5.5-min half-life) was integrated and the remaining construct structure is identical to PA-Gal4ccE (Figures 4, 5, S16, S18, and S19). Similarly, PA-Gal4ccA and B, F and G, and H and I have related construct structures except for a Cry2 PHR L348 point mutation difference. However, we did not observe the expected effects of the Cry2 PHR slow photocycle mutation on the off-kinetics of light-induced gene expression within each pair of PA-Gal4cc constructs. In addition, we also observed significant differences in the induced gene expression levels (Figures 1, 2, and 3). Thus, this Cry2 L348 point mutation might also change other features of the reconstituted PA-Gal4, such as the overall 3D structure, binding affinity for the UAS sequence, and efficiency in recruiting the transcriptional machinery. In the PA-Gal4ccH and I constructs, the truncated short version of CIB1, CIB81, was integrated. PA-Gal4ccH and I showed longer on-kinetics and preferentially induced the stepwise increase pattern of light-induced gene expression (Figures 4, 5, S16, and S19). Although the detailed temporal characteristics of this CIB1 variant have not been analyzed (Taslimi et al., 2016), CIB81 may slowly generate heterodimer complexes with Cry2.

Because of these different characteristics of our multiple PA-Gal4cc transcriptional activators, we can induce different types of gene expression patterns just by changing the selection of PA-Gal4cc-series variants even under the same blue light illumination protocols (Figures 5 and S19). This would contribute to the analysis of the functional roles of different gene expression dynamics. Some types of transcription factors can change their functional roles in the context of self-renewal and fate determination of stem cells by altering their gene expression dynamics (e.g., oscillatory versus sustained). These phenomena were discovered by the application of light-induced gene expression systems (Imayoshi et al., 2013; Imayoshi and Kageyama, 2014a).

In conclusion, we optimized the light-controllable Gal4/UAS gene expression system in mammalian cells by developing sets of PA-Gal4cc transcriptional activators. These allow the induction of different types of gene expression dynamics at fine spatiotemporal resolution in several types of mammalian cells. This technology will contribute to the systematic analysis of dynamic changes in cellular gene expression.

Limitations of the Study

The PA-Gal4cc constructs can be introduced into cells by different methods, including lipofection, electroporation, and by use of lentiviral vectors. We also demonstrated efficient light-triggered gene expression in neural stem/progenitor cells in the developing brain. Because the Gal4/UAS system is commonly used in *Drosophila*, we attempted to develop transgenic flies specifically expressing *Drosophila*-codon-optimized PA-Gal4ccE and G in mushroom body neurons (Figure S22). However, blue light-inducible gene expression was not observed in such transgenic PA-Gal4ccE-expressing flies due to too high a background reporter gene expression before exposure to light. In addition, transgenic PA-Gal4ccG-expressing flies showed only limited light-induced transcriptional activity in adult mushroom body neurons. Furthermore, light-induced activity of PA-Gal4ccE and G in the *Drosophila* S2 cell line was weak (Figure S23). This failure of application of our PA-Gal4cc in *Drosophila* could be attributed to the original optimization of the PA-Gal4cc for the human cell line HEK293T. These results imply that efficacy of light-induced transcription may be different in different cellular contexts and rigorous optimization processes are needed in different cell types and model organisms of interest.

Resource Availability

Lead Contact

Further information and requests for resources and reagents should be directed to and will be fulfilled by the Lead Contact, Itaru Imayoshi (imayoshi.itaru.2n@kyoto-u.ac.jp).

Materials Availability

All unique materials generated in this study are available from the lead Contact upon request.

Data and Code Availability

Requests for custom scripts and raw data can be directed to the Lead Contact, Itaru Imayoshi (imayoshi.itaru.2n@kyoto-u.ac.jp).

METHODS

All methods can be found in the accompanying Transparent Methods supplemental file.

SUPPLEMENTAL INFORMATION

Supplemental Information can be found online at https://doi.org/10.1016/j.isci.2020.101506.

AUTHOR CONTRIBUTIONS

M.Y. and I.I. conceived the project and designed the experiments. M.Y., S.C.N., and I.I. performed the experiments. Y.S. conducted data analysis. Y.H. produced and provided the transgenic flies. M.Y. and I.I. wrote the manuscript with inputs from all other authors.

REFERENCES

Brand, A.H., and Perrimon, N. (1993). Targeted gene expression as a means of altering cell fates and generating dominant phenotypes. Development 118, 401–415.

Crefcoeur, R.P., Yin, R., Ulm, R., and Halazonetis, T.D. (2013). Ultraviolet-B-mediated induction of protein-protein interactions in mammalian cells. Nat. Commun. 4, 1779.

Fischer, J.A., Giniger, E., Maniatis, T., and Ptashne, M. (1988). GAL4 activates transcription in Drosophila. Nature 332, 853–856.

Guntas, G., Hallett, R.A., Zimmerman, S.P., Williams, T., Yumerefendi, H., Bear, J.E., and Kuhlman, B. (2015). Engineering an improved light-induced dimer (iLID) for controlling the localization and activity of signaling proteins. Proc. Natl. Acad. Sci. U S A 112, 112–117.

Hallett, R.A., Zimmerman, S.P., Yumerefendi, H., Bear, J.E., and Kuhlman, B. (2016). Correlating in vitro and in vivo activities of light-inducible dimers: a cellular optogenetics guide. ACS Synth. Biol. 5, 53–64.

Horner, M., Muller, K., and Weber, W. (2017). Light-responsive promoters. Methods Mol. Biol. 1651, 173–186.

Hughes, R.M., Vrana, J.D., Song, J., and Tucker, C.L. (2012). Light-dependent, dark-promoted interaction between Arabidopsis cryptochrome 1 and phytochrome B proteins. J. Biol. Chem. 287, 22165–22172.

Imayoshi, I., Isomura, A., Harima, Y., Kawaguchi, K., Kori, H., Miyachi, H., Fujiwara, T., Ishidate, F., and Kageyama, R. (2013). Oscillatory control of factors determining multipotency and fate in mouse neural progenitors. Science 342, 1203–1208.

Imayoshi, I., and Kageyama, R. (2014a). bHLH factors in self-renewal, multipotency, and fate choice of neural progenitor cells. Neuron 82, 9–23.

Imayoshi, I., and Kageyama, R. (2014b). Oscillatory control of bHLH factors in neural progenitors. Trends Neurosci. 37, 531–538.

Kawano, F., Suzuki, H., Furuya, A., and Sato, M. (2015). Engineered pairs of distinct photoswitches for optogenetic control of cellular proteins. Nat. Commun. 6, 6256.

Kennedy, M.J., Hughes, R.M., Peteya, L.A., Schwartz, J.W., Ehlers, M.D., and Tucker, C.L. (2010). Rapid blue-light-mediated induction of protein interactions in living cells. Nat. Methods 7, 973–975.

Kim, J.H., Lee, S.R., Li, L.H., Park, H.J., Park, J.H., Lee, K.Y., Kim, M.K., Shin, B.A., and Choi, S.Y. (2011). High cleavage efficiency of a 2A peptide derived from porcine teschovirus-1 in human cell lines, zebrafish and mice. PLoS One 6, e18556.

Konermann, S., Brigham, M.D., Trevino, A., Hsu, P.D., Heidenreich, M., Cong, L., Platt, R.J., Scott, D.A., Church, G.M., and Zhang, F. (2013). Optical control of mammalian endogenous transcription and epigenetic states. Nature 500, 472–476.

Liu, H., Gomez, G., Lin, S., Lin, S., and Lin, C. (2012). Optogenetic control of transcription in zebrafish. PLoS One 7, e50738.

Luker, G.D., Pica, C.M., Song, J., Luker, K.E., and Piwnica-Worms, D. (2003). Imaging 26S proteasome activity and inhibition in living mice. Nat. Med. 9, 969–973.

Masamizu, Y., Ohtsuka, T., Takashima, Y., Nagahara, H., Takenaka, Y., Yoshikawa, K., Okamura, H., and Kageyama, R. (2006). Real-time imaging of the somite segmentation clock: revelation of unstable oscillators in the individual presomitic mesoderm cells. Proc. Natl. Acad. Sci. U S A 103, 1313–1318.

Motta-Mena, L.B., Reade, A., Mallory, M.J., Glantz, S., Weiner, O.D., Lynch, K.W., and Gardner, K.H. (2014). An optogenetic gene expression system with rapid activation and deactivation kinetics. Nat. Chem. Biol. 10, 196–202.

Muller, K., Engesser, R., Schulz, S., Steinberg, T., Tomakidi, P., Weber, C.C., Ulm, R., Timmer, J., Zurbriggen, M.D., and Weber, W. (2013). Multi-chromatic control of mammalian gene expression and signaling. Nucleic Acids Res. 41, e124.

Pathak, G.P., Spiltoir, J.I., Hoglund, C., Polstein, L.R., Heine-Koskinen, S., Gersbach, C.A., Rossi, J., and Tucker, C.L. (2017). Bidirectional approaches for optogenetic regulation of gene expression in mammalian cells using Arabidopsis cryptochrome 2. Nucleic Acids Res. 45, e167.

Polstein, L.R., and Gersbach, C.A. (2012). Light-inducible spatiotemporal control of gene activation by customizable zinc finger transcription factors. J. Am. Chem. Soc. 134, 16480–16483.

Quejada, J.R., Park, S.E., Awari, D.W., Shi, F., Yamamoto, H.E., Kawano, F., Jung, J.C., and Yazawa, M. (2017). Optimized light-inducible transcription in mammalian cells using Flavin Kelch-repeat F-box1/GIGANTEA and CRY2/CIB1. Nucleic Acids Res. 45, e172.

Salghetti, S.E., Muratani, M., Wijnen, H., Futcher, B., and Tansey, W.P. (2000). Functional overlap of sequences that activate transcription and signal ubiquitin-mediated proteolysis. Proc. Natl. Acad. Sci. U S A 97, 3118–3123.

Shimizu-Sato, S., Huq, E., Tepperman, J.M., and Quail, P.H. (2002). A light-switchable gene promoter system. Nat. Biotechnol. 20, 1041–1044.

Strickland, D., Lin, Y., Wagner, E., Hope, C.M., Zayner, J., Antoniou, C., Sosnick, T.R., Weiss, E.L., and Glotzer, M. (2012). TULIPs: tunable, light-controlled interacting protein tags for cell biology. Nat. Methods 9, 379–384.

Taslimi, A., Zoltowski, B., Miranda, J.G., Pathak, G.P., Hughes, R.M., and Tucker, C.L. (2016). Optimized second-generation CRY2-CIB dimerizers and photoactivatable Cre recombinase. Nat. Chem. Biol. 12, 425–430.

Voon, D.C., Subrata, L.S., Baltic, S., Leu, M.P., Whiteway, J.M., Wong, A., Knight, S.A., Christiansen, F.T., and Daly, J.M. (2005). Use of mRNA- and protein-destabilizing elements to develop a highly responsive reporter system. Nucleic Acids Res. 33, e27.

Wang, X., Chen, X., and Yang, Y. (2012). Spatiotemporal control of gene expression by a light-switchable transgene system. Nat. Methods 9, 266–269.

Wu, L., and Yang, H.Q. (2010). CRYPTOCHROME 1 is implicated in promoting R protein-mediated plant resistance to Pseudomonas syringae in Arabidopsis. Mol. Plant 3, 539–548.

Yamada, M., Suzuki, Y., Nagasaki, S.C., Okuno, H., and Imayoshi, I. (2018). Light control of the tet gene expression system in mammalian cells. Cell Rep. 25, 487–500.e6.

Yazawa, M., Sadaghiani, A.M., Hsueh, B., and Dolmetsch, R.E. (2009). Induction of protein-protein interactions in live cells using light. Nat. Biotechnol. 27, 941–945.

Supplemental Information

Optimization of Light-Inducible

Gal4/UAS Gene Expression

System in Mammalian Cells

Mayumi Yamada, Shinji C. Nagasaki, Yusuke Suzuki, Yukinori Hirano, and Itaru Imayoshi

Construct ID	Element #1		Element #2	Dark		Light		Light/Dark ratio	
	Gal4 DBD	Light-interacting protein	AD and light-interacting protein	Average	S.D.	Average	S.D.	Average	S.D.
Gal4 negative control - #1	short	–	p65 AD only	1.00	0.30	1.11	0.27	1.13	0.19
Gal4 negative control - #2	long	–	p65 AD only	6.32	1.21	7.08	0.21	1.15	0.23
Gal4 negative control - #3	short	–	NLSx2-p65 AD only	0.07	0.01	0.06	0.01	0.98	0.11
Gal4 negative control - #4	long	–	NLSx2-p65 AD only	0.15	0.01	0.17	0.02	1.17	0.20
Yeast PA-Gal4 - #1	long	CIBN	Gal4 AD-Cry2 PHR	0.16	0.03	0.19	0.00	1.21	0.21
Yeast PA-Gal4 - #2	long	Nano	Gal4 AD-iLID	0.99	0.13	0.80	0.11	0.82	0.16
GAVPO	Gal4 DBD short-VVD-p65 AD			7.94	1.90	27.51	2.35	3.56	0.59
No transfection	–	–	–	0.04	0.00	0.08	0.01	1.87	0.18
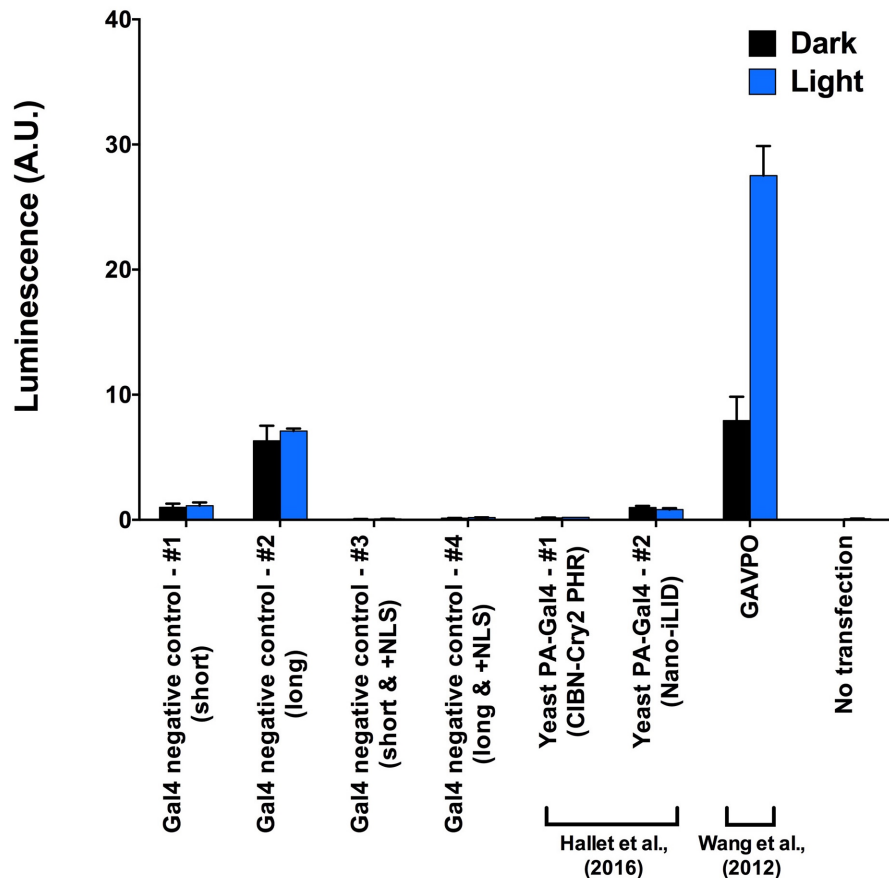
Figure S1. Evaluation of the photoactivable (PA)-Gal4 transcriptional activators developed in yeast cells, related to Figure 1. Two PA-Gal4 transcriptional activators, Yeast PA-Gal4-#1 and -#2 (Hallett et al., 2016), were transfected into HEK293T cells with the 5x UAS-Ub-NLS-luc2-Ascl1 3′ UTR reporter, and their light-dependent transcriptional activities were tested. The construct IDs, features of the construct, and the results of construct screening are shown. Each dataset consisted of three samples in the dark and three in the light. Luciferase assay data of the negative control-#1 in the dark were used for the correction of data of each construct. The data represent mean values ± standard deviation (s.d.) (n = 3).

Construct ID	Element #1		Element #2	Dark		Light		Light/Dark ratio	
	Gal4 DBD	Light-interacting protein	p65 AD and light-interacting protein	Average	S.D.	Average	S.D.	Average	S.D.
Negative control (short)	short	–	p65 AD only	1.00	0.00	1.01	0.35	1.05	0.38
Negative control (long)	long	–	p65 AD only	6.42	1.18	5.70	1.75	0.95	0.39
GAVPO		Gal4 DBD short-VVD-p65 AD		10.18	2.22	30.01	6.74	3.09	1.04
G1	short	CIB1 full	p65 AD-Cry2 PHR	0.84	0.14	5.68	1.61	6.73	1.13
G2	short	CIB1 full	p65 AD-Cry2 PHR (L348F)	0.67	0.16	3.61	1.28	5.59	2.18
G3	short	CIB1 full	p65 AD-Cry2 535	0.63	0.20	6.54	2.35	10.61	2.82
G4	short	CIB1 full	p65 AD-Cry2 535 (L348F)	1.01	0.28	3.97	1.32	4.02	0.40
G5	short	CIB1 full	NLSx2-p65 AD-Cry2PHR	0.89	0.28	3.05	1.08	3.43	0.89
G6	short	CIB1 full	NLSx2-p65 AD-Cry2 PHR (L348F)	0.74	0.13	1.75	0.63	2.43	0.40
G7	short	CIB1 full no NLS	p65 AD-Cry2 PHR	3.70	1.50	14.28	5.38	4.09	0.90
G8	short	CIB1 full no NLS	p65 AD-Cry2 PHR (L348F)	3.21	0.14	8.92	1.20	2.82	0.42
G9	short	CIB1 full no NLS	p65 AD-Cry2 535	2.11	0.76	11.80	5.20	6.13	2.58
G10	short	CIB1 full no NLS	p65 AD-Cry2 535 (L348F)	2.68	0.76	6.77	2.08	3.01	1.51
G11	short	CIB1 full no NLS	NLSx2-p65 AD-Cry2 PHR	4.02	2.97	10.93	7.02	3.40	1.98
G12	short	CIB1 full no NLS	NLSx2-p65 AD-Cry2 PHR (L348F)	2.64	0.94	6.70	2.39	2.80	0.91
G13	short	CIBN	p65 AD-Cry2 PHR	0.14	0.14	7.28	3.73	76.08	50.48
G14	short	CIBN	p65 AD-Cry2 PHR (L348F)	0.07	0.02	1.72	0.84	22.48	6.55
G15	short	CIBN	p65 AD-Cry2 535	0.09	0.08	7.60	5.71	94.55	56.12
G16	short	CIBN	p65 AD-Cry2 535 (L348F)	0.06	0.02	1.37	1.02	19.94	10.50
G17	short	CIBN	NLSx2-p65 AD-Cry2 PHR	0.35	0.37	6.23	3.05	30.96	26.90
G18	short	CIBN	NLSx2-p65 AD-Cry2 PHR (L348F)	0.15	0.08	1.85	1.14	12.54	5.45
G19	short	CIBN no NLS	p65 AD-Cry2 PHR	0.22	0.15	5.94	2.80	34.66	17.84
G20	short	CIBN no NLS	p65 AD-Cry2 PHR (L348F)	0.20	0.05	1.82	0.64	9.49	1.43
G21	short	CIBN no NLS	p65 AD-Cry2 535	0.16	0.06	5.14	2.21	32.62	0.69
G22	short	CIBN no NLS	p65 AD-Cry2 535 (L348F)	0.23	0.08	1.21	0.28	5.52	0.70
G23	short	CIBN no NLS	NLSx2-p65 AD-Cry2 PHR	1.31	1.03	8.98	1.65	9.42	4.80
G24	short	CIBN no NLS	NLSx2-p65 AD-Cry2 PHR (L348F)	0.73	0.28	2.56	0.69	3.80	0.60
G25	short	CIB81	p65 AD-Cry2 PHR	0.99	0.18	9.14	1.50	9.70	1.96
G26	short	CIB81	p65 AD-Cry2 PHR (L348F)	0.88	0.39	3.92	1.63	4.64	0.32
G27	short	CIB81	p65 AD-Cry2 535	0.44	0.18	8.11	1.31	21.24	8.33
G28	short	CIB81	p65 AD-Cry2 535 (L348F)	0.62	0.37	3.68	1.72	6.79	1.83
G29	short	CIB81	NLSx2-p65 AD-Cry2 PHR	4.73	2.00	22.19	2.32	5.23	1.70
G30	short	CIB81	NLSx2-p65 AD-Cry2 PHR (L348F)	1.95	0.72	9.34	2.70	5.04	0.76
No transfection	–	–	–	0.03	0.01	0.03	0.01	1.11	0.19
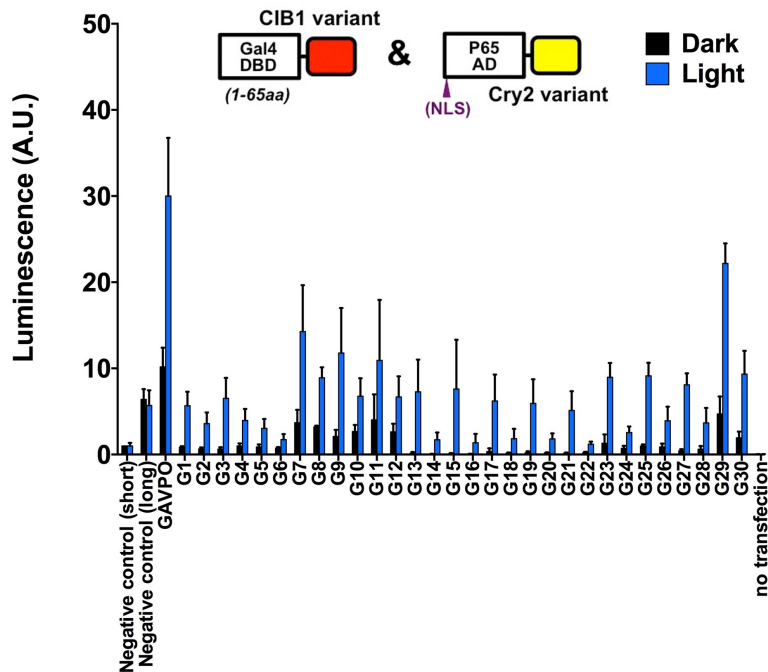
Figure S2. Functional screening of PA-Gal4cc transcriptional activators with the Gal4 DNA-binding domain (DBD) (short)-CIB1 fusion and p65-Cry2 C-terminal fusion constructs, related to Figure 1. PA-Gal4cc candidate constructs with the 5x UAS-Ub-NLS-luc2-Ascl1 3′ UTR reporter were transfected into HEK293T cells, and their light-dependent transcriptional activities were assayed. The Gal4 DBD (short, 1–65)-CIB1 variant fusion and p65 activation domain (AD)-Cry2 variant C-terminal fusion constructs were tested. The construct IDs, features of the construct, and the results of construct screening are shown. Each dataset consisted of three samples in the dark and three in the light, and the experiments were repeated three times. Luciferase assay data of the negative control (short) in the dark were used for the correction of data of each construct. The data in the table and bar graph represent mean values ± s.d. (n = 9) from three independent experiments; Each experiment consisted of three replicates. The experimental conditions are the same in Figures S2-S13.

Construct ID	Element #1		Element #2	Dark		Light		Light/Dark ratio	
	Gal4 DBD	Light-interacting protein	p65 AD and light-interacting protein	Average	S.D.	Average	S.D.	Average	S.D.
Negative control (short)	short	–	p65 AD only	1.0	0.1	1.0	0.1	1.0	0.1
Negative control (long)	long	–	p65 AD only	6.6	1.1	4.4	0.0	0.7	0.1
GAVPO		Gal4 DBD short-VVD-p65 AD		9.9	1.2	24.0	7.1	2.4	0.5
G31	long	CIB1 full	p65 AD-Cry2 PHR	0.5	0.0	0.5	0.1	0.9	0.2
G32	long	CIB1 full	p65 AD-Cry2 PHR (L348F)	0.4	0.1	0.3	0.0	0.7	0.1
G33	long	CIB1 full	p65 AD-Cry2 535	0.5	0.1	0.4	0.1	0.8	0.1
G34	long	CIB1 full	p65 AD-Cry2 535 (L348F)	0.5	0.2	0.4	0.1	0.7	0.4
G35	long	CIB1 full	NLSx2-p65 AD-Cry 2PHR	0.6	0.1	0.5	0.2	0.8	0.4
G36	long	CIB1 full	NLSx2-p65 AD-Cry2 PHR (L348F)	0.5	0.1	0.4	0.1	0.9	0.4
G37	long	CIB1 full no NLS	p65 AD-Cry2 PHR	1.0	0.3	1.2	0.3	1.1	0.3
G38	long	CIB1 full no NLS	p65 AD-Cry2 PHR (L348F)	0.9	0.2	0.6	0.1	0.7	0.3
G39	long	CIB1 full no NLS	p65 AD-Cry2 535	1.1	0.3	0.9	0.2	0.8	0.5
G40	long	CIB1 full no NLS	p65 AD-Cry2 535 (L348F)	1.0	0.5	0.7	0.3	0.7	0.7
G41	long	CIB1 full no NLS	NLSx2-p65 AD-Cry2 PHR	1.7	0.6	1.5	0.6	0.9	0.6
G42	long	CIB1 full no NLS	NLSx2-p65 AD-Cry2 PHR (L348F)	1.7	0.3	1.0	0.2	0.6	0.2
G43	long	CIBN	p65 AD-Cry2 PHR	0.4	0.0	2.2	0.4	5.3	1.4
G44	long	CIBN	p65 AD-Cry2 PHR (L348F)	0.4	0.0	0.4	0.1	1.1	0.3
G45	long	CIBN	p65 AD-Cry2 535	0.3	0.0	1.7	0.8	4.8	2.5
G46	long	CIBN	p65 AD-Cry2 535 (L348F)	0.4	0.1	0.4	0.1	1.1	0.5
G47	long	CIBN	NLSx2-p65 AD-Cry2 PHR	0.5	0.1	0.5	0.1	1.1	0.6
G48	long	CIBN	NLSx2-p65 AD-Cry2 PHR (L348F)	0.6	0.1	0.3	0.0	0.5	0.1
G49	long	CIBN no NLS	p65 AD-Cry2 PHR	0.5	0.1	1.4	0.5	2.8	1.1
G50	long	CIBN no NLS	p65 AD-Cry2 PHR (L348F)	0.5	0.2	0.6	0.0	1.2	0.4
G51	long	CIBN no NLS	p65 AD-Cry2 535	0.5	0.0	1.2	0.3	2.7	0.5
G52	long	CIBN no NLS	p65 AD-Cry2 535 (L348F)	0.5	0.1	0.5	0.1	1.0	0.1
G53	long	CIBN no NLS	NLSx2-p65 AD-Cry2 PHR	1.1	0.2	3.3	0.3	2.9	0.7
G54	long	CIBN no NLS	NLSx2-p65 AD-Cry2 PHR (L348F)	0.7	0.3	0.5	0.1	0.7	0.1
G55	long	CIB81	p65 AD-Cry2 PHR	2.5	0.7	3.5	1.3	1.4	0.9
G56	long	CIB81	p65 AD-Cry2 PHR (L348F)	2.2	0.7	1.6	0.3	0.7	0.2
G57	long	CIB81	p65 AD-Cry2 535	2.3	0.6	4.6	1.8	2.0	0.9
G58	long	CIB81	p65 AD-Cry2 535 (L348F)	2.4	0.8	2.2	0.6	0.9	0.1
G59	long	CIB81	NLSx2-p65 AD-Cry2 PHR	2.5	0.5	3.5	2.0	1.4	0.5
G60	long	CIB81	NLSx2-p65 AD-Cry2 PHR (L348F)	2.1	0.2	2.0	0.9	1.0	0.5
No transfection	–	–	–	0.2	0.0	0.2	0.0	1.0	0.1
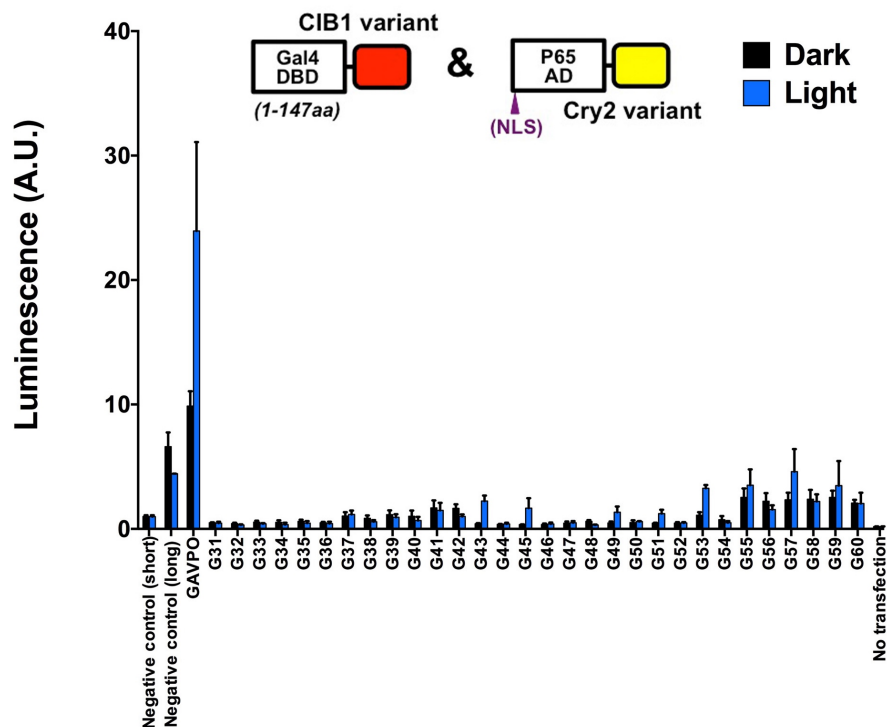
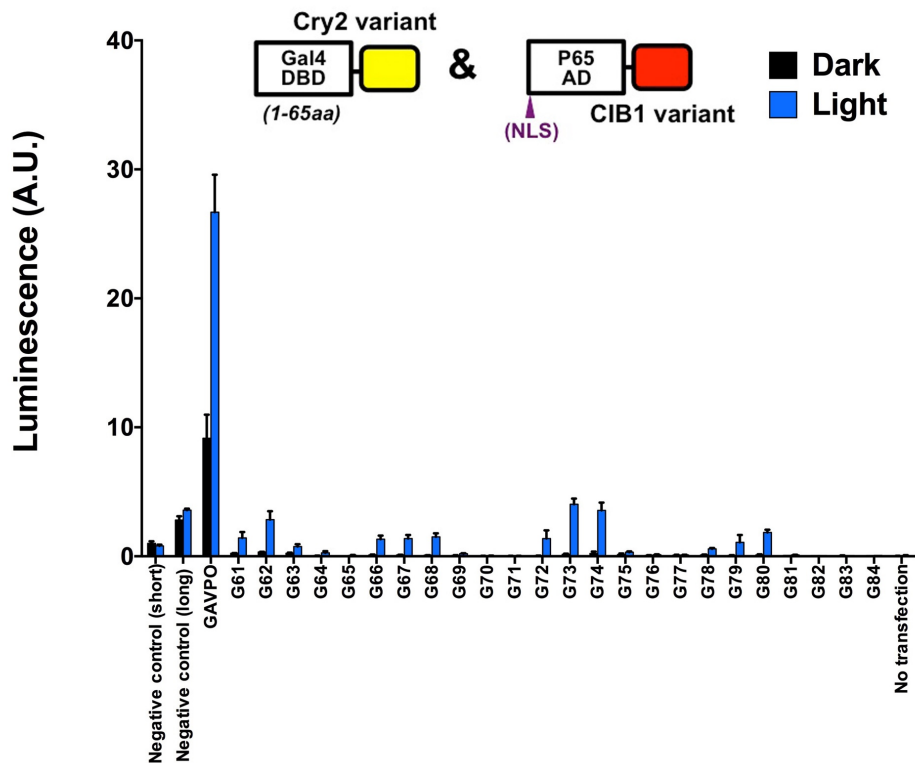**Figure S3. Functional screening of PA-Gal4cc transcriptional activators with the Gal4 DBD (long)-CIB1 fusion and p65-Cry2 C-terminal fusion constructs, related to Figure 1.** The Gal4 DBD (long, 1–147)-CIB1 variant fusion and p65 AD-Cry2 variant C-terminal fusion constructs were tested. The data represent mean values ± s.d. (n = 3).

| Construct ID	Element #1		Element #2	Dark		Light		Light/Dark ratio	
	Gal4 DBD	Light-interacting protein	p65 AD and light-interacting protein	Average	S.D.	Average	S.D.	Average	S.D.
Negative control (short)	short	–	p65 AD only	1.00	0.17	0.81	0.10	0.81	0.09
Negative control (long)	long	–	p65 AD only	2.82	0.29	3.58	0.11	1.28	0.12
GAVPO	Gal4 DBD short-VVD-p65 AD			9.15	1.84	26.69	2.90	2.96	0.44
G61	short	Cry2 PHR	p65 AD-CIB1 full	0.24	0.02	1.43	0.46	5.92	1.56
G62	short	Cry2 PHR	p65 AD-CIB1 full no NLS	0.33	0.02	2.84	0.66	8.53	2.03
G63	short	Cry2 PHR	p65 AD-CIBN	0.23	0.06	0.76	0.18	3.37	0.39
G64	short	Cry2 PHR	p65 AD-CIBN no NLS	0.05	0.01	0.28	0.13	5.48	2.07
G65	short	Cry2 PHR	NLSx2-p65 AD-CIBN no NLS	0.04	0.00	0.07	0.02	1.79	0.56
G66	short	Cry2 PHR	p65 AD-CIB81	0.11	0.03	1.33	0.27	12.13	2.68
G67	short	Cry2 PHR (L348F)	p65 AD-CIB1 full	0.10	0.02	1.38	0.28	14.32	4.37
G68	short	Cry2 PHR (L348F)	p65 AD-CIB1 full no NLS	0.09	0.01	1.50	0.28	17.94	4.81
G69	short	Cry2 PHR (L348F)	p65 AD-CIBN	0.07	0.01	0.20	0.03	2.85	0.85
G70	short	Cry2 PHR (L348F)	p65 AD-CIBN no NLS	0.03	0.01	0.04	0.01	1.33	0.12
G71	short	Cry2 PHR (L348F)	NLSx2-p65 AD-CIBN no NLS	0.03	0.00	0.04	0.01	1.13	0.13
G72	short	Cry2 PHR (L348F)	p65 AD-CIB81	0.05	0.00	1.38	0.64	26.47	12.97
G73	short	Cry2 535	p65 AD-CIB1 full	0.15	0.05	4.04	0.44	29.08	11.17
G74	short	Cry2 535	p65 AD-CIB1 full no NLS	0.22	0.15	3.56	0.60	20.41	10.07
G75	short	Cry2 535	p65 AD-CIBN	0.15	0.07	0.32	0.06	2.69	1.58
G76	short	Cry2 535	p65 AD-CIBN no NLS	0.08	0.02	0.13	0.03	1.56	0.16
G77	short	Cry2 535	NLSx2-p65 AD-CIBN no NLS	0.09	0.03	0.11	0.02	1.35	0.45
G78	short	Cry2 535	p65 AD-CIB81	0.11	0.02	0.57	0.08	5.08	0.19
G79	short	Cry2 535 (L348F)	p65 AD-CIB1 full	0.08	0.02	1.09	0.57	13.95	5.20
G80	short	Cry2 535 (L348F)	p65 AD-CIB1 full no NLS	0.11	0.04	1.85	0.21	18.07	4.89
G81	short	Cry2 535 (L348F)	p65 AD-CIBN	0.08	0.00	0.11	0.01	1.51	0.19
G82	short	Cry2 535 (L348F)	p65 AD-CIBN no NLS	0.06	0.00	0.06	0.01	1.02	0.07
G83	short	Cry2 535 (L348F)	NLSx2-p65 AD-CIBN no NLS	0.06	0.01	0.06	0.00	1.00	0.19
G84	short	Cry2 535 (L348F)	p65 AD-CIB81	0.06	0.00	0.08	0.00	1.44	0.14
No transfection	–	–	–	0.03	0.01	0.06	0.02	1.96	0.42

Figure S4. Functional screening of PA-Gal4cc transcriptional activators with the Gal4 DBD (short)-Cry2 fusion and p65-CIB1 C-terminal fusion constructs, related to Figure 1. The Gal4 DBD (short)-Cry2 variant fusion and p65 AD-CIB1 variant C-terminal fusion constructs were tested. The data represent mean values ± s.d. (n = 3).

Construct ID	Element #1		Element #2	Dark		Light		Light/Dark ratio	
	Gal4 DBD	Light-interacting protein	p65 AD and light-interacting protein	Average	S.D.	Average	S.D.	Average	S.D.
Negative control (short)	short	–	p65 AD only	1.00	0.24	1.38	0.33	1.40	0.30
Negative control (long)	long	–	p65 AD only	13.95	1.63	13.23	2.39	0.97	0.30
GAVPO	Gal4 DBD short-VVD-p65 AD			27.15	3.17	95.18	14.46	3.54	0.67
G85	long	Cry2 PHR	p65 AD-CIB1 full	3.00	0.31	15.46	4.27	5.29	2.07
G86	long	Cry2 PHR	p65 AD-CIB1 full no NLS	6.53	1.23	13.13	1.21	2.05	0.34
G87	long	Cry2 PHR	p65 AD-CIBN	2.84	0.62	7.04	2.35	2.56	0.91
G88	long	Cry2 PHR	p65 AD-CIBN no NLS	0.66	0.05	1.75	0.30	2.65	0.33
G89	long	Cry2 PHR	NLSx2-p65 AD-CIBN no NLS	0.31	0.03	0.85	0.16	2.77	0.79
G90	long	Cry2 PHR	p65 AD-CIB81	1.07	0.24	2.74	0.18	2.68	0.84
G91	long	Cry2 PHR (L348F)	p65 AD-CIB1 full	11.30	2.94	20.69	3.20	1.99	0.94
G92	long	Cry2 PHR (L348F)	p65 AD-CIB1 full no NLS	19.57	5.08	23.23	0.98	1.23	0.25
G93	long	Cry2 PHR (L348F)	p65 AD-CIBN	2.07	0.31	6.58	0.28	3.22	0.41
G94	long	Cry2 PHR (L348F)	p65 AD-CIBN no NLS	0.50	0.06	1.49	0.28	2.99	0.57
G95	long	Cry2 PHR (L348F)	NLSx2-p65 AD-CIBN no NLS	0.28	0.06	0.59	0.09	2.14	0.18
G96	long	Cry2 PHR (L348F)	p65 AD-CIB81	1.46	0.27	3.46	0.60	2.49	0.96
G97	long	Cry2 535	p65 AD-CIB1 full	0.78	0.20	1.32	0.43	1.68	0.10
G98	long	Cry2 535	p65 AD-CIB1 full no NLS	1.10	0.19	2.06	0.65	1.85	0.30
G99	long	Cry2 535	p65 AD-CIBN	0.43	0.04	0.57	0.15	1.34	0.27
G100	long	Cry2 535	p65 AD-CIBN no NLS	0.39	0.05	0.49	0.06	1.27	0.34
G101	long	Cry2 535	NLSx2-p65 AD-CIBN no NLS	0.32	0.06	0.29	0.05	0.92	0.02
G102	long	Cry2 535	p65 AD-CIB81	0.49	0.06	0.54	0.11	1.10	0.11
G103	long	Cry2 535 (L348F)	p65 AD-CIB1 full	0.37	0.08	0.98	0.31	2.67	0.59
G104	long	Cry2 535 (L348F)	p65 AD-CIB1 full no NLS	0.51	0.05	1.29	0.16	2.55	0.53
G105	long	Cry2 535 (L348F)	p65 AD-CIBN	0.27	0.05	0.33	0.09	1.21	0.37
G106	long	Cry2 535 (L348F)	p65 AD-CIBN no NLS	0.25	0.02	0.29	0.02	1.18	0.02
G107	long	Cry2 535 (L348F)	NLSx2-p65 AD-CIBN no NLS	0.22	0.02	0.25	0.03	1.14	0.13
G108	long	Cry2 535 (L348F)	p65 AD-CIB81	0.29	0.03	0.30	0.06	1.05	0.28
No transfection	–	–	–	0.13	0.02	0.21	0.07	1.58	0.23
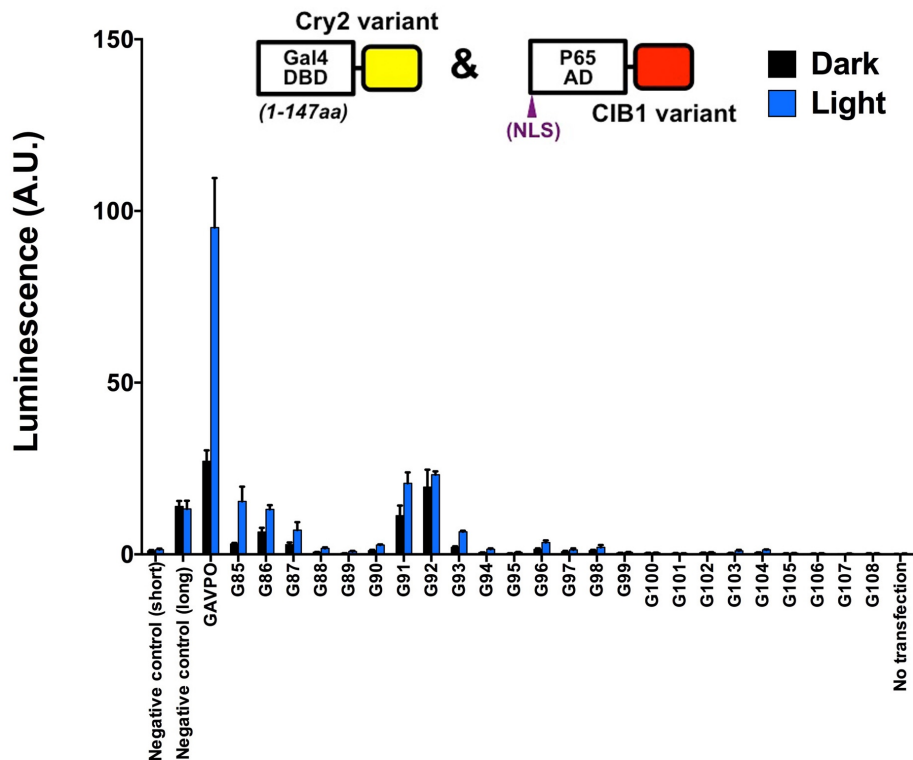
Figure S5. Functional screening of PA-Gal4cc transcriptional activators with the Gal4 DBD (long)-Cry2 fusion and p65-CIB1 C-terminal fusion constructs, related to Figure 1. The Gal4 DBD (long)-Cry2 variant fusion and p65 AD-CIB1 variant C-terminal fusion constructs were tested. The data represent mean values ± s.d. (n = 3).

Construct ID	Element #1		Element #2	Dark		Light		Light/Dark ratio	
	Gal4 DBD	Light-interacting protein	p65 AD and light-interacting protein	Average	S.D.	Average	S.D.	Average	S.D.
Negative control (short)	short	–	p65 AD only	1.00	0.00	0.93	0.20	0.94	0.20
Negative control (long)	long	–	p65 AD only	8.12	1.41	6.50	1.05	0.87	0.09
GAVPO			Gal4 DBD short-VVD-p65 AD	14.30	7.20	54.65	7.87	4.65	2.77
G109	short	CIB1 full	Cry2 PHR-p65 AD	2.82	0.60	10.13	1.79	3.95	0.34
G110	short	CIB1 full	Cry2 PHR (L348F)-p65 AD	1.26	0.44	19.49	11.86	15.25	4.44
G111	short	CIB1 full	Cry2 PHR-p65 AD-NLSx2	3.42	0.07	7.27	4.14	2.36	1.42
G112	short	CIB1 full	Cry2 PHR (L348F)-p65 AD-NLSx2	2.21	0.40	8.76	6.20	4.05	2.47
G113	short	CIB1 full no NLS	Cry2 PHR-p65 AD	8.87	2.01	25.13	5.42	2.89	0.07
G114	short	CIB1 full no NLS	Cry2 PHR (L348F)-p65 AD	4.21	0.50	34.90	2.25	8.90	0.40
G115	short	CIB1 full no NLS	Cry2 PHR-p65 AD-NLSx2	9.42	2.44	11.19	0.54	1.25	0.39
G116	short	CIB1 full no NLS	Cry2 PHR (L348F)-p65 AD-NLSx2	7.43	1.52	18.39	3.51	2.62	0.97
G117	short	CIBN	Cry2 PHR-p65 AD	1.06	0.44	13.18	4.37	14.97	10.73
G118	short	CIBN	Cry2 PHR (L348F)-p65 AD	0.39	0.08	21.03	8.16	52.77	11.27
G119	short	CIBN	Cry2 PHR-p65 AD-NLSx2	2.07	0.89	4.99	1.33	2.86	1.85
G120	short	CIBN	Cry2 PHR (L348F)-p65 AD-NLSx2	0.94	0.15	12.05	1.24	13.05	0.73
G121	short	CIBN no NLS	Cry2 PHR-p65 AD	1.40	0.87	11.60	2.94	11.27	8.94
G122	short	CIBN no NLS	Cry2 PHR (L348F)-p65 AD	1.15	0.68	28.36	2.13	30.36	16.25
G123	short	CIBN no NLS	Cry2 PHR-p65 AD-NLSx2	2.84	0.32	6.54	0.69	2.34	0.02
G124	short	CIBN no NLS	Cry2 PHR (L348F)-p65 AD-NLSx2	2.91	2.67	10.82	5.51	4.87	2.55
G125	short	CIB81	Cry2 PHR-p65 AD	2.38	0.02	9.73	0.80	4.09	0.37
G126	short	CIB81	Cry2 PHR (L348F)-p65 AD	0.90	0.35	10.90	3.82	12.47	0.83
G127	short	CIB81	Cry2 PHR-p65 AD-NLSx2	15.64	4.30	14.25	0.59	0.95	0.24
G128	short	CIB81	Cry2 PHR (L348F)-p65 AD-NLSx2	8.12	1.62	20.14	3.34	2.58	0.93
No transfection	–	–	–	0.14	0.08	0.17	0.05	1.36	0.45
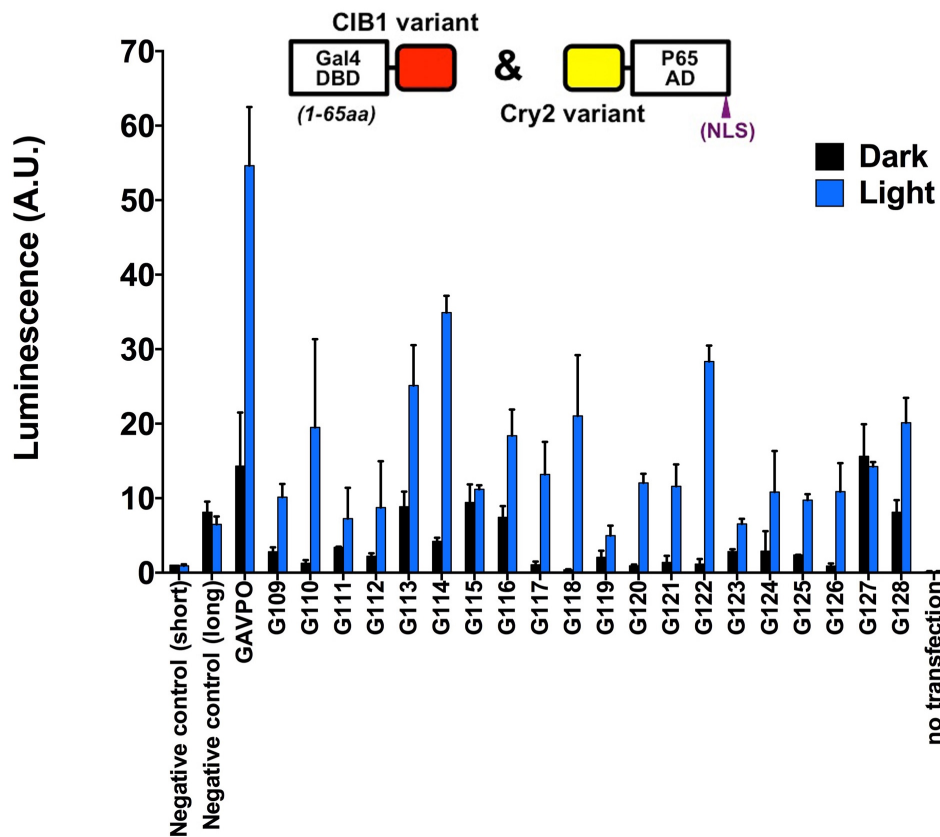
Figure S6. Functional screening of PA-Gal4cc transcriptional activators with the Gal4 DBD (short)-CIB1 fusion and Cry2-p65 N-terminal fusion constructs, related to Figure 1. The Gal4 DBD (short)-CIB1 variant fusion and CIB1 variant-p65 AD N-terminal fusion constructs were tested. The data in the table and bar graph represent mean values ± s.d. (n = 6) from three independent experiments; Each experiment consisted of duplicates.

| Construct ID	Element #1		Element #2	Dark		Light		Light/Dark ratio	
	Gal4 DBD	Light-interacting protein	p65 AD and light-interacting protein	Average	S.D.	Average	S.D.	Average	S.D.
Negative control (short)	short	–	p65 AD only	1.0	0.3	1.2	0.7	1.3	0.8
Negative control (long)	long	–	p65 AD only	8.1	4.2	9.3	3.1	1.5	1.2
GAVPO			Gal4 DBD short-VVD-p65 AD	17.9	4.0	85.7	50.4	5.3	4.0
G129	long	CIB1 full	Cry2 PHR-p65 AD	0.5	0.1	1.8	0.2	3.4	0.8
G130	long	CIB1 full	Cry2 PHR (L348F)-p65 AD	0.6	0.1	0.9	0.5	1.7	1.2
G131	long	CIB1 full	Cry2 PHR-p65 AD-NLSx2	0.7	0.1	1.2	0.9	1.9	1.8
G132	long	CIB1 full	Cry2 PHR (L348F)-p65 AD-NLSx2	0.5	0.1	2.0	1.4	4.7	4.5
G133	long	CIB1 full no NLS	Cry2 PHR-p65 AD	1.8	0.5	5.9	1.5	3.7	1.6
G134	long	CIB1 full no NLS	Cry2 PHR (L348F)-p65 AD	1.2	0.1	4.4	0.7	3.6	0.5
G135	long	CIB1 full no NLS	Cry2 PHR-p65 AD-NLSx2	2.8	0.2	2.9	0.7	1.0	0.3
G136	long	CIB1 full no NLS	Cry2 PHR (L348F)-p65 AD-NLSx2	2.1	0.6	2.4	1.2	1.1	0.3
G137	long	CIBN	Cry2 PHR-p65 AD	1.0	0.1	3.5	1.7	3.7	2.0
G138	long	CIBN	Cry2 PHR (L348F)-p65 AD	0.4	0.1	9.0	6.8	28.1	27.9
G139	long	CIBN	Cry2 PHR-p65 AD-NLSx2	1.9	0.5	13.8	5.4	7.6	3.4
G140	long	CIBN	Cry2 PHR (L348F)-p65 AD-NLSx2	0.8	0.3	13.9	8.0	17.5	10.7
G141	long	CIBN no NLS	Cry2 PHR-p65 AD	1.1	0.4	8.7	1.1	8.4	2.1
G142	long	CIBN no NLS	Cry2 PHR (L348F)-p65 AD	0.4	0.1	11.8	4.6	29.8	15.9
G143	long	CIBN no NLS	Cry2 PHR-p65 AD-NLSx2	2.8	1.4	15.6	3.8	6.1	2.6
G144	long	CIBN no NLS	Cry2 PHR (L348F)-p65 AD-NLSx2	0.6	0.3	8.6	3.5	17.3	8.0
G145	long	CIB81	Cry2 PHR-p65 AD	16.5	6.1	43.2	31.7	3.4	3.1
G146	long	CIB81	Cry2 PHR (L348F)-p65 AD	1.0	0.2	11.1	5.5	11.5	7.0
G147	long	CIB81	Cry2 PHR-p65 AD-NLSx2	10.8	3.1	15.4	7.0	1.4	0.6
G148	long	CIB81	Cry2 PHR (L348F)-p65 AD-NLSx2	2.0	0.6	5.8	3.3	3.5	2.9
No transfection	–	–	–	0.2	0.0	0.2	0.0	1.2	0.1
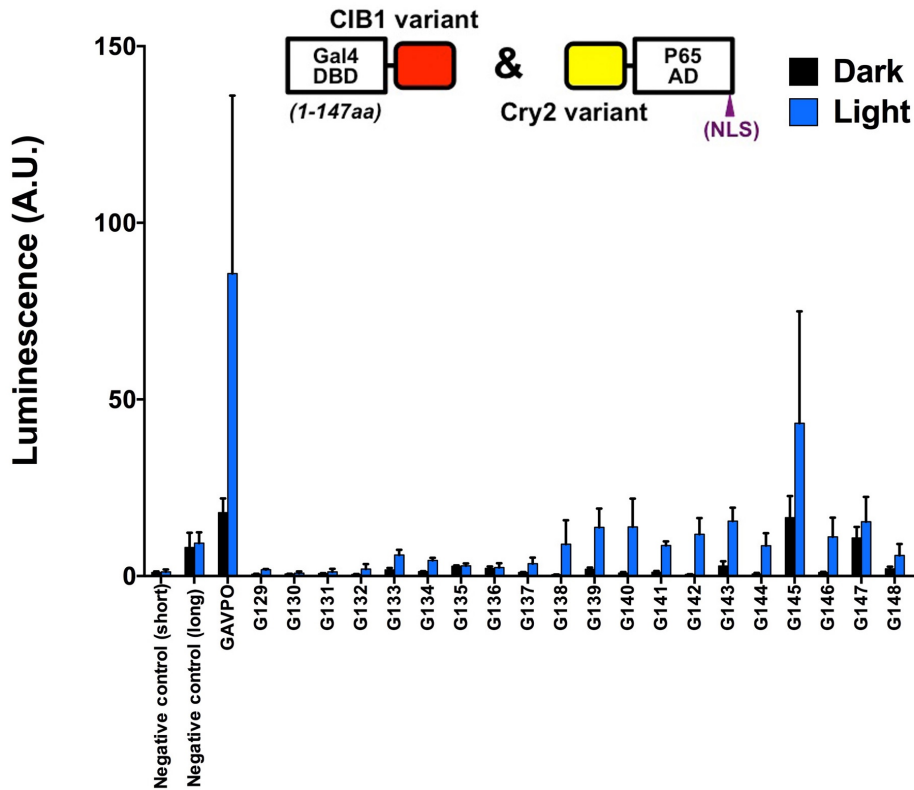
Figure S7. Functional screening of PA-Gal4cc transcriptional activators with the Gal4 DBD (long)-CIB1 fusion and Cry2-p65 N-terminal fusion constructs, related to Figure 1. The Gal4 DBD (long)-CIB1 variant fusion and Cry2 variant-p65 AD N-terminal fusion constructs were tested. The data represent mean values ± s.d. (n = 3).

Construct ID	Element #1		Element #2	Dark		Light		Light/Dark ratio	
	Gal4 DBD	Light-interacting protein	p65 AD and light-interacting protein	Average	S.D.	Average	S.D.	Average	S.D.
Negative control (short)	short	–	p65 AD only	1.00	0.00	0.90	0.32	0.91	0.33
Negative control (long)	long	–	p65 AD only	3.39	2.10	3.52	2.76	1.08	0.28
GAVPO	Gal4 DBD short-VVD-p65 AD			6.63	0.78	21.86	4.42	3.37	0.32
G149	short	Cry2 PHR	CIBN-p65 AD	1.43	0.93	6.03	2.88	4.81	1.58
G150	short	Cry2 PHR	CIBN no NLS-p65 AD	0.56	0.29	9.79	3.65	19.81	7.62
G151	short	Cry2 PHR	CIBN-p65 AD-NLSx2	0.43	0.16	0.69	0.18	1.65	0.25
G152	short	Cry2 PHR	CIBN no NLS-p65 AD-NLSx2	0.38	0.21	1.20	0.57	3.65	1.01
G153	short	Cry2 PHR (L348F)	CIBN-p65 AD	0.24	0.14	9.75	5.69	44.69	4.32
G154	short	Cry2 PHR (L348F)	CIBN no NLS-p65 AD	0.06	0.01	10.13	2.34	174.44	53.52
G155	short	Cry2 PHR (L348F)	CIBN-p65 AD-NLSx2	0.24	0.12	0.67	0.23	3.06	0.99
G156	short	Cry2 PHR (L348F)	CIBN no NLS-p65 AD-NLSx2	0.19	0.07	1.81	0.70	9.93	3.47
G157	short	Cry2 535	CIBN-p65 AD	0.92	0.55	5.57	2.05	7.33	3.46
G158	short	Cry2 535	CIBN no NLS-p65 AD	0.31	0.14	8.03	0.80	30.08	11.64
G159	short	Cry2 535	CIBN-p65 AD-NLSx2	0.43	0.22	0.72	0.23	1.87	0.58
G160	short	Cry2 535	CIBN no NLS-p65 AD-NLSx2	0.45	0.22	1.60	0.62	3.90	0.47
G161	short	Cry2 535 (L348F)	CIBN-p65 AD	0.28	0.16	5.24	3.02	20.67	7.74
G162	short	Cry2 535 (L348F)	CIBN no NLS-p65 AD	0.07	0.02	3.48	1.96	45.91	17.64
G163	short	Cry2 535 (L348F)	CIBN-p65 AD-NLSx2	0.29	0.17	0.56	0.25	2.22	0.64
G164	short	Cry2 535 (L348F)	CIBN no NLS-p65 AD-NLSx2	0.15	0.09	0.88	0.56	6.02	2.01
No transfection	–	–	–	0.02	0.01	0.02	0.01	0.96	0.08
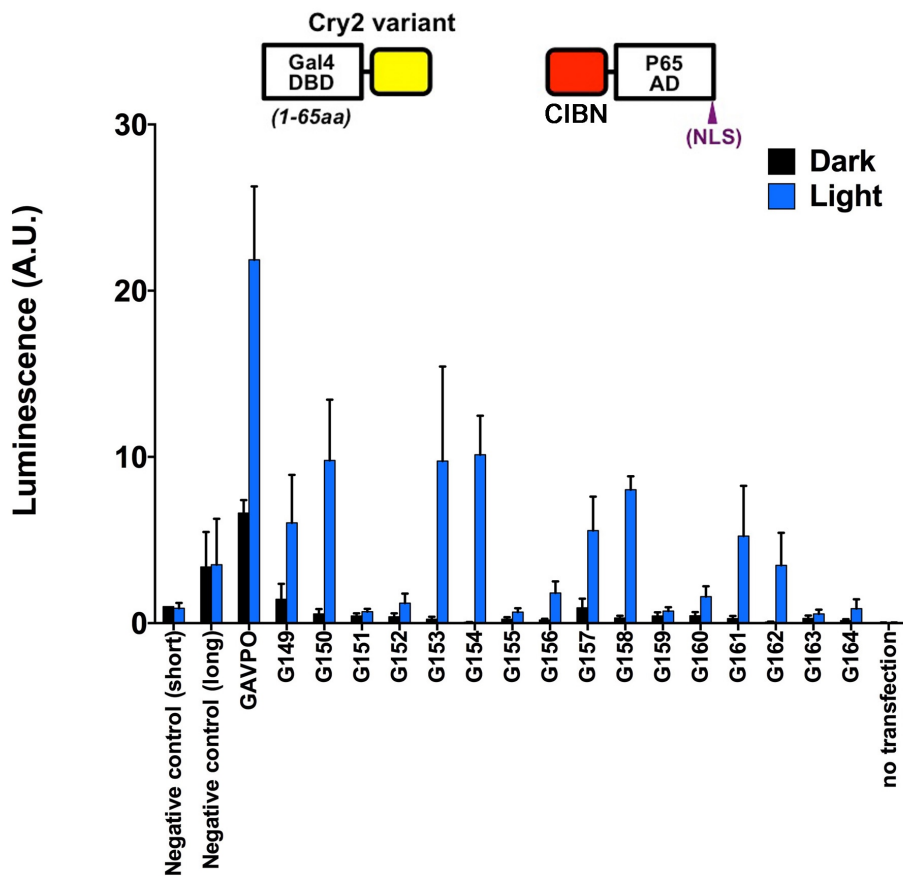
Figure S8. Functional screening of PA-Gal4cc transcriptional activators with the Gal4 DBD (short)-Cry2 fusion and CIBN-p65 N-terminal fusion constructs, related to Figure 1. The Gal4 DBD (short)-Cry2 variant fusion and CIBN-p65 AD N-terminal fusion constructs were tested. The data in the table and bar graph represent mean values ± s.d. (n = 9) from three independent experiments; Each experiment consisted of three replicates.

| Construct ID	Element #1		Element #2	Dark		Light		Light/Dark ratio	
	Gal4 DBD	Light-interacting protein	p65 AD and light-interacting protein	Average	S.D.	Average	S.D.	Average	S.D.
Negative control (short)	short	–	p65 AD only	1.0	0.2	0.9	0.1	0.9	0.2
Negative control (long)	long	–	p65 AD only	5.1	1.8	7.8	1.0	1.8	1.0
GAVPO	Gal4 DBD short-VVD-p65 AD			14.0	2.1	42.0	4.5	3.0	0.3
G165	long	Cry2 PHR	CIBN-p65 AD	4.3	0.6	10.7	2.4	2.5	0.8
G166	long	Cry2 PHR	CIBN no NLS-p65 AD	1.7	0.2	8.1	1.2	4.9	0.8
G167	long	Cry2 PHR	CIBN-p65 AD-NLSx2	2.7	0.3	3.6	0.3	1.3	0.0
G168	long	Cry2 PHR	CIBN no NLS-p65 AD-NLSx2	1.4	0.2	3.3	0.5	2.4	0.6
G169	long	Cry2 PHR (L348F)	CIBN-p65 AD	5.6	0.8	13.9	0.8	2.5	0.3
G170	long	Cry2 PHR (L348F)	CIBN no NLS-p65 AD	1.6	0.2	6.5	0.1	4.1	0.6
G171	long	Cry2 PHR (L348F)	CIBN-p65 AD-NLSx2	1.9	0.3	3.1	0.1	1.7	0.2
G172	long	Cry2 PHR (L348F)	CIBN no NLS-p65 AD-NLSx2	1.6	0.1	4.2	0.9	2.7	0.7
G173	long	Cry2 535	CIBN-p65 AD	0.8	0.2	3.7	0.6	5.0	1.9
G174	long	Cry2 535	CIBN no NLS-p65 AD	0.2	0.0	1.6	0.3	9.3	2.2
G175	long	Cry2 535	CIBN-p65 AD-NLSx2	0.7	0.1	1.2	1.0	1.7	1.3
G176	long	Cry2 535	CIBN no NLS-p65 AD-NLSx2	0.4	0.0	2.4	0.5	6.6	0.8
G177	long	Cry2 535 (L348F)	CIBN-p65 AD	0.5	0.1	2.9	0.1	6.4	1.6
G178	long	Cry2 535 (L348F)	CIBN no NLS-p65 AD	0.1	0.0	1.3	0.1	10.0	0.5
G179	long	Cry2 535 (L348F)	CIBN-p65 AD-NLSx2	0.4	0.1	0.9	0.1	2.3	0.6
G180	long	Cry2 535 (L348F)	CIBN no NLS-p65 AD-NLSx2	0.3	0.0	1.2	0.1	4.8	0.9
No transfection	–	–	–	0.1	0.0	0.1	0.0	1.0	0.0
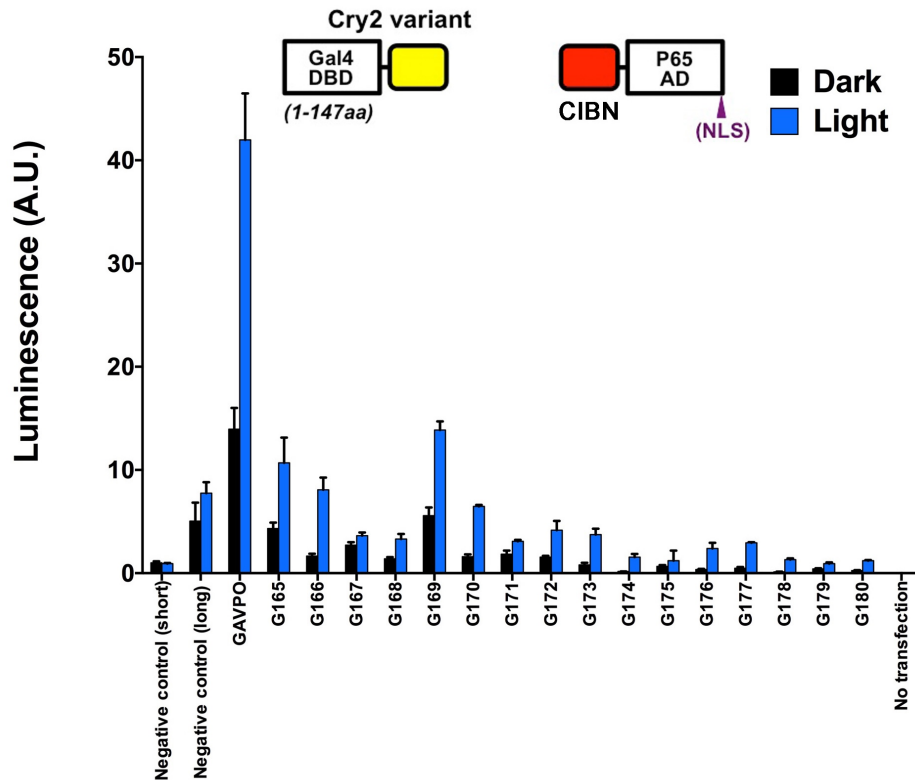
Figure S9. Functional screening of PA-Gal4cc transcriptional activators with the Gal4 DBD (long)-Cry2 fusion and CIBN-p65 N-terminal fusion constructs, related to Figure 1. The Gal4 DBD (long)-Cry2 variant fusion and CIBN-p65 AD N-terminal fusion constructs were tested. The data represent mean values ± s.d. (n = 3).

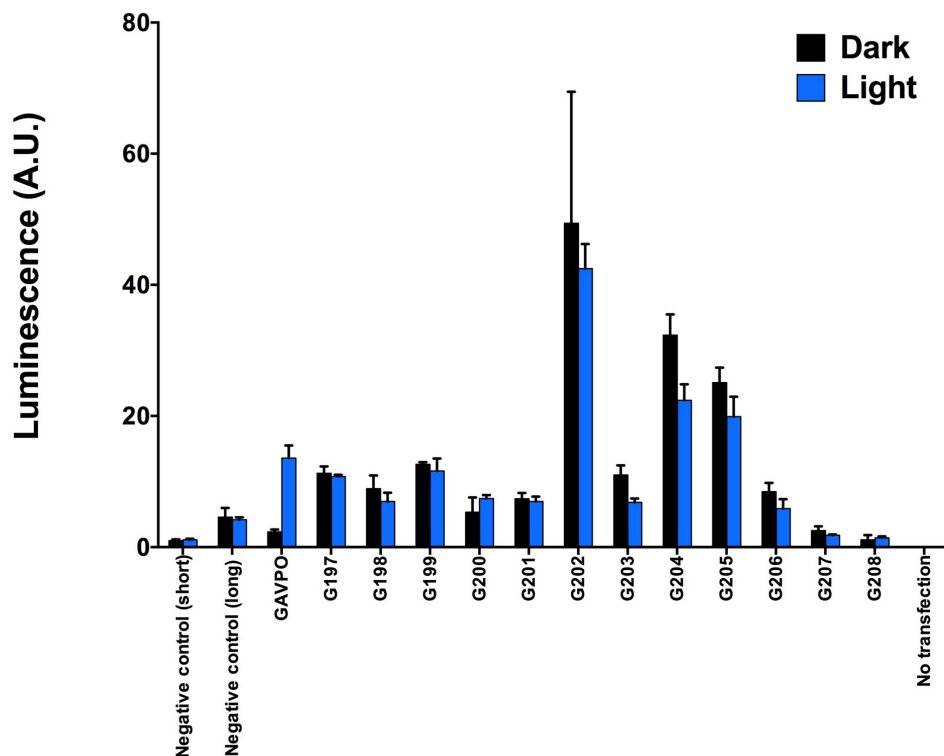| Construct ID	Element #1		Element #2	Dark		Light		Light/Dark ratio	
	Gal4 DBD	Light-interacting protein	p65 AD and light-interacting protein	Average	S.D.	Average	S.D.	Average	S.D.
Negative control (short)	short	–	p65 AD only	1.00	0.23	0.80	0.15	0.81	0.14
Negative control (long)	long	–	p65 AD only	7.34	1.85	7.55	0.84	1.06	0.22
GAVPO	Gal4 DBD short-VVD-p65 AD			9.82	3.83	22.68	2.85	2.59	1.09
G181	short	nMag	pMag-p65 AD	0.36	0.10	0.29	0.01	0.85	0.23
G182	long	nMag	pMag-p65 AD	4.03	0.22	2.88	0.56	0.71	0.12
G183	short	nMag	pMag-p65 AD_NLSx2	0.50	0.05	0.31	0.06	0.61	0.10
G184	long	nMag	pMag-p65 AD_NLSx2	0.29	0.04	0.26	0.03	0.92	0.17
G185	short	nMag High1	pMag High1-p65 AD	0.69	0.16	0.41	0.14	0.61	0.19
G186	long	nMag High1	pMag High1-p65 AD	0.64	0.04	1.30	0.19	2.03	0.36
G187	short	nMag High1	pMag High1-p65 AD_NLSx2	0.29	0.08	0.25	0.05	0.92	0.35
G188	long	nMag High1	pMag High1-p65 AD_NLSx2	0.36	0.02	2.03	0.61	5.63	2.02
No transfection	–	–	–	0.04	0.00	0.04	0.00	0.95	0.03
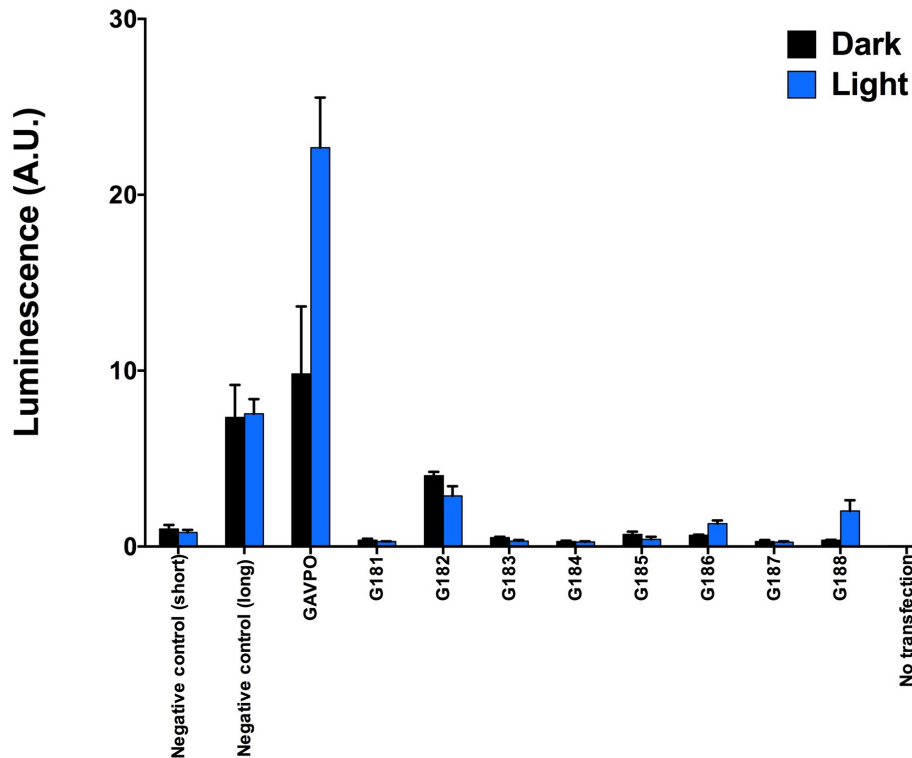
Figure S10. Functional screening of PA-Gal4cc transcriptional activators with the Magnet optical dimer formation system, related to Figure 1. The PA-Gal4 candidate constructs having Magnet photo-switches were tested. The data represent mean values ± s.d. (n = 3).

Construct ID	Element #1		Element #2	Dark		Light		Light/Dark ratio	
	Gal4 DBD	Light-interacting protein	p65 AD and light-interacting protein	Average	S.D.	Average	S.D.	Average	S.D.
Negative control (short)	short	–	p65 AD only	1.00	0.28	0.87	0.18	0.88	0.12
Negative control (long)	long	–	p65 AD only	4.84	1.79	5.18	0.39	1.17	0.42
GAVPO	Gal4 DBD short-VVD-p65 AD			3.72	1.01	17.40	1.35	4.86	1.08
G189	short	ePDZ	p65 AD-LOVpep	8.92	1.52	7.26	2.13	0.85	0.35
G190	short	ePDZ	p65 AD-LOVpep+	4.96	1.19	3.71	0.17	0.77	0.17
G191	long	ePDZ	p65 AD-LOVpep	3.37	0.29	2.33	0.19	0.69	0.07
G192	long	ePDZ	p65 AD-LOVpep+	2.38	0.46	1.95	0.62	0.81	0.12
G193	short	LOVpep	p65 AD-ePDZ	0.51	0.11	0.35	0.01	0.71	0.14
G194	long	LOVpep	p65 AD-ePDZ	1.95	0.62	1.83	0.18	1.03	0.41
G195	short	LOVpep+	p65 AD-ePDZ	0.40	0.04	0.34	0.04	0.87	0.21
G196	long	LOVpep+	p65 AD-ePDZ	2.46	0.17	1.72	0.15	0.70	0.01
No transfection	–	–	–	0.03	0.00	0.03	0.00	0.92	0.08
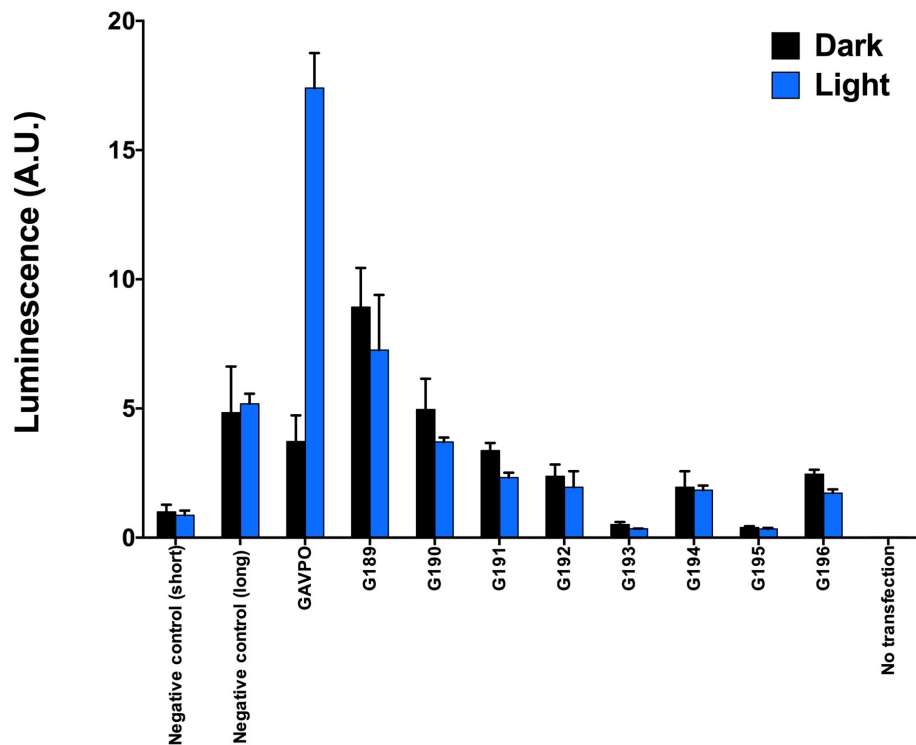
Figure S11. Functional screening of PA-Gal4cc transcriptional activators with the TULIPs optical dimer formation system, related to Figure 1. The PA-Gal4 candidate constructs having TULIPs photo-switches were tested. The data represent mean values ± s.d. (n = 3).

Construct ID	Element #1		Element #2	Dark		Light		Light/Dark ratio	
	Gal4 DBD	Light-interacting protein	p65 AD and light-interacting protein	Average	S.D.	Average	S.D.	Average	S.D.
Negative control (short)	short	–	p65 AD only	1.00	0.18	1.11	0.16	1.15	0.33
Negative control (long)	long	–	p65 AD only	4.59	1.41	4.18	0.38	0.97	0.31
GAVPO	Gal4 DBD short-VVD-p65 AD			2.32	0.38	13.59	1.91	6.07	1.92
G197	short	oLID	NLSx2-p65 AD-Nano	11.26	1.05	10.78	0.27	0.96	0.10
G198	long	oLID	NLSx2-p65 AD-Nano	8.93	2.01	6.97	1.33	0.83	0.32
G199	short	oLID	p65 AD-Micro	12.63	0.32	11.63	1.88	0.92	0.13
G200	long	oLID	p65 AD-Micro	5.32	2.28	7.43	0.50	1.66	0.96
G201	short	Nano	p65 AD-oLID	7.38	0.89	6.96	0.74	0.95	0.09
G202	long	Nano	p65 AD-oLID	49.39	20.07	42.49	3.73	0.96	0.35
G203	short	Micro	p65 AD-oLID	11.02	1.46	6.82	0.60	0.63	0.14
G204	long	Micro	p65 AD-oLID	32.33	3.18	22.40	2.42	0.69	0.05
G205	short	oLID	Nano-p65 AD	25.11	2.26	19.91	3.02	0.80	0.18
G206	long	oLID	Nano-p65 AD	8.47	1.34	5.88	1.44	0.72	0.29
G207	short	oLID	Nano-p65 AD-NLSx2	2.52	0.67	1.80	0.14	0.76	0.27
G208	long	oLID	Nano-p65 AD-NLSx2	1.14	0.72	1.42	0.22	1.73	1.33
No transfection	–	–	–	0.05	0.01	0.04	0.01	0.89	0.07

Figure S12. Functional screening of PA-Gal4cc transcriptional activators with the oLID optical dimer formation system, related to Figure 1. The PA-Gal4 candidate constructs having oLID photo-switches were tested. The data represent mean values ± s.d. (n = 3).

| Construct ID	Element #1		Element #2	Dark		Light		Light/Dark ratio	
	Gal4 DBD	Light-interacting protein	p65 AD and light-interacting protein	Average	S.D.	Average	S.D.	Average	S.D.
Negative control (short)	short	–	p65 AD only	1.00	0.10	0.84	0.05	0.84	0.07
Negative control (long)	long	–	p65 AD only	4.49	0.43	3.73	0.21	0.84	0.07
GAVPO	Gal4 DBD short-VVD-p65 AD			11.76	1.82	22.64	5.17	1.91	0.17
G209	short	iLID	NLSx2-p65 AD-Nano	31.91	1.04	17.49	7.44	0.54	0.22
G210	long	iLID	NLSx2-p65 AD-Nano	10.55	1.22	7.79	0.17	0.74	0.07
G211	short	iLID	p65 AD-Micro	36.01	2.32	21.77	3.18	0.61	0.12
G212	long	iLID	p65 AD-Micro	3.97	0.16	2.48	0.06	0.63	0.04
G213	short	Nano	p65 AD-iLID	14.68	5.71	9.66	5.29	0.64	0.14
G214	long	Nano	p65 AD-iLID	12.82	5.84	9.87	2.34	0.86	0.38
G215	short	Micro	p65 AD-iLID	8.49	1.52	6.82	1.89	0.84	0.35
G216	long	Micro	p65 AD-iLID	12.73	6.54	10.66	1.77	0.94	0.34
G217	short	iLID	Nano-p65 AD	80.13	13.40	65.13	10.64	0.85	0.30
G218	long	iLID	Nano-p65 AD	32.65	5.70	18.05	11.88	0.57	0.38
G219	short	iLID	Nano-p65 AD-NLSx2	6.91	1.73	2.93	2.44	0.37	0.30
G220	long	iLID	Nano-p65 AD-NLSx2	5.81	1.46	4.68	1.05	0.87	0.40
G221	short	Nano	iLID-p65 AD	4.27	1.10	3.51	1.06	0.82	0.14
G222	long	Nano	iLID-p65 AD	45.41	10.39	50.25	11.26	1.12	0.14
G223	short	Nano	iLID-p65 AD-NLSx2	0.49	0.04	0.39	0.07	0.81	0.21
G224	long	Nano	iLID-p65 AD-NLSx2	0.99	0.43	0.97	0.17	1.25	0.92
No transfection	–	–	–	0.06	0.03	0.10	0.01	1.95	0.91
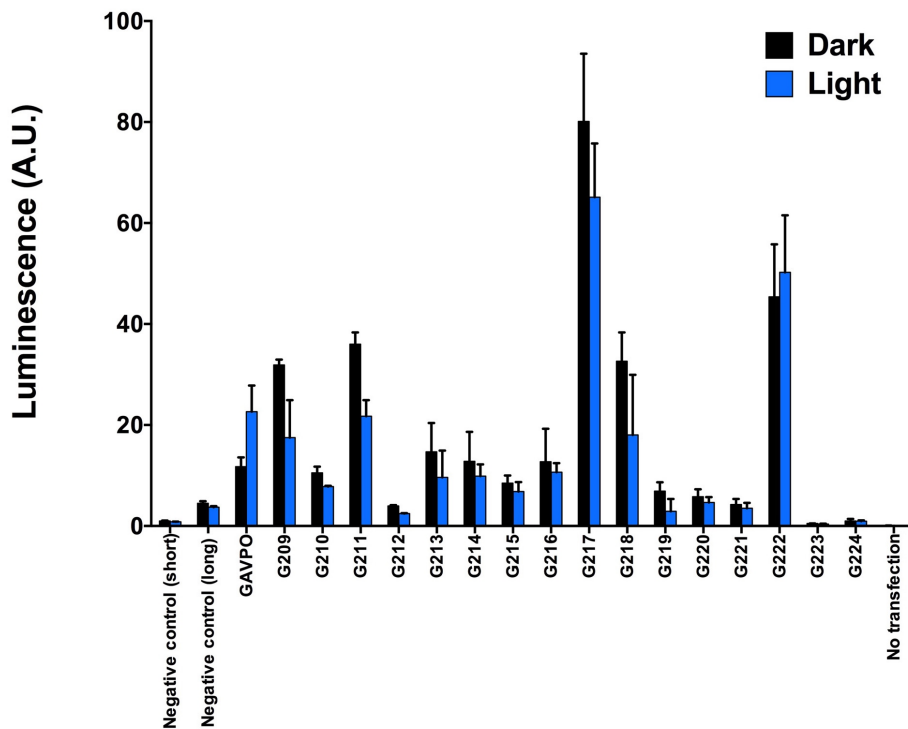
Figure S13. Functional screening of PA-Gal4cc transcriptional activators with the iLID optical dimer formation system, related to Figure 1. The PA-Gal4 candidate constructs having iLID photo-switches were tested. The data represent mean values ± s.d. (n = 3).
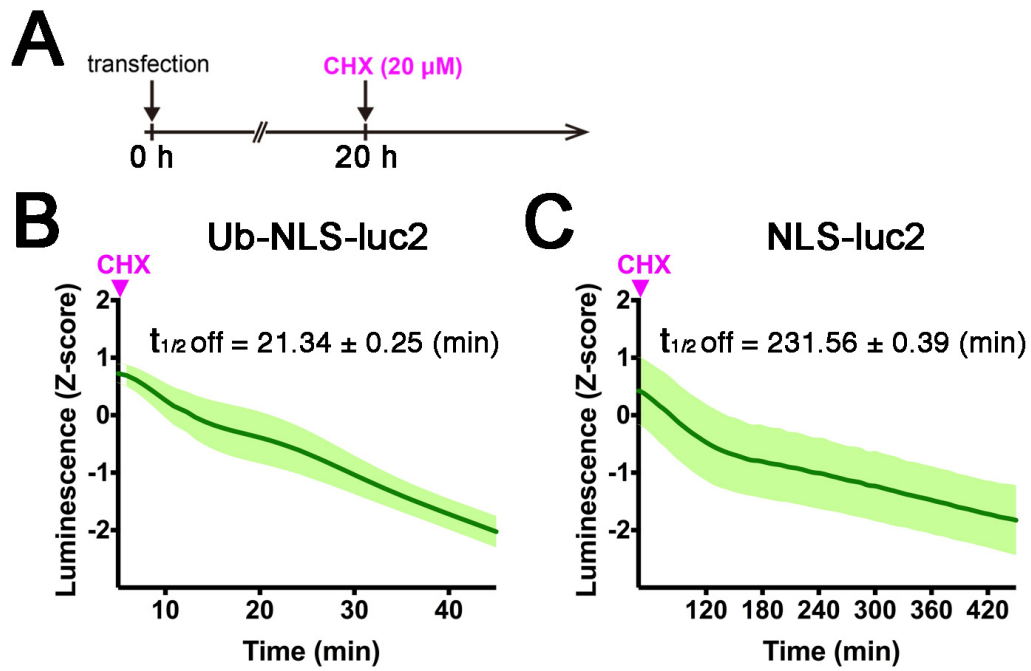
Figure S14. Characterization of the Ub-NLS-luc2 reporter, related to Figure 1. (**A**) Bioluminescence of HEK293T cells transiently transfected with Ub-NLS-luc2 (**B**) or NLS-luc2 (**C**) was measured in the presence of cycloheximide (CHX; 20 µM) (n = 19). Luminescence from Ub-NLS-luc2 and NLS-luc2 transfected cells was decreased with half-lives of ≈21.3 and 231.6 min, respectively. Their temporal changes of the reporter activity were transformed into z-scores to determine the half-lives of the reporter degradations. The data represent mean values ± s.d..

Constructs	Average	S.D.
Negative control 1: Gal4 DBD short & p65 AD (co-transfection)	1.00	0.00
Gal4 DBD short – p65 AD	373.20	108.45
Gal4 DBD short – VP16 AD	34.99	14.64
Gal4 DBD short – VP64 AD	0.85	0.18
Negative control 2: Gal4 DBD long & p65 AD (co-transfection)	0.88	0.63
Gal4 DBD long – p65 AD	91.82	13.29
Gal4 DBD long – VP16 AD	101.55	38.06
Gal4 DBD long – VP64 AD	132.38	20.14
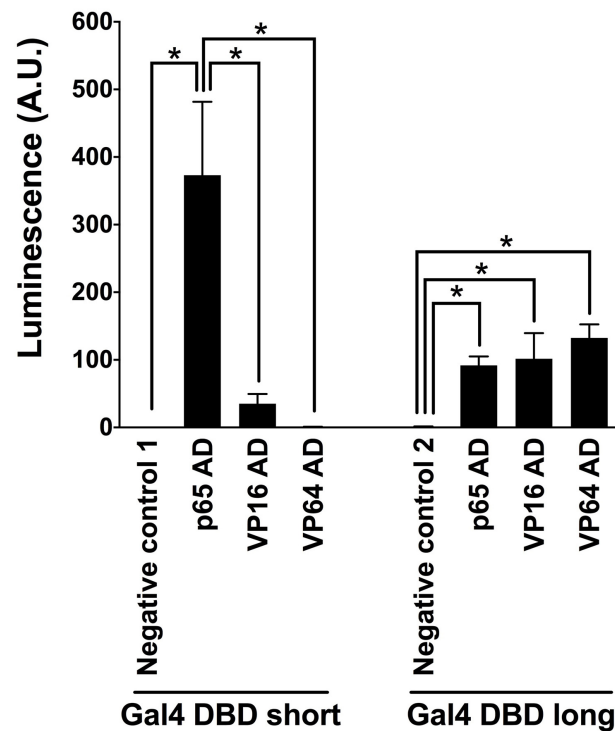
Figure S15. Comparison of p65, VP16 and VP64 transcription ADs, related to Figure 1. Three transcription activation domains (i.e. p65 AD, VP16 AD and VP64 AD) were directly fused to the short or long Gal4 DBDs. Transcription activity of these Gal4 transcription activators was tested in HEK293T cells with transient transfections. The pEF-Gal4 DBD short or long and pEF-p65 AD without any PA dimer formation molecules were co-transfected as the negative control. Luciferase assay data of the negative control 1 were used for the correction of data of each construct. The data in the table and bar graph represent mean values ± s.d. (n = 9) from three independent experiments; Each experiment consisted of three replicates. *$p < 0.05$; One-way ANOVA followed by Tukey's post hoc test.

A

Corresponding main figure panels	Total time for light illumination	Rank order of the degree of fold-activation (High to low)
Figure 2C	6 min	PA-Gal4cc-H, I, G, C, A, E, B, F, J, D
Figure 2F	48 min	PA-Gal4cc-H, I, G, A, C, E, B, J, F, D
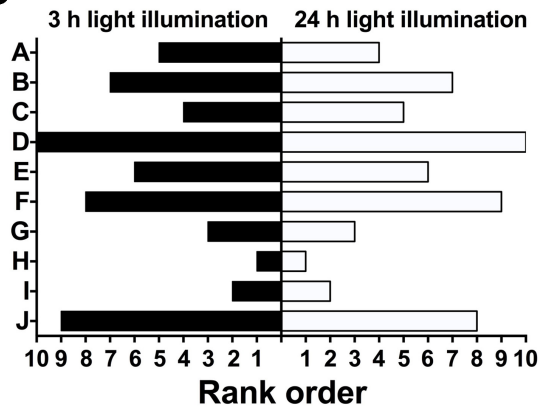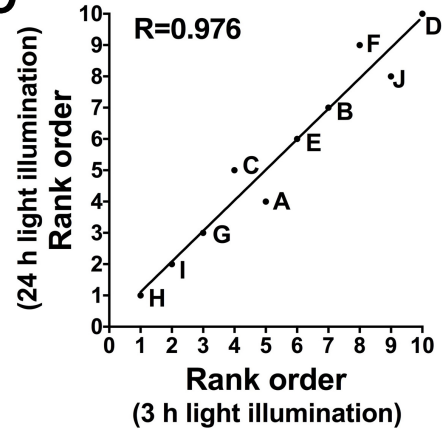
Figure S16. Summary for the effects of different light-illumination protocols on the light-induced gene expressions, related to Figure 2. (A-C) The rank order of the degree of fold-activation (light/dark ratio) of PA-Gal4cc constructs was compared between the 3-hr and 24-h blue-light exposures. The rank order was mostly preserved in the two different light illumination protocols.
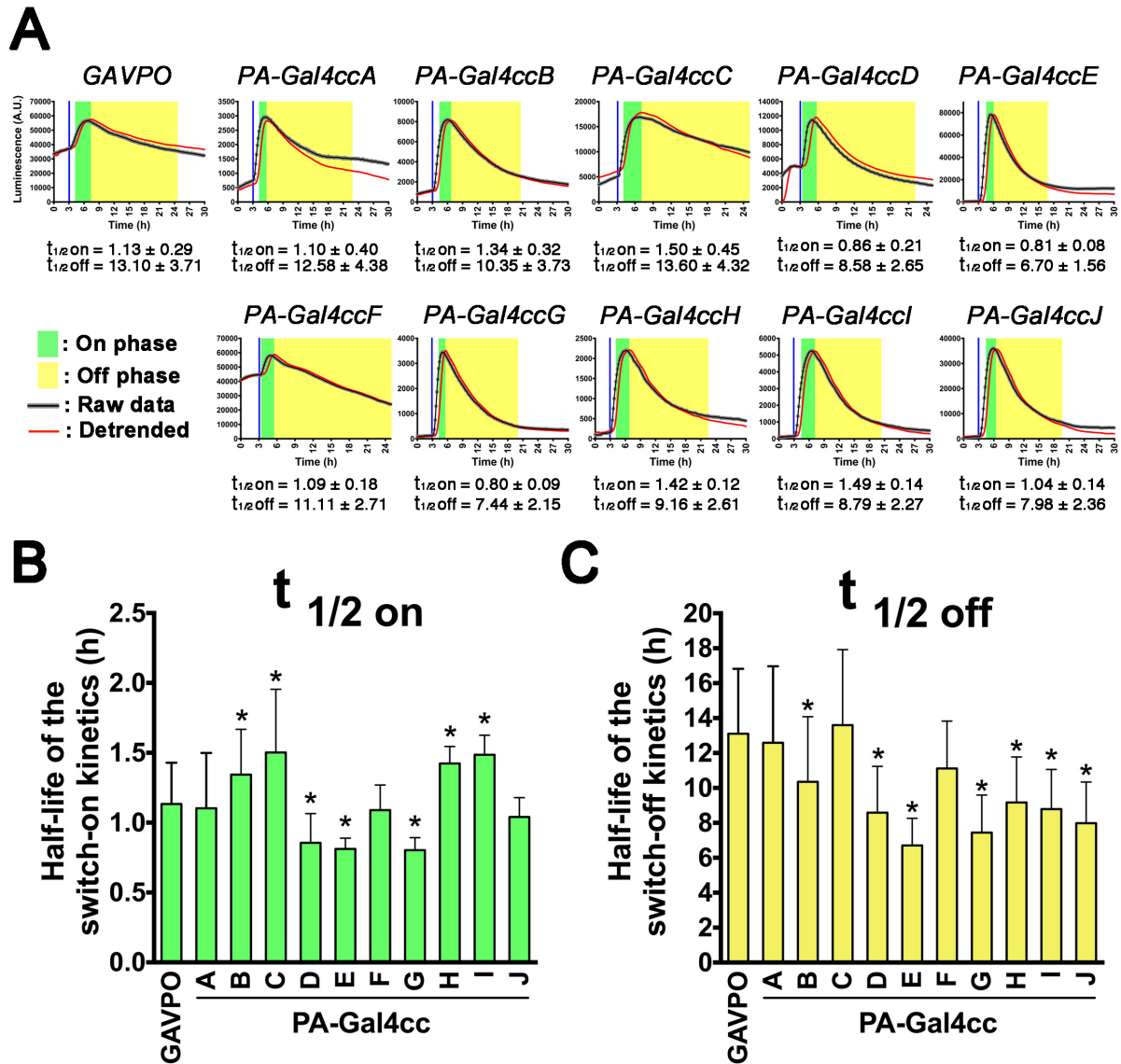
Figure S17. Temporal features of PA-Gal4cc-mediated transcription using the normal stable luciferase reporter, related to Figure 4. (**A**) HEK293T cells were transfected with the PA-Gal4cc constructs and 5x UAS-luc2-Hes1 3′ UTR reporter and exposed to a single blue light pulse. The timing of blue light exposure is indicated by vertical blue lines. The blue light was applied to cells 30 h after the transfection. The transcription On- and Off-phases are highlighted in *green* and *yellow*, respectively. (**B,C**) Using the single light pulse data set, kymograph analysis was used to determine the half-lives of the switch-on/off kinetics of the PA-Gal4cc transcriptional activators. The data represent mean ± s.d.. *$p < 0.05$; One-way ANOVA followed by Dunnett's post hoc test (GAVPO vs. each PA-Gal4cc). The rank order of the half-life of the switch-on/off kinetics between the PA-Gal4cc constructs was summarized in Figure S18.

A

Corresponding main figure panels	Transcription reporter	Rank order of half-life (Fast to slow)
Figure 4B	Ub-NLS-luc2	t1/2 on: PA-Gal4cc-J, G, E, D, H, C, B, A, F, I
Figure 4C		t1/2 off: PA-Gal4cc-G, E, D, J, I, H, B, F, C, A

B

Corresponding main figure panels	Transcription reporter	Rank order of half-life (Fast to slow)
Figure S17B	Normal luc2	t1/2 on: PA-Gal4cc-G, E, D, J, F, A, B, H, I, C
Figure S17C		t1/2 off: PA-Gal4cc-E, G, J, D, I, H, B, F, A, C
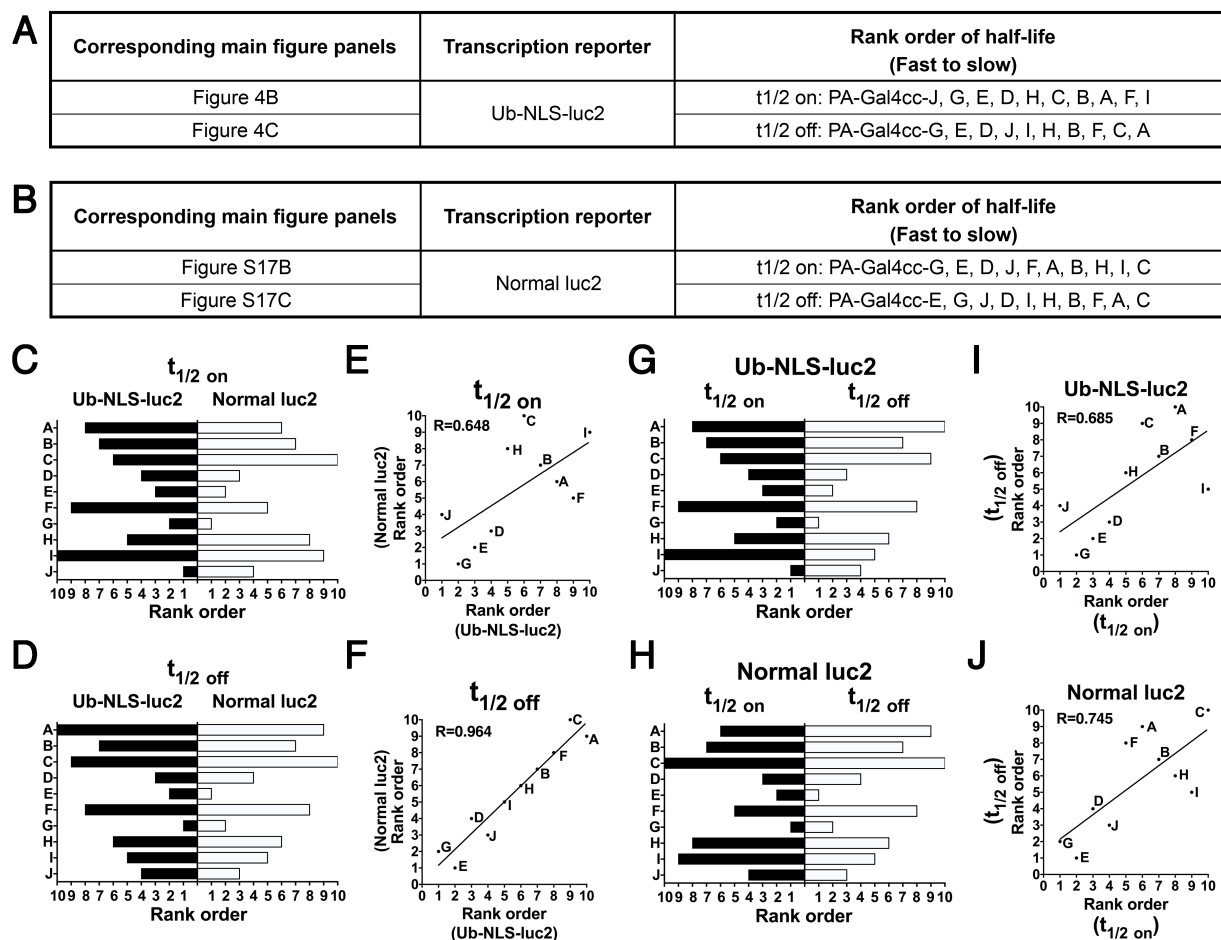
Figure S18. Summary for the rank orders of the switch-on/off kinetics of PA-Gal4cc constructs, related to Figures 4 and S17. (A-J) The rank orders of the switch-on/off kinetics of PA-Gal4cc in the two experiments with different reporters were summarized. Although the rank orders of the switch-off kinetics showed strong correlation (**D,F**), those of the switch-on kinetics were moderately preserved (**C,E**) between the experiments with the Ub-NLS-luc2 and normal luc2 reporters. The correlations of the rank orders of the switch-on/off kinetics of each PA-Gal4cc were compared in the experiments with the Ub-NLS-luc2 (**G,I**) and normal luc2 reporters (**H,J**). In the both cases, the switch-on/off kinetics of each PA-Gal4cc is positively correlated.
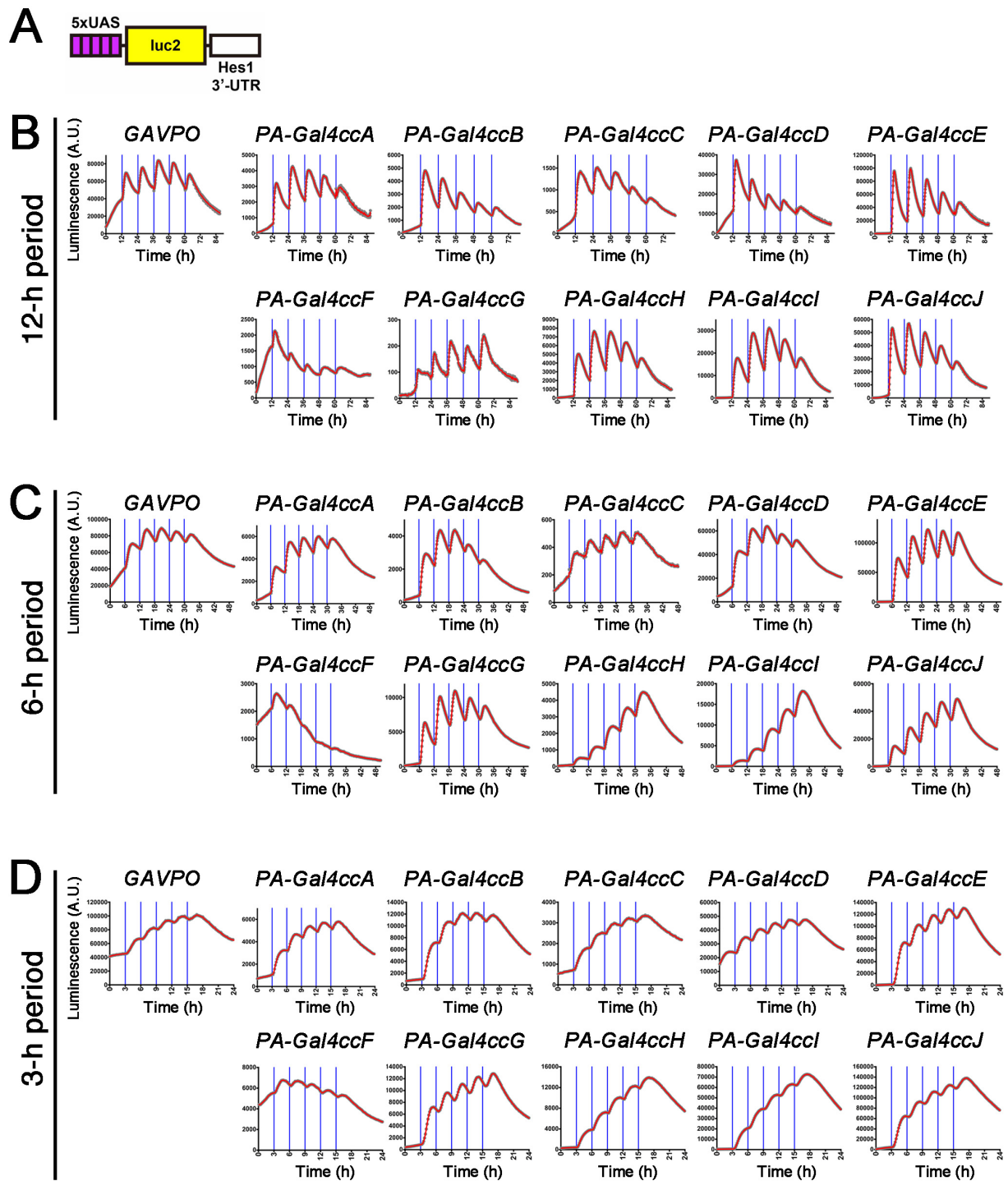
Figure S19. Periodic activation of PA-Gal4cc transcriptional activators with the normal stable luciferase reporter, related to Figure 5. (**A**) The reporter construct used in this experiment consisted of 5x UAS, normal stable luc2, and *Hes1* 3′ UTR sequences. (**B-D**) Transiently-transfected HEK293T cells, in which PA-Gal4cc and 5x UAS-luc2-Hes1 3′ UTR reporter had been introduced via lipofection, were repeatedly exposed to blue light pulses at 12 (**B**), 6 (**C**), or 3 h (**D**) intervals. The timing of blue light exposure is indicated by vertical blue lines. The first blue light illumination was initiated 24 h after the transfection. Experiments were repeated at least three times with similar results.
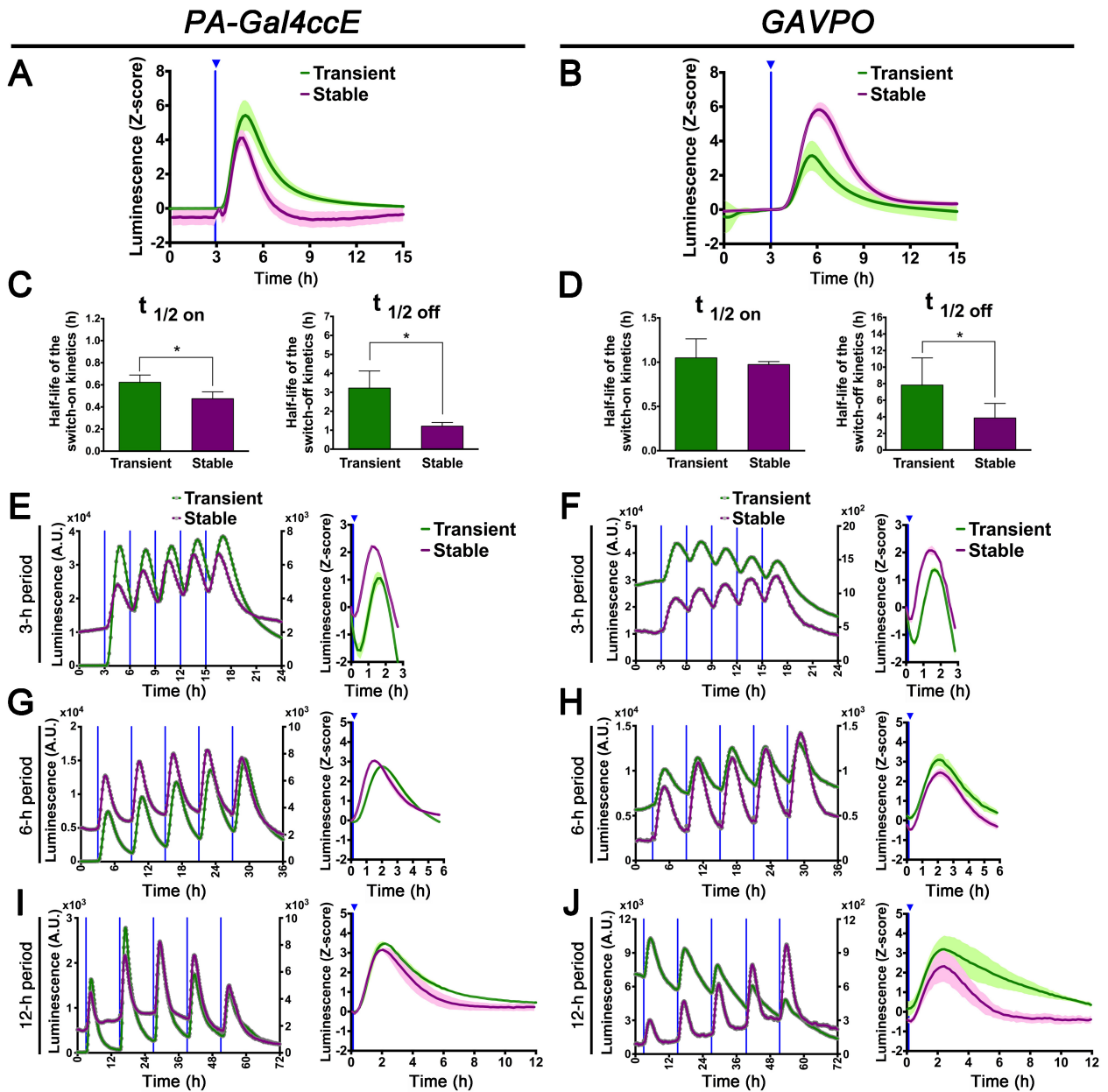
Figure S20. Comparison of temporal features of the PA-Gal4ccE and GAVPO between the transiently transfected and lentivirus-stably introduced conditions, related to Figures 4-6. (A-D) The PA-Gal4ccE or GAVPO transiently transfected- or lentiviral vector-transduced HEK293T cells were exposed to a single blue light pulse. Their temporal changes of the reporter activity were transformed into z-scores (see Transparent Methods). The half-lives of the switch-on/off kinetics of light-induced gene expression were determined and compared between the transiently transfected and lentivirus-stably introduced conditions. The data represent mean ± s.d. (PA-Gal4ccE: n = 23, GAVPO: n=32). *$p < 0.05$; two-tailed Student's t-test. **(E-J)** The PA-Gal4ccE or GAVPO introduced HEK293T cells were repeatedly exposed to blue light pulses at 3 **(E,F)**, 6 **(G,H)**, or 12 h **(I,J)** intervals. The temporal changes in the reporter activity of the second to fourth light-responses of each condition were extracted, transformed into z-scores, and displayed in the right panels. The data represent mean values ± s.d. (n = 3) The Step-2 PA-Gal4ccE cells of Figure S21 were used in these experiments.
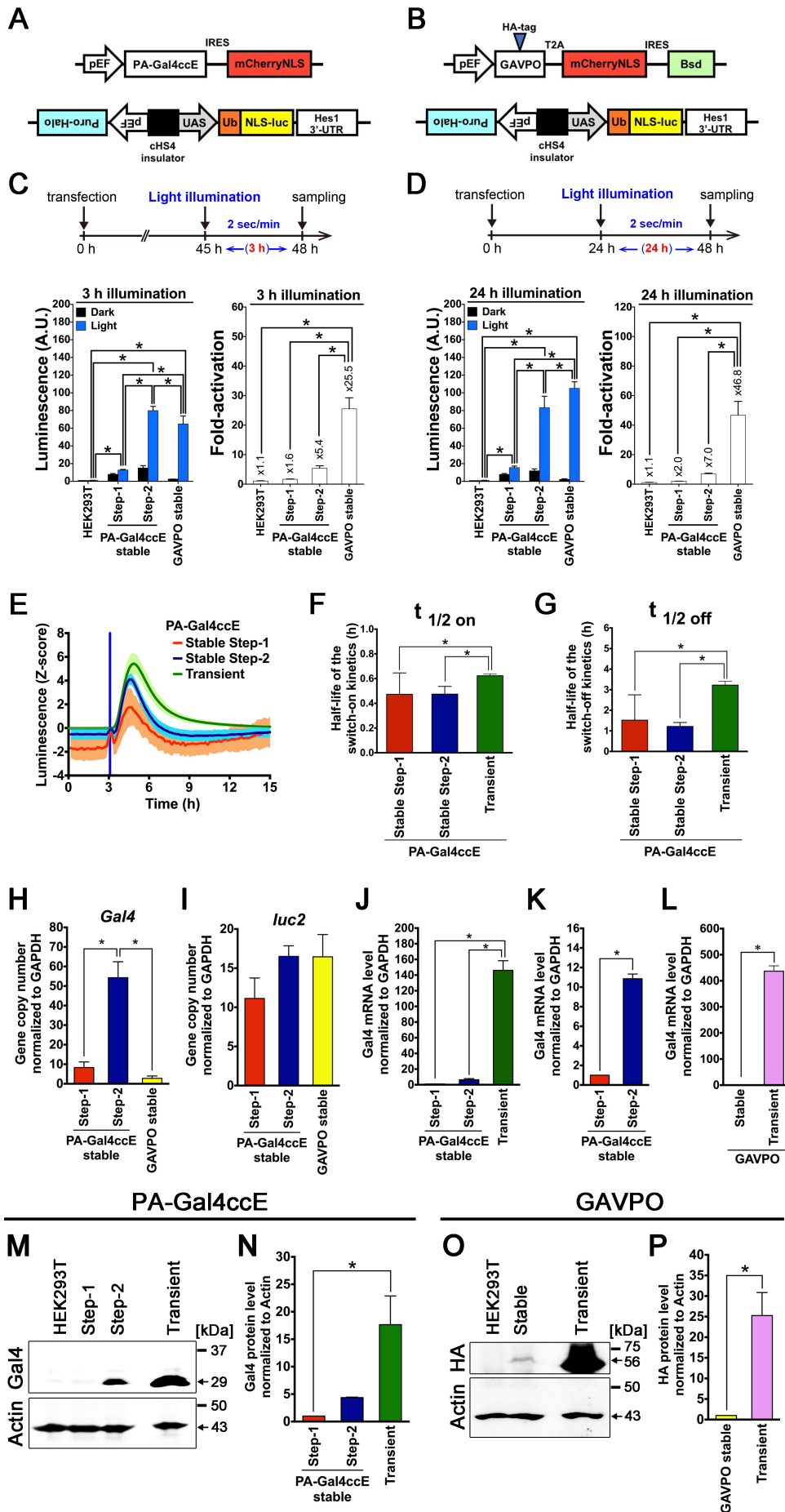
Figure S21. Detailed characterization of PA-Gal4ccE- or GAVPO-stably expressing cells with lentivirus vectors, related to Figures 4-6. (A,B) Schematic illustration of the lentivirus vectors expressing PA-Gal4ccE, GAVPO and the destabilized luciferase transcription reporter. (**A**) For the analysis of PA-Gal4ccE-stable cells, we tested cells at the two different selection steps. Step-1 cells are the stably transduced HEK293T cell population selected by antibiotics, puromycin. Step-2 cells were the further selected cell population from Step-1 cells by FACS. Step-2 cells expressed high-levels of transduction markers, mCherry and Halo-tag. (**B,D**) GAVPO-stable cells were generated by co-transduction of lentivirus vectors and selected by blasticidin and puromycin. (**C,D**) Comparison of the two different light exposure protocols to activate stably expressing PA-Gal4ccE and GAVPO. The illumination protocols used for the luciferase assay are indicated. Measured luciferase activities and fold-increase of luciferase activity (Light/Dark) are displayed. PA-Gal4ccE Step-2 cells and GAVPO cells, but not Step-1 cells, showed robust light-induced reporter expressions with the both light exposure protocols. The data represent mean values ± s.d. (n = 6) from three independent experiments. (**E-G**) Stably or transiently PA-Gal4ccE-introduced cells were exposed to a single blue light pulse. Using the single light pulse data set, kymograph analysis was used to determine the half-lives of the switch-on/off kinetics of light-induced gene expression (Step-1: n = 6, Step-2: n = 11, Transient: n = 23). (**H,I**) The genomic copy numbers of integrated lentivirus vectors were assayed by quantitative PCR. The copy number of Gal4 DBD sequence (**H**) and reporter luc2 (**I**) sequence was determined in the PA-Gal4ccE Step-1,2 and GAVPO cells (n = 4). (**J-L**) The mRNA expression levels of PA-Gal4ccE (**J,K**) and GAVPO (**L**) were determined by RT-qPCR. For comparison, the transiently transfected cells with the PA-Gal4ccE or GAVPO expression plasmid vectors were also subjected to the RT-qPCR analysis. The independent samples of PA-Gal4ccE Step-1 and Step-2 cells were also compared (**K**) (n = 12 in **J**, n = 8 in **K**, n = 12 in **L**). (**M-P**) The protein expression levels of PA-Gal4ccE (**M,N**) and GAVPO (**O,P**) were determined by western blotting. For comparison, the transiently transfected cells with the PA-Gal4ccE or GAVPO expression plasmid vectors were also subjected to the western blotting analysis (n = 3 in **N** and **P**). The data represent mean ± s.d.. *$p < 0.05$; One-way ANOVA followed by Tukey's post hoc test in **C,D,F,G,H,I,J,N**. Two-tailed Student's t-test in **K,L,P**.
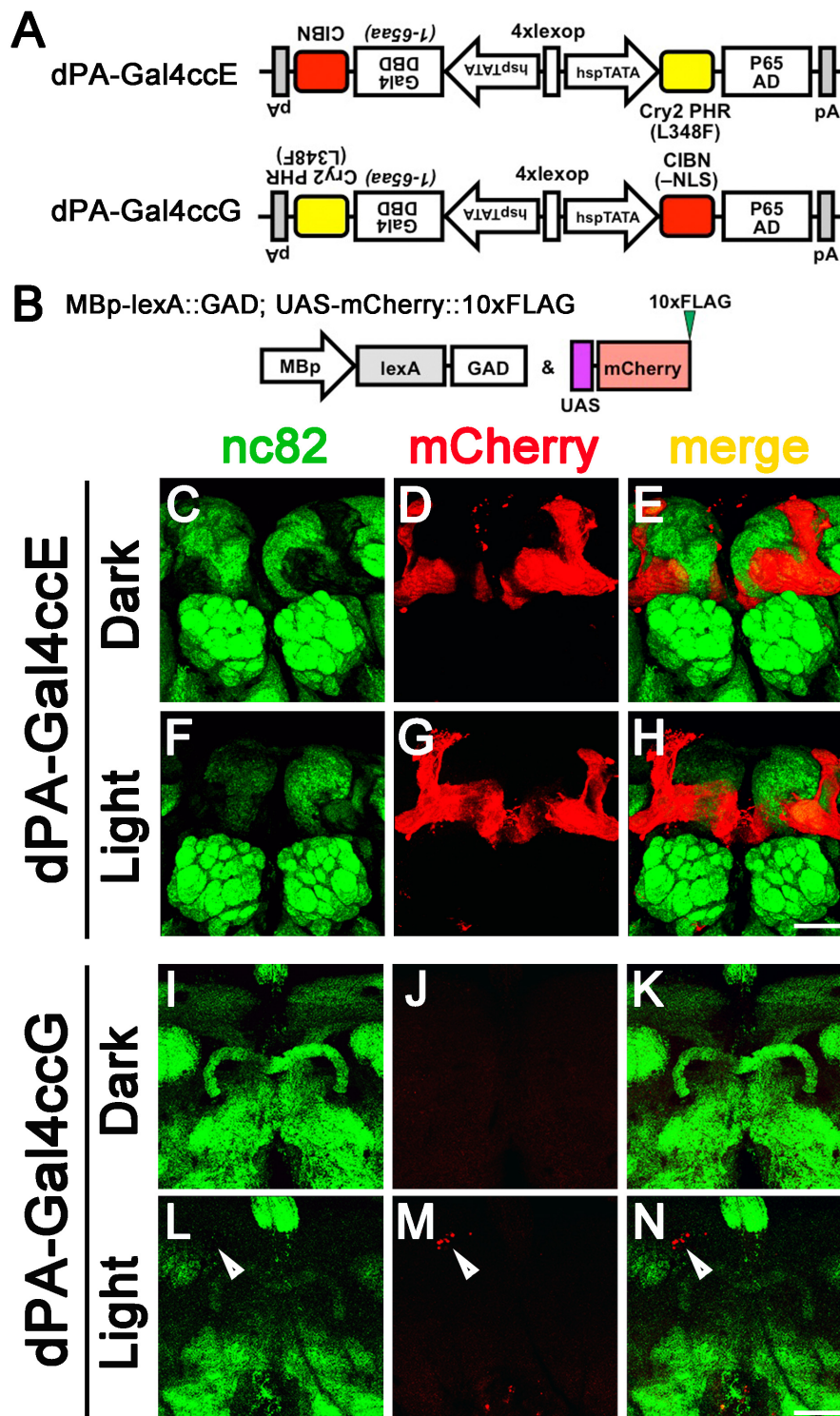
Figure S22. Generation of transgenic flies specifically expressing *Drosophila*-codon optimized PA-Gal4ccE and G in mushroom body neurons, related to Discussion. (**A**) Schematic illustration of the transgenic constructs expressing *Drosophila*-codon optimized PA-Gal4ccE and G (dPA-Gal4ccE and G) in mashroom body neurons. (**B**) These transgenic flies were crossed with a MBp-lexA::GAD; UAS-mCherry::10xFLAG reporter line. (**C-H**) In the PA-Gal4ccE-expressing flies, the expression of mCherry reporter was found independently from light illuminations. The nc82 monoclonal antibody was used to visualize neuropils. (**I-N**) In the PA-Gal4ccG-expressing flies, the light-induced mCherry expression was observed by the limited number of mashroom body neurons. Scale bars, 50 μm.

Construct ID	Element #1		Element #2	Dark		Light		Light/Dark ratio	
	Gal4 DBD	Light-interacting protein	p65 AD and light-interacting protein	Average	S.D.	Average	S.D.	Average	S.D.
Gal4 negative control - #1	short	–	p65 AD only	1.0	0.1	1.1	0.2	1.1	0.1
Gal4 negative control - #2	long	–	p65 AD only	2.6	0.7	2.3	0.3	0.9	0.4
dPA-Gal4ccE	short	CIBN	Cry2PHR (L348F)-p65 AD	14.2	0.5	35.4	6.6	2.5	0.4
dPA-Gal4ccG	short	Cry2PHR (L348F)	CIBN no NLS-p65 AD	1.5	0.3	4.5	0.9	3.1	1.0
GAVPO	Gal4 DBD short-VVD-p65 AD			1.5	0.2	1.5	0.2	1.1	0.3
No transfection	–	–	–	0.0	0.0	0.0	0.0	0.4	0.0
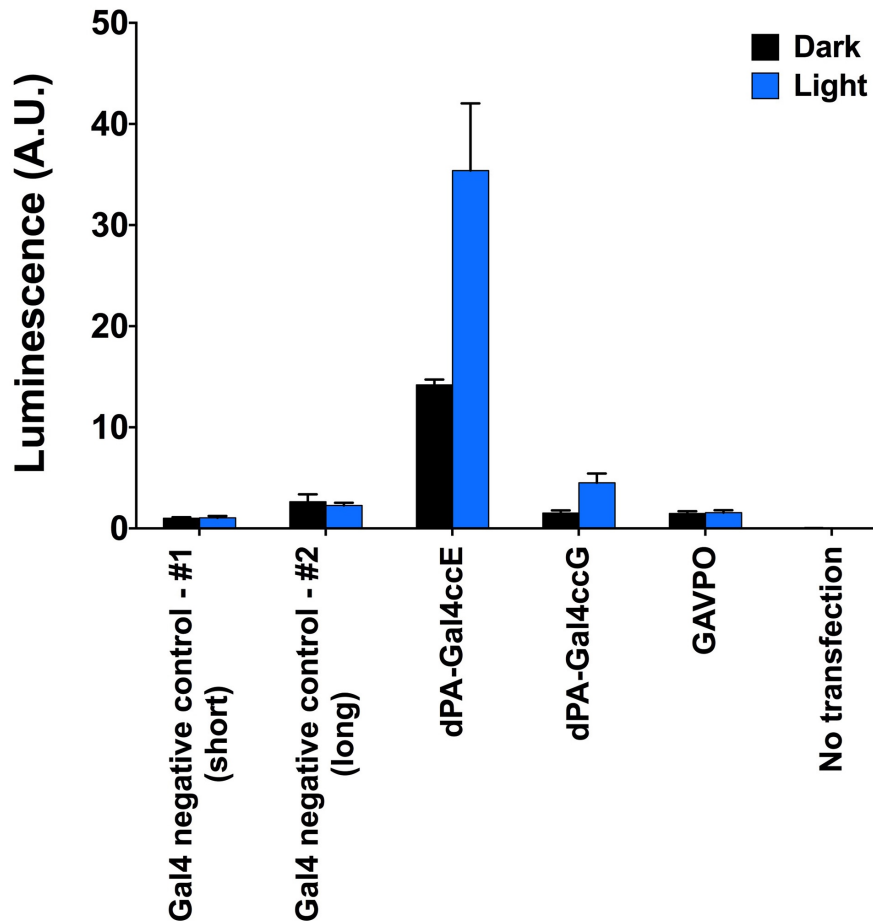
Figure S23. Evaluation of the dPA-Gal4cc transcriptional activators in the *Drosophila* S2 cells, related to Figure 1. Two PA-Gal4 transcriptional activators, dPA-Gal4ccE and G, were transfected into S2 cells with the UAS-luciferase reporter, and their light-dependent transcriptional activities were tested. The construct IDs, features of the construct, and the results of construct screening are shown. Each dataset consisted of three samples in the dark and three in the light. Luciferase assay data of the negative control-#1 in the dark were used for the correction of data of each construct. The data represent mean values ± s.d. (n = 3).

Construct ID	Element #1	Element #2	Dark Average	Dark S.D	Statistical comparison of GAVPO vs PA-Gal4cc	Light Average	Light S.D	Statistical comparison of GAVPO vs PA-Gal4cc	Light/Dark ratio Average	Light/Dark ratio S.D	Statistical comparison of GAVPO vs PA-Gal4cc	Statistical comparison of separated vs PA-Gal4cc (T2A ver.)
Negative control (short)	Gal4 DBD short & p65 AD		1.00	0.00		0.78	0.11		0.78	0.11		
Negative control (long)	Gal4 DBD long & p65 AD		7.64	3.94		6.61	4.36		0.84	0.35		
GAVPO	Gal4 DBD short-VVD-p65 AD		3.95	1.01	–	15.37	2.89	–	4.11	1.51	–	
A-separated G23	Gal4 DBD short-CIBN no NLS & NLSx2-p65 AD-Cry2 PHR		0.57	0.20	*	10.10	1.05	n.s.	19.26	3.71	n.s.	*
A	Gal4 DBD short-CIBN no NLS-T2A-NLSx2-p65 AD-Cry2 PHR		0.24	0.15	*	11.75	5.69	n.s.	51.76	11.20	n.s.	
B-separated G24	Gal4 DBD short-CIBN no NLS & NLSx2-p65 AD-Cry2 PHR (L348F)		0.53	0.10	*	2.41	0.40	*	4.71	1.32	n.s.	*
B	Gal4 DBD short-CIBN no NLS-T2A-NLSx2-p65 AD-Cry2 PHR (L348F)		0.25	0.13	*	4.75	2.63	n.s.	19.61	3.12	n.s.	
C	Gal4 DBD short-CIBN no NLS-T2A-NLSx2-p65 AD-Cry2 535		0.23	0.10	*	12.21	1.63	n.s.	58.90	18.98	*	
D-separated G117	Gal4 DBD short-CIBN & Cry2 PHR-p65 AD		1.21	0.76	*	16.03	1.45	n.s.	18.92	13.31	n.s.	n.s.
D	Gal4 DBD short-CIBN-T2A-Cry2 PHR-p65 AD		1.92	0.34	*	21.77	8.43	n.s.	11.30	2.95	n.s.	
E-separated G118	Gal4 DBD short-CIBN & Cry2 PHR (L348F)-p65 AD		0.38	0.13	*	28.70	7.40	*	86.12	49.07	*	n.s.
E	Gal4 DBD short-CIBN-T2A-Cry2 PHR (L348F)-p65 AD		0.35	0.06	*	22.07	10.42	n.s.	66.87	37.39	*	
F-separated G150	Gal4 DBD short-Cry2 PHR & CIBN no NLS-p65 AD		1.07	0.36	*	16.40	5.50	n.s.	15.68	2.92	n.s.	n.s.
F	Gal4 DBD short-Cry2 PHR-T2A-CIBN no NLS-p65 AD		1.14	0.36	*	21.53	2.55	n.s.	20.98	7.26	n.s.	
G-separated G154	Gal4 DBD short-Cry2 PHR (L348F) & CIBN no NLS-p65 AD		0.14	0.05	*	6.09	6.99	n.s.	36.44	28.73	n.s.	n.s.
G	Gal4 DBD short-Cry2 PHR (L348F)-T2A-CIBN no NLS-p65 AD		0.14	0.07	*	8.25	2.93	n.s.	62.22	9.55	*	
H-separated G29	Gal4 DBD short-CIB81 & NLSx2-p65 AD-Cry2 PHR		2.42	1.17	*	34.02	6.45	*	16.69	6.71	n.s.	*
H	Gal4 DBD short-CIB81-T2A-NLSx2-p65 AD-Cry2 PHR		0.21	0.04	*	33.29	5.47	*	168.73	54.37	*	
I-separated G30	Gal4 DBD short-CIB81 & NLSx2-p65 AD-Cry2 PHR (L348F)		2.81	1.44	n.s.	25.06	4.60	n.s.	11.69	8.03	n.s.	*
I	Gal4 DBD short-CIB81-T2A-NLSx2-p65 AD-Cry2 PHR (L348F)		0.15	0.06	*	7.30	2.43	n.s.	50.12	5.85	n.s.	
J-separated G126	Gal4 DBD short-CIB81 & Cry2 PHR (L348F)-p65 AD		1.08	0.45	*	16.20	3.43	n.s.	16.80	5.41	n.s.	n.s.
J	Gal4 DBD short-CIB81-T2A-Cry2 PHR (L348F)-p65 AD		0.82	0.26	*	9.32	0.87	n.s.	12.43	4.23	n.s.	

Table S1. Summary for validation of PA-Gal4cc constructs in transiently-transfected HEK293T cells, related to Figure 1. The data represent mean values ± s.d. (n = 9) from three independent experiments; Each experiment consisted of three replicates. Luciferase assay data of the negative control (short) in the dark were used for the correction of data of each construct. Statistical comparisons were conducted for the values of Dark, Light and Light/Dark ratio between the GAVPO vs. each PA-Gal4cc with ANOVA followed by Dunnett's post hoc test. Two-tailed Student's *t*-test between the Light/Dark ratio of each separated and T2A construct pair was also conducted. The asterisks indicate $p < 0.05$.

Corresponding main figure panels	Construct ID	Length of light ilumination	Dark		Statistical comparison of GAVPO vs PA-Gal4cc	Light		Statistical comparison of GAVPO vs PA-Gal4cc	Statistical comparison of Gal4-VN8x6 vs PA-Gal4cc	Light/Dark ratio		Statistical comparison of GAVPO vs PA-Gal4cc
			Average	S.D.		Average	S.D.			Average	S.D.	
Figure 2B&2C	GAVPO	3 h	10.58	5.69	–	31.65	4.23	–	*	3.81	2.34	–
	A		0.40	0.17	*	17.91	5.58	n.s.	*	49.08	21.57	n.s.
	B		0.38	0.20	*	7.68	1.95	*	*	23.93	11.33	n.s.
	C		0.37	0.14	*	21.38	5.22	n.s.	*	60.98	15.51	n.s.
	D		2.24	0.71	*	24.53	15.85	n.s.	*	13.69	13.36	n.s.
	E		1.17	0.80	*	22.95	6.12	n.s.	*	44.02	43.64	n.s.
	F		1.52	0.52	*	27.24	8.16	n.s.	*	18.16	2.89	n.s.
	G		0.27	0.02	*	15.79	4.19	n.s.	*	63.05	20.59	n.s.
	H		0.19	0.06	*	28.11	5.74	n.s.	*	168.94	80.65	*
	I		0.15	0.06	*	11.47	4.22	*	*	77.92	2.29	*
	J		1.29	1.00	*	15.70	5.51	n.s.	*	16.56	10.02	n.s.
	Gal4-VN8x6		72.65	3.21		78.51	16.10		–	1.10	0.22	

Table S2. Summary for comparison of PA-Gal4cc-mediated transcriptions with the 3 h-light exposure protocol, related to Figure 2. The data represent mean values ± s.d. (n = 9) from three independent experiments; Each experiment consisted of duplicates. Luciferase assay data of the negative control (short) in the dark (*data not shown*) were used for the correction of data of each construct. Statistical comparisons were conducted for the values of Dark, Light and Light/Dark ratio between the GAVPO vs. each PA-Gal4cc with ANOVA followed by Dunnett's post hoc test. Another statistical comparison was also conducted for the values of Dark between the Gal4-VN8x6 vs. each PA-Gal4cc with ANOVA followed by Dunnett's post hoc test. The asterisks indicate *p* < 0.05.

Corresponding main figure panels	Construct ID	Length of light ilumination	Dark		Statistical comparison of GAVPO vs PA-Gal4cc	Light		Statistical comparison of GAVPO vs PA-Gal4cc	Statistical comparison of Gal4-VN8x6 vs PA-Gal4cc	Light/Dark ratio		Statistical comparison of GAVPO vs PA-Gal4cc
			Average	S.D.		Average	S.D.			Average	S.D.	
Figure 2E&2F	GAVPO	24 h	2.76	1.00	–	28.92	10.12	–	n.s.	12.44	7.32	–
	A		0.14	0.02	*	39.53	0.57	n.s.	n.s.	288.22	50.73	n.s.
	B		0.13	0.03	*	11.51	2.11	n.s.	*	101.61	52.76	n.s.
	C		0.17	0.03	*	31.29	2.55	n.s.	n.s.	182.41	23.32	n.s.
	D		1.46	0.18	*	36.27	6.99	n.s.	n.s.	25.70	3.05	n.s.
	E		0.43	0.06	*	50.61	1.51	n.s.	n.s.	122.68	15.18	n.s.
	F		1.17	0.08	*	108.99	17.07	*	*	92.93	18.95	n.s.
	G		0.11	0.01	*	33.76	8.53	n.s.	n.s.	305.52	103.22	n.s.
	H		0.10	0.03	*	169.91	17.09	*	*	1835.10	411.52	*
	I		0.08	0.01	*	57.90	13.58	*	*	689.82	120.74	*
	J		0.29	0.01	*	28.47	1.44	n.s.	n.s.	101.14	4.37	n.s.
	Gal4-VN8x6		34.79	1.55		34.35	3.02		–	1.00	0.12	

Table S3. Summary for comparison of PA-Gal4cc-mediated transcriptions with the 24 h-light exposure protocol, related to Figure 2. The data represent mean values ± s.d. (n = 6) from three independent experiments; Each experiment consisted of duplicates. Luciferase assay data of the negative control (short) in the dark (*data not shown*) were used for the correction of data of each construct. Statistical comparisons were conducted for the values of Dark, Light and Light/Dark ratio between the GAVPO vs. each PA-Gal4cc with ANOVA followed by Dunnett's post hoc test. Another statistical comparison was also conducted for the values of Dark between the Gal4-VN8x6 vs. each PA-Gal4cc with ANOVA followed by Dunnett's post hoc test. The asterisks indicate $p < 0.05$.

Corresponding main figure panels	Experiment type or highlighted feature	PA-Gal4cc									
		A	B	C	D	E	F	G	H	I	J
Figure 2A-2C	3 h light illumination	+	-	++	++	++	++	+	++	-	+
Figure 2D-2F	24 h light illumination	+	-	+	+	+	++	+	++	+	+
Figure 3A-3C	Light pulse duration dependency	+	+	++	-	+	-	+	++	++	-
Figure 3D-3F	Light pulse number dependency	+	+	+	-	-	-	++	++	++	-
Figure 4A,4B	Fast t1/2 on	+	+	+	+	+	-	+	+	-	+
Figure 4A,4C	Fast t1/2 off	-	-	-	++	++	-	++	-	+	+
Figure 5	Oscillatory expression	-	+	-	+	+	-	+	-	-	-
Figure 5	Step-wise expression	+	-	+	-	-	-	+	+	+	+
Figure 6	Stable cell	NA	NA	NA	NA	+	NA	NA	NA	NA	NA
Figure 7	Patterned illumination	NA	NA	NA	NA	+	NA	NA	+	NA	NA
Figure 8	In utero electroplation	NA	NA	NA	NA	+	NA	NA	NA	NA	NA

Table S4. Examples of application of different PA-Gal4cc transcription factors, related to Figures 2-8. Tested experimental types or highlighted features of each PA-Gal4cc are summarized. ++: strongly recommended or superior, +: recommended or good, −: not strongly recommended or fair, NA: not applied.

Transparent Methods

Constructs

For functional screening of PA-Gal4cc candidate constructs, sequences encoding the short version of Gal4, which contains the DNA-binding domain (DBD) of Gal4 (residues 1–65), or the long version of Gal4 containing the DBD and dimerization domains (residues 1–147), were amplified using pEF-hGAVPO (Imayoshi et al., 2013, Yamada et al., 2018, Wang et al., 2012) and pM Vector of the Matchmaker™ Mammalian Assay Kit 2 (Clontech/TAKARA, 630305), respectively. The transcriptional activation domain of p65 (p65 AD) was amplified using pEF-hGAVPO. The optimized mammalian codon sequences encoding the derivatives of Cry2 (Cry2 PHR, Cry2 PHR [L348F], Cry2 535, and Cry2 535 [L348F]), and CIB1 and its derivatives (CIB1 without nuclear localization sequences [NLS], CIBN, CIBN without NLS sequences, and CIB81), were synthesized by FASMAC (Kanagawa, Japan) (Yamada et al., 2018, Hallett et al., 2016, Kennedy et al., 2010, Taslimi et al., 2016).

Using these sequences, Gal4 (residues 1–65 or 1–147) or p65 AD was fused to Cry2- or CIB1 derivatives, and the NLS or T2A sequences were introduced/attached by conventional overlap polymerase chain reaction (PCR) extension, restriction enzyme digestion, and ligation methods. These constructs were cloned into expression vector plasmids with the human elongation factor 1a (EF) promoter sequence and polyadenylation sequences (pEF-BOS) and their derivatives (Mizushima and Nagata, 1990). All prepared constructs were verified by DNA sequencing. The plasmids encoding CRY-GalΔDD (92035), CIB-VP16 (92036) and CIB-VP64 (92037) used in figure 1 were purchased from Addgene (Pathak et al., 2017). In the validation of transcription ADs (**Figure S15**), the DNA sequences encoding p65 (residues 286–550 of human p65), VP16 (residues 413–490 of herpes simplex virus transcription factor VP16) and VP64 (tandem 4-copy repeats of VP16 AD) were applied.

PA-Gal4 constructs using other optical dimer formation systems, such as tunable light-controlled interacting protein tags (TULIPs) (Hallett et al., 2016, Strickland et al., 2012), original light-inducible dimer/improved light-inducible dimer (oLID/iLID) (Hallett et al., 2016, Guntas et al., 2015), Vivid (VVD) and Magnet (Kawano et al., 2015, Wang et al., 2012) were generated by the same procedures.

In the plasmid constructions for lentivirus vectors, coding sequences of the PA-Gal4cc constructs were inserted into multiple cloning sites of CSII-EF-MCS-IRES2-mCherryNLS plasmids (Yamada et al., 2018, Imayoshi et al., 2013, Miyoshi, 2004). For the UAS reporter constructs, CSII-EF-MCS (Miyoshi, 2004) was digested with *AgeI* to remove the EF promoter, and the UAS sequence and the 3′ UTR of the mouse *Hes1* gene was cloned in the opposite orientation to long terminal repeat (LTR)-mediated transcription. A Ub-NLS-luc2 coding sequence was inserted immediately after the UAS sequence. The cHS4 insulator-pEF-Puro-halo sequence was inserted upstream of the UAS sequence for puromycin and haloTag® (Promega, G6050) selection.

Cell culture

HEK293T cells (American Type Culture Collection [ATCC]) were cultured at 37°C and 5% CO2 in Dulbecco's Modified Eagle´s Medium (DMEM; Nacalai Tesque, 08458-16) supplemented with 10% fetal bovine serum (FBS;

ThermoFisher, Hyclone, SH30071.03) and 100 units/mL penicillin and 100 mg/mL of streptomycin (Nacalai Tesque, 09367-34). HEK293T cells were passaged using 0.05% Trypsin/EDTA (Nacalai Tesque, 32778-05). *Drosophila* Schneider 2 (S2) cells (ThermoFisher, R69007) were cultured in Schneider's medium (ThermoFisher, 21720-024) supplemented with 10% FBS (Sigma, 13K272) and 100 units/mL penicillin and 100 mg/mL of streptomycin (Nacalai Tesque, 09367-34) at room temperature. S2 cells were grew at semi-adherent monolayer in cell culture flasks with shaking. S2 cell suspension was transferred into new flasks every 3-4 days.

Lentivirus packaging

Lentiviral particles were produced via lipofection of HEK293T cells with packaging plasmids. Briefly, supernatants were collected 48 h after transfection and concentrated by centrifugation at 6,000 g for 16 h. The viral pellet was resuspended in PBS and the viral aliquot was frozen. Viral titers were approximately 10^{8-9} infectious units/mL. Cultured cells were infected by purified lentiviral particles with a multiplicity of infection (MOI) = ~10–20. Transduced cells were selected by blasticidin (Bsd) S (10 μg/mL; ThermoFisher, R21001) and/or puromycin (2 μg/mL; Sigma, P8833) for the cells co-expressing Bsd and/or Puro, or by fluorescence-activated cell sorting (FACS; BD Biosciences, FACSAriaII) for cells co-expressing mCherry or haloTag.

Light source

For blue light irradiation of cultured cells in CO_2 incubators, we used an LED light source, LEDB-SBOXH (OptoCode). For blue light illumination under the microscope (except for patterned light application), blue light was generated by a pE-2 LED excitation system (CoolLED) equipped with a 470 nm LAM.

Patterned light application

A Mosaic 3 pattern illuminator (Andor) coupled to a blue light-emitting diode (Excelitas Technologies, X-Cite® 120LED) was attached to the microscope and used for light delivery through the objective.

Luciferase assays

Luciferase activity of the lysed cells was assayed according to the manufacturer's protocol (Promega, Luciferase Assay System, E1501).

Live-cell monitoring of luciferase activity

Luminescence signals at the population level were recorded by a live cell monitoring system (Churitsu Electric Corp., CL24B-LIC/B) equipped with a highly sensitive photomultiplier tube (PMT) and an LED blue light source (OptoCode, LEDB-SBOXH). Cells were plated on black 24-well plates in 1 mM luciferin-containing medium (Nacalai Tesque, 0149385), and photon-counting measurements were recorded.

Luciferase imaging

Cells were plated at 50–60% confluence on 35-mm glass bottomed dishes and incubated at 37°C in 5% CO_2. One mM luciferin was then added to the culture medium. Bioluminescence images were acquired on an upright microscope (Olympus, IX83) with a 20× or 40× dipping objective. Digital images were acquired using a cooled CCD camera (Andor, iKon-M DU934P-BV). The filters and camera control were adjusted automatically using software (Universal Imaging Corp., MetaMorph®). Stray light was eliminated by turning off the electric system. The imaging system was used in a dark room.

Characterization of PA-Gal4cc

For functional screening of the PA-Gal4cc candidate constructs, HEK293T cells were plated at $4\sim5 \times 10^4$ cells/well in a 24-well plate, and cultured for 24 h at 37°C in 5% CO_2. The cells were then transfected with Lipofectamine® LTX (ThermoFisher, 15338100) according to the manufacturer's protocols. Three plasmids were co-transfected at a 25:25:8 ratio: pEF-Gal4 DBD fused with Cry2/CIB-derivative, pEF-p65 AD fused with Cry2/CIB-derivative, and CSII-5x UAS-Ub-NLS-luc2-Ascl1 3′ UTR reporter (Imayoshi et al., 2013). Expression plasmids of Gal4 DBD short, Gal4 DBD long, and p65 AD without any PA dimer formation molecules were used for negative control experiments. The pEF-Gal4 DBD short and pEF-p65 AD, and pEF-Gal4 DBD long and pEF-p65 AD were co-transfected as the negative control (short) and the negative control (long), respectively. The total amount of DNA was 0.58 μg/well. Forty-five hours after transfection, the cells were exposed to blue light (7.2 W/m^2; 2-s pulse every 1 min) for 3 h. Thereafter, cells were lysed and their luciferase activity was measured using a plate reader (PerkinElmer, ARVO X3). Control cells were kept in the dark after plasmid transfection. For the analysis of constructs having the T2A sequence, the expression vector, pBluescript plasmid, and the reporter were mixed at a 25:25:8 ratio and transfected. The pBluescript plasmid was used to adjust the total amount of transfected DNA.

For comparing maximum induced gene expression levels between the PA-Gal4cc and constitutively active Gal4 transcriptional activator, the pEF-Gal4-VN8x6 plasmid was used (Salghetti et al., 2000). HEK293T cells were plated in a 24-well plate at $4\sim5 \times 10^4$ cells/well and transfected. Twenty-four hours after transfection, the cells were exposed to blue light (7.2 W/m^2; 2-s pulse every minute) for 24 h.

To analyze the relationship between the duration of blue light illumination on-phase in the on-off cycle and the level of induced gene expression, HEK293T cells were plated in a 24-well plate at $4\sim5 \times 10^4$ cells/well and transfected. Thirty-six hours after transfection, blue light (7.2 W/m^2) was applied for 15 min at the following on-phase: 0, 0.1, 0.5, 2.5, and 12.5 sec/min. One hour after the onset of illumination, cells were lysed and their luciferase activity was measured.

To analyze the relationship between the number of applied blue light pulses and the level of induced gene expression, HEK293T cells were plated in a 24-well plate at $4\sim5 \times 10^4$ cells/well and transfected. Thirty-six hours after transfection, blue light (7.2 W/m^2; 2-s pulse every minute) was applied to cells as follows: 0, 1, 2, 8, and 16 times. One hour after the onset of illumination, cells were lysed and their luciferase activity measured.

To establish the temporal characteristics of PA-Gal4cc, transfected or lentivirus-transduced HEK293T cells were used. Cells were plated in black 24-well plates and exposed to blue light (7.2 W/m^2) for 2 min. Luminescence

signals at the population level were recorded by a live-cell monitoring system (Churitsu Electric Corp., CL24B-LIC/B). For monitoring transiently transfected cells, HEK293T cells were plated at 1×10^4 cells/well and transfected 24 h later. The first blue light illumination was initiated 24 or 30 h after transfection. For monitoring lentivirus-transduced HEK293T cells, the cells were plated at 1×10^4 cells/well. The first blue light illumination was initiated 48 or 54 h after seeding.

To examine the ability of the PA-Gal4/UAS system to spatially control gene expression in the targeted cells, transfected HEK293T cells were plated at 50–60% confluence on 35-mm glass bottomed dishes (IWAKI, 3910-035) and incubated at 37°C in 5% CO_2 in the chamber stage of the microscope before illumination. Patterned light was generated by the MOSAIC 3 device (Andor) and applied to the cells. Light (10-ms pulse) was applied to cells 50 times, and temporal changes in luminescence signals were recorded. The first blue light illumination was initiated 24 or 30 h after transfection. When the blue light source power was set to 100%, and 200 pixel × 200 pixel regions were targeted through the 40× objective lens (Olympus, UApo 40× Oil Iris3/340; NA was modified to 0.55), the measured light energy was 1.3 W/m^2.

For the validation of the PA-Gal4/UAS system in the neural stem/progenitor cells of the developing mouse brain, the pEF-mCherryNLS, pEF-PA-Gal4ccE and CSII-5x UAS-Ub-NLS-luc2-Ascl1 3′ UTR reporter plasmids were mixed at a 2:9:9 ratio, and co-transfected into E13.5 dorsal telencephalon progenitors by *ex utero* electroporation (Imayoshi et al., 2013). Plasmid DNA (2.5 μg/μl) was microinjected into a telencephalic ventricle, and *ex utero* electroporation (6 pulses, 50 mV, square wave generator (BEX, CUY21), 5-mm paddle electrodes) was performed for transfection of plasmids into neural stem/progenitor cells at the ventricular surface of the neocortex. Brains were immediately dissected, embedded in 3% low-melting point agarose, cut into 250-μm organotypic slices with a vibratome (Leica, VT1000), transferred to 12-mm well culture insert (Merck, Millicell, PICM01250), and cultured in slice culture medium (DMEM/F-12 (GIBCO, 11039) supplemented with 0.6 mmol/L L-Glutamine, 5% horse serum, and penicillin/streptomycin). Slices were incubated at 37°C, 5% CO_2 for 24 h, and then subjected to the light illumination experiments.

Characterization of destabilized luciferase reporters

To determine the half-lives of the transcriptional reporter degradations, time-dependent changes in luciferase signals were monitored in the presence of protein synthesis inhibitor, cycloheximide. HEK293T cells were plated in black 24-well plates at 1-5 x10^3 cells/well and transfected 24 h later. Plasmid DNA (0.01 μg), pEF-Ub-NLS-luc2 or pEF-luc2 was transfected with Lipofectamine® LTX (ThermoFisher, 15338100). Twenty hours after transfection, the cells were treated with 20 μM cycloheximide (CHX; Nacalai Tesque, 06741-04). Luminescence signals at the population level were recorded by a live-cell monitoring system (Churitsu Electric Corp., CL24B-LIC/B). One sec exposure measurement was performed in each well every 1 min.

Real-time PCR analysis

Quantitative real-time PCR was used to determine the copy numbers of the lentivirus transduced cells. PA-Gal4ccE- or GAVPO-stably expressing HEK293T cells were plated in a 24-well plate at 1×10^5 cells/well and cultured in the dark conditioned CO_2 incubator. Genomic DNA (gDNA) was isolated with NucleoSpin DNA RapidLyse (MACHEREY-NAGEL, U0100B) according to the manufacturer's protocol. Each DNA sample was dissolved in 50 μl lysis buffer (5 mM Tris/HCl, pH8.5) and 0.5 μl of DNA solution was used for a real-time PCR reaction. The following primers were used; GAPDH forward, 5'-gcgacacccactcctccacc-3'; GAPDH reverse, 5'-ttaagagccagtctctggcc-3'; Gal4 forward, 5'-atgaagctgctgagcagcatcgag-3'; Gal4 reverse, 5'-cagttgttcttcaggcacttggcg-3'; luc2 forward, 5'-acatatcgaggtggacattacctac-3'; luc2 reverse, 5'-atgaagaactgcaagctattctcg-3'. The amount of specific gDNAs was quantitated with THUNDERBIRD SYBR qPCR Mix (TOYOBO, QPS-201). The amplification protocol was at 95°C for 60s for pre-denaturation, 95°C for 15s and 60 °C for 35s repeatedly for 40 cycles. Incorporation of the SYBR ROX dye into the PCR products was monitored in real time with Applied Biosystems 7500 (Applied Biosystems), thereby allowing determination of the threshold cycle (Ct) at which exponential amplification of PCR products begins. The gDNA copy number for each gene was quantified based on the Ct standard curve generated with the corresponding control gDNA.

To quantitatively test the mRNA expression levels of PA-transcription factors, PA-Gal4ccE- or GAVPO-stably expressing HEK293T cells were plated in a 24-well plate at 1×10^5 cells/well and cultured in the dark condition. Total RNA was isolated with TRIZOL Reagent (ThermoFisher, 15596-018) and subjected to reverse transcription with ReverTra Ace (TOYOBO, TRT-101) according to the manufacturer's protocols. The following primers were used; GAPDH forward, 5'-ggtggtctcctctgacttcaa-3'; GAPDH reverse, 5'-tctctcttcctcttgtgctcttg-3'. The Gal4 primer set was same as the gDNA analysis. The amount of specific mRNAs was quantitated by real-time PCR analysis with THUNDERBIRD SYBR qPCR Mix (TOYOBO, QPS-201) and Applied Biosystems 7500. The same amplification protocol as the gDNA analysis was applied. The relative quantification of the mRNA expressions was determined using the ΔΔCt method. Using this method, we obtained the fold changes in mRNA expression normalized to an internal control gene (GAPDH), and relative to one calibrator sample. For comparison, PA-Gal4ccE- or GAVPO-transiently expressed cells were prepared by the following procedure. HEK293T cells were plated in a 24-well plate at 4×10^4 cells/well and transfected 24 h later. Plasmid DNA (0.25 μg), pEF-PA-Gal4ccE or pEF-GAVPO was transfected with Lipofectamine® LTX (ThermoFisher, 15338100) and cultured in the dark condition, and analyzed twenty-four hours after transfection.

Western blotting analysis

PA-Gal4ccE- or GAVPO-stably expressing HEK293T cells were plated in a 6-well plate at 1×10^6 cells/well and cultured in the dark conditioned CO_2 incubator. Twenty-four hours after seeding, the cells were lysed and analyzed by the western blotting. For comparison, PA-Gal4ccE- or GAVPO-transiently expressed cells were prepared by the following procedure. HEK293T cells were plated in a 6-well plate at 2-3 × 10^5 cells/well and transfected 24 h later. Plasmid DNA (2 μg), pEF-PA-Gal4ccE or pEF-GAVPO was transfected with Lipofectamine® LTX (ThermoFisher, 15338100) and cultured in the dark conditioned CO_2 incubator. The cells were lysed twenty-four hours after transfection. The following primary antibodies (final dilution and source) were used: rabbit anti-Gal4 (1:1000; Santa

cruz, sc-577), rat anti-HA (1:2000; Roche, 11867423001, clone 3F10) and mouse anti-Actin (1:5000; Chemicon, MAB1501, clone C4). As the secondary antibodies, the following HRP-conjugated antibodies (final dilution and source) were used: donkey anti-rabbit IgG (1:2500, GE Healthcare, NA9340V), goat anti-rat IgG (1:2500, GE Healthcare, NA935) and sheep anti-mouse IgG (1:2500, GE Healthcare, NA9310V). The chemiluminescence signals emitted by ECL reagent (GE Healthcare, ECL Prime, RPN2232) were detected with LAS-3000 (FUJIFILM).

Generation of transgenic flies

The transgenic flies expressing *Drosophila melanogaster*-codon optimized PA-Gal4ccE and G (dPA-Gal4ccE and G) were generated by germline transformation using standard procedures (Hirano et al., 2013). The transgene structures were described in **Figure S22**. We selected a founder line for each dPA-Gal4cc transgenic fly by the highest transgene expression, and crossed with the MBp-lexA::GAD; UAS-mCherry::10xFLAG reporter line. The triple transgenic flies were kept in the dark condition before light illuminations, and then illuminated by blue light (7.2 W/m^2; 2-s pulse every 1 min) for 13-17 h with LEDB-SBOXH (OptoCode).

Characterization of dPA-Gal4cc in S2 cells

To examine the ability of the dPA-Gal4/UAS system to control gene expression in S2 cells, the cells were plated at 5×10^5 cells/well on a 12-well plate. The cells were then transfected with HilyMax (DOJINDO, H357) according to the manufacturer's protocols. Three plasmids were co-transfected at a 1:1:1 ratio: pEF-Gal4 DBD, pEF-p65 AD and pUAST-dLuc (Drosophila melanogaster-codon optimized luciferase) reporter, or dPA-Gal4cc expression vector, pBluescript plasmid and the reporter. The pBluescript plasmid was used to adjust the total amount of transfected DNA. The total amount of DNA was 3 μg/well. Forty-two hours after transfection, the cells were exposed to blue light (7.2 W/m^2; 2-s pulse every 1 min) for 3 h. Thereafter, cells were lysed and their luciferase activity was measured with a plate reader (PerkinElmer, ARVO X3). Control cells were kept in the dark after plasmid transfection.

Image analysis and quantification

Image analysis was performed using ImageJ software and custom plug-ins (Yamada et al., 2018, Imayoshi et al., 2013, Isomura et al., 2017). In brief, for analyzing an image sequence file of bioluminescence imaging, 'Spike-noise filter' was applied to a stack file to remove noise signals caused by cosmic rays. CCD readout noise was also removed by 'Temporal background reduction filter'. In this normalization procedure, the background value measured in the outside of the imaging regions for each time-flame was subtracted from the signal intensity. In some experiments, nuclear localized mCherry was expressed by transfection or electroporation, and used to detect and track moving cells (Imayoshi et al., 2013). Average signal intensity inside the nucleus were measured, illustrated and analyzed by Prism® 6.0 software (GraphPad).

Estimation of the activation and deactivation kinetics of light-induced gene expression

The half-lives of the switch-on/off kinetics of light-induced gene expression in PA-Gal4cc transformed cells were determined as described below. First, each waveform was detrended to remove the linear trends of activities independent of photostimulation. In the detrend processing, linear regression was performed on data points fewer than the median absolute deviation of the waveform, then values predicted by the regression were subtracted from all points of the waveform. A low pass filter (order = 4, cut-off frequency = 0.2) was also applied to remove the high frequency components. Then, the processed waveforms were transformed into z-scores.

Second, the starting point of event epochs induced by photostimulation was estimated by comparing each value in the waveform with a probabilistic threshold, where random numbers with the same length of the waveform vector were generated from a Gaussian distribution ($\mu = 0$, $\sigma = \sigma_{waveform}$). The probabilistic threshold was generated by the same method in all analyses. Each value in the waveform was compared with that in the threshold at the corresponding time point. This process was iterated 100 times, and time points when the probability exceeding the threshold was more than 50% were treated as events (i.e., light-induced gene expression). This procedure was performed in order to determine the start, peak, and tentative end of events even when the waveforms after the observed peak converged to slightly above the given constant threshold. The values of τ_{on} of light-induced gene expressions were estimated as the time from the beginning of the event epoch to the peak.

The end point of light-induced gene expression was estimated by analyzing the distribution of distance between the observed waveform and probabilistic threshold in each time point. We assumed that near the termination of light-induced gene expression, the distance would be smaller than in the middle. We fitted the distance distribution by Gaussian distribution, and then estimated the end of light-induced gene expression as time points satisfying the both criteria; (1) The time point of the end of light-induced gene expression is included in the left tail 2.5% of the fitted distributions of distance between the observed waveform and probabilistic threshold. (2) The time point of termination located after, but nearest to the peak of observed waveform. The values of τ_{off} were estimated as the time from the peak to end of the estimated light-induced gene expression.

This analysis was repeated 100 times for each time-series data of the monitored cell, and the calculated average τ_{on} and τ_{off} values of the same PA-Gal4cc construct were used for determining the half-lives of the switch-on/off kinetics of light-induced gene expression. All programs for this analysis were written in MATLAB R2018a (MathWorks Inc., MA, USA).

Statistical analysis

Statistical analyses were performed with Prism® 6.0 software (GraphPad). P values less than 0.05 were considered significant. Statistical methods used in the analysis are described in the figure or table legends.

STAR+METHODS

KEY RESOURCES TABLE

REAGENT or RESOURCE	SOURCE	IDENTIFIER
Antibodies		
Rabbit polyclonal anti-Gal4	Santa cruz	Cat#sc-577
Rat monoclonal anti-HA (clone 3F10)	Roche	Cat#11867423001
Mouse monoclonal anti-Actin (clone C4)	Chemicon	Cat#MAB1501
Donkey HRP-conjugated anti-rabbit IgG	GE Healthcare	Cat#NA9340V
Goat HRP-conjugated anti-rat IgG	GE Healthcare	Cat#NA935
Sheep HRP-conjugated anti-mouse IgG	GE Healthcare	Cat#NA9310V
Bacterial and Virus Strains		
CSII-EF-PA-Gal4cc-IRES2-mCherryNLS	This paper	N/A
CSII-UAS-Ub-NLS-luc2-Hes1 3′ UTR	This paper	N/A
CSII-EF-GAVPO-T2A-mCherryNLS	Imayoshi et al., 2013	N/A
Chemicals, Peptides, and Recombinant Proteins		
DMEM	Nacalai Tesque	Cat#08458-16
Penicillin/streptomycin	Nacalai Tesque	Cat#09367-34
Trypsin/EDTA	Nacalai Tesque	Cat#32778-05
FBS Hyclone	ThermoFisher	Cat#SH30071.03
FBS	Sigma	Cat#13K272
Schneider's medium	ThermoFisher	Cat#21720-024
D-luciferin sodium salt	Nacalai Tesque	Cat#0149385
Blasticidin S HCl	ThermoFisher	Cat#R21001
puromycin	Sigma	Cat#P8833
haloTag	Promega	Cat#G6050
DMEM/F-12	GIBCO	Cat#11039
cycloheximide	Nacalai Tesque	Cat#06741-04
Critical Commercial Assays		
Luciferase Assay System	Promega	Cat#E1501
Lipofectamine® LTX	ThermoFisher	Cat#15338100
NucleoSpin DNA RapidLyse	MACHEREY-NAGEL	Cat#U0100B
THUNDERBIRD SYBR qPCR Mix	TOYOBO	Cat#QPS-201

TRIZOL Reagent	ThermoFisher	Cat#15596-018
ReverTra Ace	TOYOBO	Cat#TRT-101
ECL Prime	GE Healthcare	Cat#RPN2232
HilyMax	DOJINDO	Cat#H357
Deposited Data		
Raw and analyzed data	This paper	N/A
Experimental Models: Cell Lines		
HEK293T	ATCC	Cat#CRL-3216
Drosophila Schneider 2 (S2)	ThermoFisher	Cat#R69007
Experimental Models: Organisms/Strains		
dPA-Gal4ccE transgenic *Drosophila melanogaster* strain	This paper	N/A
dPA-Gal4ccG transgenic *Drosophila melanogaster* strain	This paper	N/A
Oligonucleotides		
Primer: GAPDH forward: GCGACACCCACTCCTCCACC	This paper	N/A
Primer: GAPDH reverse: TTAAGAGCCAGTCTCTGGCC	This paper	N/A
Primer: Gal4 forward: ATGAAGCTGCTGAGCAGCATCGAG	This paper	N/A
Primer: Gal4 reverse: CAGTTGTTCTTCAGGCACTTGGCG	This paper	N/A
Primer: luc2 forward: ACATATCGAGGTGGACATTACCTAC	This paper	N/A
Primer: luc2 reverse: ATGAAGAACTGCAAGCTATTCTCG	This paper	N/A
Primer: GAPDH forward: GGTGGTCTCCTCTGACTTCAA	This paper	N/A
Primer: GAPDH reverse: TCTCTCTTCCTCTTGTGCTCTTG	This paper	N/A
Recombinant DNA		
pEF-mCherryNLS	Yamada et al., 2018; Imayoshi et al., 2013	N/A
pEF-luc2	Yamada et al., 2018	N/A

pEF-Ub-NLS-luc2	This paper	N/A
pEF-hGAVPO	Yamada et al., 2018; Imayoshi et al., 2013, Wang et al., 2012	N/A
pEF-BOS	Mizushima and Nagata, 1990	N/A
pEF-Gal4 DBD short	This paper	N/A
pEF-Gal4 DBD long	This paper	N/A
pEF-Gal4 DBD fused with Cry2/CIB-derivative	This paper	N/A
pEF-p65 AD fused with Cry2/CIB-derivative	This paper	N/A
pEF-PA-Gal4cc	This paper	N/A
CSII-5x UAS-Ub-NLS-luc2-Ascl1 3′ UTR	Imayoshi et al., 2013	N/A
pEF-Gal4-VN8x6	Salghetti et al., 2000	N/A
CRY-GalΔDD (B1013)	Pathak et al., 2017	Addgene plasmid #92035
CIB-VP16 (B1014)	Pathak et al., 2017	Addgene plasmid #92036
CIB-VP64 (B1016)	Pathak et al., 2017	Addgene plasmid #92037
pEF-p65 AD	This paper	N/A
pEF-VP16 AD	This paper	N/A
pEF-VP64 AD	This paper	N/A
CSII-EF-MCS	Miyoshi, 2004	N/A
CSII-EF-MCS-IRES2-Bsd	Yamada et al., 2018; Imayoshi et al., 2013; Miyoshi, 2004	N/A
CSII-EF-MCS-IRES2-mCherryNLS	Yamada et al., 2018; Imayoshi et al., 2013; Miyoshi, 2004	N/A
pEF-TU LIPs	This paper	N/A
pEF-oLID/iLID	This paper	N/A
pEF-Vivid	This paper	N/A
pEF-Magnet	This paper	N/A
pM Vector of the Matchmaker™ Mammalian Assay Kit 2	Clontech/TAKARA	Cat#630305
4xlexop-dPA-Gal4ccE	This paper	N/A

4xlexop-dPA-Gal4ccG	This paper	N/A
pUAST-dLuc	This paper	N/A
Software and Algorithms		
MetaMorph®	Universal Imaging Corp.	Version 7.8.10.0
ImageJ software and custom plug-ins	Yamada et al., 2018; Imayoshi et al., 2013; Isomura et al., 2017	N/A
Prism® software	GraphPad Software	Version 6.0
MATLAB	MathWorks	Version 9.2
Curve Fitting Toolbox	MathWorks	version 3.5.5
Signal Processing Toolbox	MathWorks	version 7.4
Other		
LED light source	OptoCode	Cat#LEDB-SBOXH
LED light source	CoolLED	Cat#pE-2 LED
Digital mirror device (DMD)	Andor	Cat#Mosaic 3
blue light-emitting diode	Excelitas Technologies	Cat#X-Cite® 120LED
Microscope for bioluminescence imaging	Olympus	Cat#IX83
40× objective lens	Olympus	Cat#UApo 40× Oil Iris3/340
CCD camera	Andor	Cat#iKon-M DU934P-BV
live cell monitoring system	Churitsu Electric Corp.	Cat#CL24B-LIC/B

CONTACT FOR REAGENT AND RESOURCE SHARING

Further information and requests for resources and reagents should be directed to and will be fulfilled by the Lead Contact, Itaru Imayoshi (imayoshi.itaru.2n@kyoto-u.ac.jp).

EXPERIMENTAL MODEL AND SUBJECT DETAILS

Animal handling and experimental protocols were approved by the Animal Care Committee of Kyoto University (permit numbers: Lif-K18019, Lif-K19016) and conformed to all relevant regulatory standards.

Supplemental references

HIRANO, Y., MASUDA, T., NAGANOS, S., MATSUNO, M., UENO, K., MIYASHITA, T., HORIUCHI, J. & SAITOE, M. 2013. Fasting launches CRTC to facilitate long-term memory formation in Drosophila. *Science,* 339**,** 443-6.

ISOMURA, A., OGUSHI, F., KORI, H. & KAGEYAMA, R. 2017. Optogenetic perturbation and bioluminescence imaging to analyze cell-to-cell transfer of oscillatory information. *Genes Dev,* 31**,** 524-535.

MIYOSHI, H. 2004. Gene delivery to hematopoietic stem cells using lentiviral vectors. *Methods Mol Biol,* 246**,** 429-38.

MIZUSHIMA, S. & NAGATA, S. 1990. pEF-BOS, a powerful mammalian expression vector. *Nucleic Acids Res,* 18**,** 5322.